Harpur Hill, Buxton
Derbyshire, SK17 9JN
T: +44 (0)1298 218000
F: +44 (0)1298 218986
W: www.hsl.gov.uk

HEALTH & SAFETY LABORATORY

Technical Assessment of Petroleum Road Fuel Tankers
Work Package 1 - Full scale testing and associated modelling
TANKER TOPPLE TEST METHODS AND RESULTS

ES/14/39/04rev07

Report Approved for Issue By:	Nigel Corlett BEng(Hons), MSc, PhD, ACSM
Date of Issue:	02 September 2015
Lead Author:	Michael Stewart MSc, PhD, FIMechE
Contributing Author(s):	Chris Atkin BEng (Hons) CEng, MIMechE, James Hobbs MEng, PhD, CEng, MIMechE
Technical Reviewer(s):	Richard Isherwood BEng (Hons) CEng, MIMechE
Editorial Reviewer:	Rob Richardson BEng (Hons) CEng, MIMechE
HSL Project Number:	PE05832

DISTRIBUTION

Steve Gillingham	Principal Engineer, Department for Transport
Nigel Corlett	HSL, Head of Engineering and Personal Safety Unit
Authors	
Duncan Webb	HSL Project manager
HSL Reports and Papers Library	pdf only

Technical Assessment of Petroleum Road Fuel Tankers

Disclaimer

Certain aspects of this report, and any results and conclusions set out within it, may be disputed by the tank manufacturer.

Report Approved for Issue by:	**Nigel Corlett BEng(Hons), MSc, PhD, ACSM**
Date of issue:	**02 September 2015**
Lead Author:	**Michael Stewart MSc, PhD, FIMechE**
Contributing Author(s):	**Chris Atkin BEng, CEng. MIMechE, James Hobbs MEng, PhD, CEng, MIMechE**
HSL Project Manager:	**Duncan Webb BSc (Hons)**
Technical Reviewer(s):	**Richard Isherwood BEng (Hons) CEng, MIMechE**
Editorial Reviewer:	**Rob Richardson BEng (Hons) CEng, MIMechE**
HSL Project Number:	**PE05832**

CONTENTS

last page = 113

1 LIST OF FIGURES

2 LIST OF TABLES

3 EXECUTIVE SUMMARY

Background

Following examination, certain petroleum road fuel tankers have been found to not be fully compliant with the provisions of Chapter 6.8 of the European Agreement on the Carriage of Dangerous Goods by Road (ADR). Amongst other things, these tankers are seen to exhibit extensive lack-of-fusion defects in the circumferential weld seams which, based on a leak-before-break assessment[i], could rupture under rollover and ADR load conditions.

The Department for Transport (DfT) commissioned research consisting of three work packages (WPs):

- WP1 – Full scale testing and associated modelling; Health and Safety Laboratory (HSL).
- WP2 – Detailed Fracture and Fatigue Engineering Critical Assessment (ECA); TWI Ltd.
- WP3 – Accident data and regulatory implications, and production of an overall summary report of the research; TRL Ltd.

HSL has taken forward the tasks set out in WP1 to:

1. Develop an independent non-proprietary structural hydrodynamic model of GRW tankers, validate this model against the results of tanker tests, and report modelling findings, including the potential for tanker structural performance tests.
2. Design, construct and commission a test rig for tests of tankers, including selecting and procuring suitable instrumentation for data gathering.
3. Determine suitability of tankers for large scale tests and acquire tankers, as appropriate, in accordance with project objectives as specified by DfT.
4. Undertake tests on tankers, including preparing the tankers, assessing the tanker test method and results, and reporting the findings.
5. Capture collision and/or deformation data from relevant impacts, for example by laser scanning, to corroborate modelling and tanker tests, and reconcile any inconsistencies.
6. Engage in peer review activities on the overall DfT research programme.

This report describes work undertaken to deliver tasks 2 and 4.

Objectives

The objectives for tasks 2 and 4 were:

- design, construct and commission a test rig for tankers which offers a reliable and repeatable method to provide experimental data for use in both improving the understanding of tanker impact behaviour and validating HSL's Finite Element (FE) modelling; and
- prepare and test tankers to provide experimental data for use in both improving the understanding of tanker impact behaviour, and to validate HSL's FE modelling.

Main Findings

Overall, the outcomes of a *proof of concept* test and tests on two GRW tankers, J2580 and J3910, demonstrated that the topple test was a reliable test method. The test data was reproducible and was used to validate HSL's Finite Element (FE) model, and improve the understanding of tanker impact behaviour during rollover.

[i] *'Short-term Fitness for Service Assessment of [non-compliant] Road Tankers, TWI (Draft) Report 23437/1/13, September 2013 and 'Project 23437 Contract Amendment: Additional FEA for assessment of [non-compliant] road tankers, TWI (Draft) Report 23437/2/13, October 2013.*

Test Methods, including tanker preparation

Three tankers were topple tested. First, a *proof of concept* test was conducted on a 'guinea pig' aluminium petroleum road fuel tanker. The aim of this test was to establish, with minimal test instrumentation on the tanker, that the basic test method and data logging system were sound, and so all the key features of tanker preparation, test and recovery were included in this test. The second and third tests were on GRW tanker J2580 (8-banded 6-compartment, 2008), and GRW tanker J3910 (8-banded 6-compartment, 2011): full test instrumentation was used in both tests.

After considering various approaches, HSL developed a topple test whereby a prepared tanker was tilted under controlled conditions until it became unstable and fell onto its offside under the influence of gravity. The tanker was filled with water because fuels were not practical for environmental and safety reasons. Impact on the offside of the tanker avoided damaging filling ports on the tanker's nearside. Information on GRW tankers was used to calculate the approximate angle at which GRW tankers would become unstable and ramps were designed to provide an initial tilt angle less than this calculated angle. The ramps were secured to a concrete test pad, with a plate steel landing pad providing a robust and repeatable impact area. After preparation, an empty tanker was placed on the ramps with its offside at, and parallel to, the bottom of the ramps.

Once ready for test, the tanker was filled with the required volume of water (equivalent to the mass of fuel for the GRW tankers) distributed across all compartments. It was then toppled sideways, pivoting around the outer edge of its offside wheels to fall onto the landing pad. The tanker was rotated into the topple position using two parallel winching systems with wide slings to spread the load and prevent high stress levels on the tanker body when winch forces were applied to the slings. Each winching system included a chain hoist and load cell and was anchored to the concrete pad. Rotating the tanker into the topple position was controlled by ensuring the load on each winch line was similar. When the point of instability was reached, the winching lines slackened and the tanker toppled onto its side due to the force of gravity.

Rectangular steel supports ('steel wheels') replaced the tanker's offside wheels to remove the risk of the tyres coming off the wheel rims during the test, and to avoid variability from uncontrolled shear movement in these tyres during the topple. The tanker was not tested with a tractor unit to avoid uncontrolled variations between tests caused by tractor unit rotation and to avoid possible failure of the kingpin due to unconventional loading. Instead, a steel frame (the '5^{th} wheel' assembly) was fitted at the tanker's kingpin plate to give the support normally provided by the tractor and to keep the tanker at the desired coupling height for the test. The tanker's suspension was blocked and held rigid to remove sources of uncontrolled variation, such as changes in the ride height, and to keep the tank position fixed relative to the suspension during the topple. Any items on the tanker not integral to the tank and suspension, or which might adversely affect the impact, or which might contain fuel, hydraulic oil or other environmentally harmful materials, were sealed or removed.

The full data gathering instrumentation for GRW tankers J2580 and J3910 comprised strain gauges, pressure transducers and accelerometers to provide data for use in validating the finite element model and characterising general impact behaviour. In total, 40 such instruments were used in these two tests. Accelerometer blocks were located at the centre point on the outside of both the front and rear bulkheads. Arrays of strain gauges and pressure transducers were mounted in compartments C1b (rear half of front compartment) and C4 (third compartment from the rear) as follows:

- seven pressure transducers in each compartment, located at the midpoint of the compartment close to the inner tanker wall, radiating circumferentially top to bottom on the offside (impact side), the centre being at the estimated point of impact;

- twelve strain gauges in each compartment, mounted as strain gauge pairs in matching positions on the inside and the outside of the offside tanker shell. For GRW tankers J2580 and J3910 one location was near the rear bulkhead weld measuring longitudinal strain and one location was at the midpoint of the compartment measuring both longitudinal and hoop strain. For GRW tanker J3910 only, a further location was near the front bulkhead weld measuring longitudinal strain.

Two independent data loggers were used, one for each of compartments C1b and C4. During the test these loggers were synchronised with the high speed video and acquired data at 50 000 samples per second, or one recording every 0.02 millisecond. The *proof of concept* test was recorded using a range of video cameras, and the tests on GRW tankers J2580 and J3910 were recorded using thirteen video cameras ranging from standard speed (25 frames per second) to high speed (1 000 frames per second). Frames from the high speed video were analysed to obtain accurate measurements of acceleration and impact velocity at the front and rear of the tanker.

Before test, the internal welds at the extrusion bands in GRW tankers J2580 and J3910 were visually inspected; the locations of fillet welds between the extrusion band and the shell were mapped for both tankers and the locations of weld misalignments mapped for GRW tanker J3910. GRW tanker J2580 bulkheads were welded to the extrusion bands on the convex side of the bulkhead only, while GRW tanker J3910 bulkheads were welded to the extrusion bands on both sides of the bulkhead. In addition, the extrusion profiles were different between the two tankers, with a lug on the concave side of the bulkhead for GRW tanker J2580. Before the test of GRW tanker J3910, the external circumferential weld caps were surveyed to provide data for WP2. Grids of circles, intended to indicate the deformation close to the welds for WP2, were marked on the outside of this tanker above the likely impact zone at compartments C1b and C4. Tankers were laser scanned before and after test to confirm if tanker preparation caused any changes, and to record changes to tanker shape after impact.

Once surveyed and prepared, including fitting all instrumentation, the manway lids were refitted and pneumatic pressure tests conducted to confirm that GRW tankers J2580 and J3910 were fully sealed and loadworthy. Immediately before the test, the tankers were filled with water (using a calibrated water meter) to give a mass that was equivalent to the maximum rated load mass of the tankers. GRW tankers J2580 and J3910 were, thus, both filled with 31 376 litres of water, with each compartment filled to about 70% of its maximum capacity. These volumes were below the rated volumes for fuel because of the higher density of water.

Immediately after impact, leaks and other impact features found by visual examination were recorded. The tanker was then emptied and lifted back upright onto its wheels. After recovery there was further visual examination and, for GRW tankers J2580 and J3910, pressure tests were conducted to establish the internal integrity of the compartments and bulkheads.

Topple test results

The overall impact duration was a few seconds for all the tests, with most deformation occurring in the first 100 ms. The impact was close to uniform along the length of the tanker, and the impact velocities lay within the range of 1.75 to 2.62 rad/s[ii] as follows:

- The front and rear of the *proof of concept* tanker hit the ground within a few milliseconds of each other. The impact speed at the rear of the tanker was 4.25 m/s (around 2 rad/s) – due to the nature of the test, impact speed was not measured at the front of the tanker.
- GRW tanker J2580 impacted with speeds of 4.50 m/s (1.82 rad/s) at the front and 4.10 m/s (1.86 rad/s) at the rear of the tanker, with the rear hitting the ground less than 1 ms before the front of the tanker.

[ii] *Velocities in this range have been reported for rollovers in real accidents*

- GRW tanker J3910 impacted with speeds of 4.55 m/s (1.84 rad/s) at the front and 4.25 m/s (1.93 rad/s) at the rear of the tanker, with the rear hitting the ground less than 7 ms before front of the tanker.

The pressure data in both compartments were similar for GRW tankers J2580 and J3910. Short duration pressure peaks between 2 and 7.7 bar were observed during the first 20 to 30 ms of the impact; these were above the 2 bar peak used in previous rollover modelling. However, between around 20 and 40 ms after impact the pressures were around 2 bar, and after this the pressures reduced further.

The strain data in both compartments were similar for GRW tankers J2580 and J3910. Strains near the welds were higher than those at the compartment centre, with some yielding and plastic deformation observed in the strain behaviour near the welds. During impact, for both GRW tankers, high speed video captured free travelling flexural waves propagating away from the impact line around the circumference of the tanker. Such waves should result in more pronounced ripples in the circumferential strain than the longitudinal strain at the centre of the compartment and, for both GRW tankers, this was found to be the case. Signals from three of the internal strain gauges on GRW tanker J3910 were lost during filling. Although these signals re-appeared during the impact, data from these gauges was only used as an indicator of trends. This loss of data did not significantly compromise the successful outcome of the tests.

After the test, all the tankers exhibited a similar offside deformation shape with the impact area flattened. The deformation profile was similar along the length of the GRW tankers, with the level of deformation increasing from front to rear of the GRW tankers. The deformation data (i.e. the length of the flattened impact chord and reduction in tanker diameter), were similar for GRW tankers J2580 and J3910. For example, the impact had caused a permanent reduction in tanker diameter of approximately 100 mm at the rear and 82 mm at the front of GRW tanker J2580; and of approximately 107 mm at the rear and 82 mm at the front of GRW tanker J3910.

GRW J2580 impact damage. Immediately after the test, the only visible leak from the tanker was between the rear bulkhead and extrusion band at the top of the impact area. Subsequent visual inspection found a rupture within the fillet weld between the rear bulkhead and extrusion band at the top of the impact area, with no visible damage at the bottom of the impact area. During emptying there was no evidence of any breaches between compartments. However, pneumatic pressure tests showed that all compartments had lost their internal integrity. HSL supplied TWI with samples from GRW tanker J2580, including the impact zone from the off-side rear, for post-mortem assessment under WP2. During post-mortem examination, TWI observed an apparent through-wall crack along the circumferential weld at the top of the impact zone. This crack can be seen on close examination of HSL photographs of the tanker after being lifted back onto its wheels. Detailed fractographic analysis of the J2580 and J3910 samples is addressed in the WP2 report.

GRW J3910 impact damage. Immediately after the test, the only visible leak from the tanker was between the front bulkhead and extrusion band at the top of the impact area. Subsequent visual inspection found a rupture in the toe of the fillet weld between the front bulkhead and extrusion band at the top of the impact area, and also a crack in the toe of the same weld at the bottom of the impact area. During emptying there was evidence of leaks at the bulkhead between compartments 1 and 2, and between compartments 4 and 5. Pneumatic pressure tests confirmed that internal integrity had been lost between compartments 1 and 2, and between compartments 4 and 5, while the other bulkheads and compartments had maintained their internal integrity. HSL supplied TWI with a sample from GRW tanker J3910, including the impact zone from the off-side front, for post-mortem assessment under WP2.

GRW have indicated that the damage around the joints between the extrusion band and the bulkhead/baffles is consistent with that seen in real-world rollovers.

4 INTRODUCTION

This work has been carried out as part of the Department for Transport's (DfT) technical assessment of petroleum road fuel tankers.

Following examination, certain petroleum road fuel tankers have been found to not be fully compliant with the provisions of Chapter 6.8 of the European Agreement on the Carriage of Dangerous Goods by Road (ADR). Amongst other things, these tankers are seen to exhibit extensive lack-of-fusion defects in the circumferential weld seams which, based on a leak-before-break assessment[iii], could rupture under rollover and ADR load conditions.

The Department for Transport (DfT) commissioned research consisting of three work packages (WPs):

- WP1 – Full scale testing and associated modelling; Health and Safety Laboratory (HSL).
- WP2 – Detailed Fracture and Fatigue Engineering Critical Assessment (ECA); TWI Ltd.
- WP3 – Accident data and regulatory implications, and production of an overall summary report of the research; TRL Ltd.

HSL has taken forward the tasks set out in WP1 to:

1. Develop an independent non-proprietary structural hydrodynamic model of GRW tankers, validate this model against the results of tanker tests, and report modelling findings, including the potential for tanker structural performance tests.
2. Design, construct and commission a test rig for tests of tankers, including selecting and procuring suitable instrumentation for data gathering.
3. Determine suitability of tankers for large scale tests and acquire tankers, as appropriate, in accordance with project objectives as specified by DfT.
4. Undertake tests on tankers, including preparing the tankers, assessing the tanker test method and results, and reporting the findings.
5. Capture collision and/or deformation data from relevant impacts, for example by laser scanning, to corroborate modelling and tanker tests, and reconcile any inconsistencies.
6. Engage in peer review activities on the overall DfT research programme.

This report covers the work undertaken to meet the objectives for tasks 2 and 4:

- design, construct and commission a test rig for tankers which offers a reliable and repeatable method to provide experimental data for use in both improving the understanding of tanker impact behaviour and validating HSL's Finite Element (FE) modelling; and
- prepare and test tankers to provide experimental data for use in both improving the understanding of tanker impact behaviour, and to validate HSL's FE modelling.

The main measurements that will be used to validate HSL's FE model are:

1. Deformations from laser scan data
2. Impact velocity measurements
3. Pressure measurements
4. Strain measurements
5. Accelerometer measurements

This report is one of a package of reports describing HSL's work on WP1. The reports in this package are given in Table 1.

[iii] *'Short-term Fitness for Service Assessment of [non-compliant] Road Tankers, TWI (Draft) Report 23437/1/13, September 2013 and 'Project 23437 Contract Amendment: Additional FEA for assessment of [non-compliant] road tankers, TWI (Draft) Report 23437/2/13, October 2013.*

Table 1 HSL reports describing Work Package 1

ES/14/39/00	Technical Assessment of Petroleum Road Fuel Tankers; Work Package 1 - Full scale testing and associated modelling; Overall Summary
ES/14/39/07	Technical Assessment of Petroleum Road Fuel Tankers; Work Package 1 - Full scale testing and associated modelling; Assessment and Supply of Tankers
ES/14/39/04	Technical Assessment of Petroleum Road Fuel Tankers; Work Package 1 - Full scale testing and associated modelling; Tanker Topple Test Methods and Results **THIS REPORT**
ES/14/39/05	Technical Assessment of Petroleum Road Fuel Tankers; Work Package 1 - Full scale testing and associated modelling; Modelling to Provide Load Case Data for Rollover – Approach and Initial Development
ES/14/39/06	Technical Assessment of Petroleum Road Fuel Tankers; Work Package 1 - Full scale testing and associated modelling; Modelling to Provide Load Case Data for Rollover - Validation and Application

4.1 TOPPLE TESTS CONDUCTED

Tests were carried out on three different tankers on the following dates:

Proof of concept tanker	03 April 2014
GRW tanker J2580	02 May 2014
GRW tanker J3910	04 July 2014

To ensure that the test and measurement methods were reliable and effective, a *proof of concept* test was carried out as mentioned above. The aluminium petroleum road tanker used for the *proof of concept* test was a 'stuffed box' construction[iv]. The purpose of this test was to:

- ensure that the tanker could be lifted and manoeuvred into the test position on the ramp without causing any damage to the tanker;
- ensure that the winching method could raise the tanker to the topple position in a controlled manner, and the tanker would then topple under gravity and land on the horizontal test pad with its longitudinal axis parallel to the ground; and
- ensure that, before during and after impact, and with several metres of tanker movement the instrumentation and cabling system continued to transmit and measure the data.

The two GRW tankers, J2580 (2008) and J3910 (2011), were both 8-banded 6-compartment designs. These tankers were of "banded" construction – i.e. extrusion bands were used to join the sections of the tanker together. In this report the term 'band' is used to mean extrusion band. Relevant details of their design and construction are given in this report, with other details given in HSL reports ES/14/39/05, ES/14/39/06 and ES/14/39/07.

[iv] *In a 'stuffed' construction, the tanker shell is one single construction, and the bulkheads/baffles are fitted inside and welded to the inner wall of this shell.*

5 TANKER TEST METHOD

5.1 SUMMARY OF DIFFERENT TEST METHODS CONSIDERED

In early discussions with DfT on impact testing of tankers, the consortium considered three different methodologies to carry out the tests as shown in Table 2.

Table 2 Summary of the test methods considered

Method	Advantages	Limitations
1. Tanker rollover whilst in motion	Closer to a real-life scenario.	This method is not the most suitable for validating a numerical model as there will be a larger variation in the dynamic response of each tanker being tested compared with 3. (below). For example, the impact velocities will vary more between each test than in 3. Also there will probably be a greater variation in which part of the tank strikes the ground first.
2. Drop tests of a tank	A well-controlled test. The tank orientation could be controlled so impact occurs on specific areas of interest. Would follow a similar test method for packages used to transport radioactive materials (covered by IAEA regulations). May be useful when considering accident scenarios involving direct impacts on the tank (e.g. rear impact or side impact crashes)	Test method more suitable for assessments of the tank alone. Test is different to rollover conditions. Dynamic response of the internal fluid may not be typical of an accident scenario.
3. Sideways topple test of a tanker when stationary	A well-controlled test without the practical difficulties in 1. and 2. Will provide data that should be suitable for validation of a model. Closer to a real-life scenario than 2. Closer to the ADR regulatory test for IBCs (clause 6.5.6.11 described Section 5.2 below).	Not as close to a road-going accident scenario as 1.

The methodology followed, in agreement with DfT, was the topple test (number 3 in Table 2), with the tanker filled with water to represent the fuel: petroleum, diesel or fuel oil were not practical for environmental and safety reasons. The tanker would be toppled in a sideways direction onto flat ground, so the topple height was almost zero as the pivot line was close to the ground. This was considered the most practical and appropriate method within the timescales required to deliver the test work.

The tanker would be positioned close to the point of instability and then 'nudged' to roll it onto its side using a controlled and repeatable method. The impact is on the tanker's offside, because the ports on the nearside need to be accessible for filling. This is shown in Figure 1.

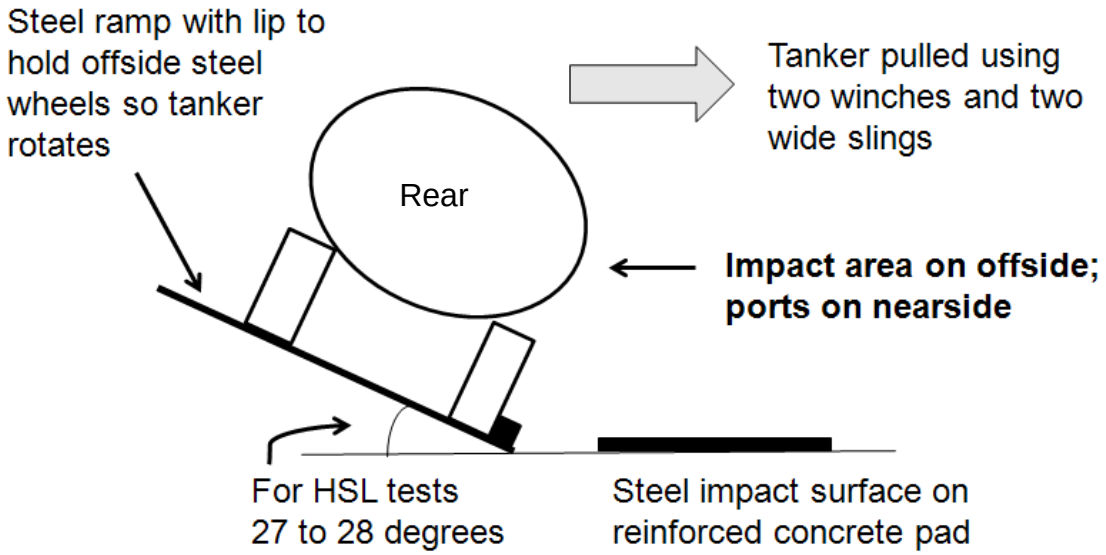

Figure 1 The key features of the HSL tanker topple test

HSL calculated that a tanker of the type to be tested, filled to its maximum gross weight with water rather than road fuel, is stable at around 27 to 33 degrees of tilt. Therefore an initial angle of around 27 to 28 degrees would reduce the horizontal pull force required to topple the tanker.

5.2 ADR TEST METHOD FOR TANKS

The ADR regulations [1] were referenced to assess what impact test methods are required for tanks. In ADR there are currently no mandatory impact test requirements for petroleum road fuel tankers. However, there are topple test requirements for intermediate bulk containers (IBCs)[v], which are shown below for information.

[v] *An Intermediate bulk container (IBC) is a reusable industrial container designed for the transport and storage of bulk liquid and granulate substances. They can normally be stacked, and common sizes are 1 040 litres and 1 250 litres. Cube shaped IBCs give particularly good storage capacity compared to palletized drums.*

6.5.6.11 Topple Test

6.5.6.11.1 Applicability

For all types of flexible IBC, as a design type test.

6.5.6.11.2 Preparation of the IBC for test.

The IBC shall be filled to not less than 95% of its capacity and to its maximum permissible gross mass, the contents being evenly distributed.

6.5.6.11.3 Method of testing.

The IBC shall be caused to topple on to any part of its top on to a rigid, non-resilient, smooth, flat and horizontal surface.

6.5.6.11.4 Topple Height

Packing Group I	*Packing Group II*	*Packing Group III*
1.8m	*1.2m* **(same group as an LGBF code petroleum tanker)**	*0.8m*

6.5.6.11.5 Criteria for passing the test.

No loss of contents. A slight discharge, e.g. from closures or stitch holes, upon impact shall not be considered to be a failure of the IBC provided that no further leakage occurs.

HSL installed a 20 mm thick steel landing pad bolted to a 150 mm deep reinforced concrete slab to satisfy 6.5.6.11.3. Regarding 6.5.6.11.2, HSL did not fill the tankers to maximum volumetric capacity for reasons discussed in Section 7.

5.3 RAMP DESIGN

HSL placed the tanker at a pre-set angle on a ramp as described in Section 5.1. As well as reducing the winching force required to topple the tanker, it also reduced the risk of the tanker sliding towards the winches as the force was applied.

HSL designed two steel ramps constructed at an angle of 25^{o} (one to go under the trailer, and the other to go under a bespoke 5^{th} wheel assembly (described in Section 5.4)).

The ramps consisted of a 20 mm thick top plate welded to a triangular steel frame underneath; the frame was constructed of rectangular hollow sections (RHS) to provide the angle and support the load of a fully-loaded tanker.

Stability calculations showed that, for a fully-loaded tanker, this would require a winching force in the range of four to seven tonnes. To reduce this force, HSL manufactured 2^{o} wedges to go underneath the upper wheels to raise the angle to $27^{o} – 28^{o}$ as shown in Figure 2. This reduced the calculated winching force to between two and five tonnes.

FES140601_01

Figure 2 Tanker on the ramps showing the wedges under the nearside wheels in preparation for a topple test (*proof of concept* test)

Figure 2 also shows the two restraint slings that HSL used to secure the tanker on the ramp. HSL had carried out calculations to demonstrate the tanker would be stable on the ramp at this angle (whilst empty, during filling and when filled). However, as a safety precaution these two restraint slings were attached to the tanker and each anchored to a separate steel bracket bolted into the concrete pad (similar to those for the winching lines shown in Figure 8). Therefore, if the tanker did become unstable and started to topple (e.g. in high winds) the restraints would hold the load[vi].

The tanker is shown on the ramps in Figure 3.

[vi] *In still conditions, the tests showed the tanker does remain stable on the ramp without the need for the restraints.*

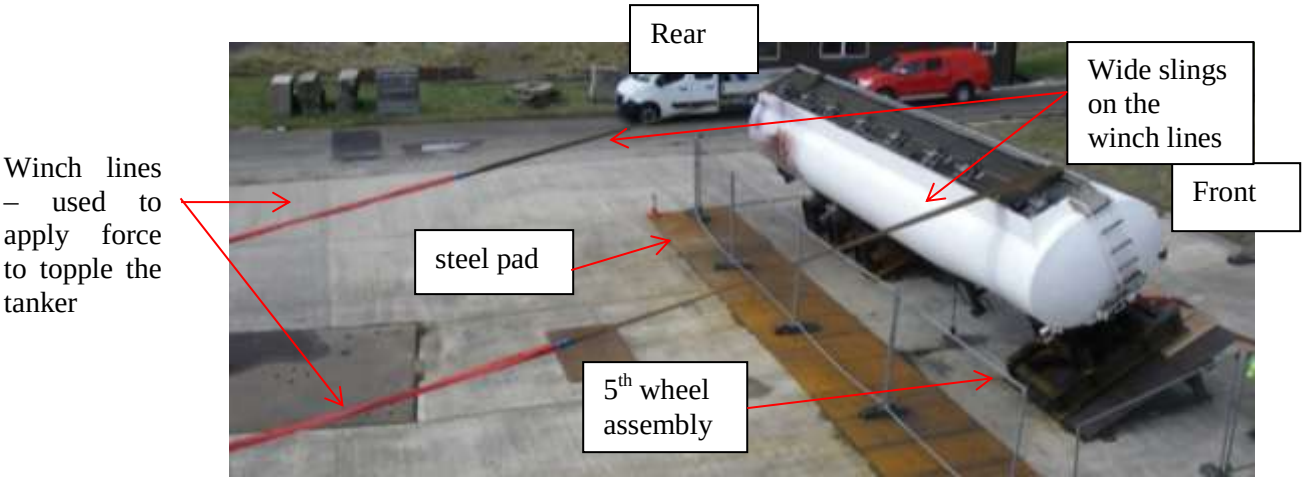

FES140502_01

Figure 3 *Proof of concept* tanker on the ramps before test

To prevent the tanker sliding off the ramp, and to provide a pivot point, a 20 mm x 20 mm steel strip was welded along the lower side of the ramps (this can be seen in Figure 5).

5.4 TANKER PREPARATION

All tanker components that could affect the impact, such as brackets, mudguards, flexible hoses, the box containing firefighting equipment etc. were removed. The pipework to and from the pump was removed, and inlets and outlets at the pump were blocked to prevent any residual fuel spills during the test. This ensured that the tank would impact directly on the ground during the test, and the method would be repeatable for tests on other tankers.

The tanker was not tested with a tractor unit as tractor unit rotation, and possible failure of the kingpin due to unconventional loading, would have caused variations in the test that would not be repeatable from one test to the next. Predicting this behaviour in the FE model would have been extremely difficult. A steel frame, the 5th wheel assembly, was bolted to the kingpin plate on the underside of the tanker near the front to provide support (see Figure 4). The assembly was designed and manufactured by HSL using I-beams and cross-bracing. It supported the tanker at the same nominal height and replicated the wheel track as if coupled to a tractor unit.

VPS 1404007_002

Figure 4 Front of the tanker and 5th wheel assembly (*proof of concept test)*

To eliminate the risk of the tyres coming off the rims, and shear movement in the tyres as the tanker is winched to the topple position, the nearside wheels were replaced with rectangular steel supports: referred to as *steel wheels* (see Figure 5).

FES140502_02

Figure 5 Tanker on ramps with steel wheels fitted to its offside and the steel strip on the ramp (*proof of concept* test)

Both the 5th wheel assembly and the steel wheels were designed to keep the vehicle track (the width from the outside of the tyres on one side to the outside of the tyres on the other side) as close to the true dimension as practical (2 550 mm). In addition, the tanker suspension was blocked on all tankers by installing brackets between the axles and chassis rail (Figure 6).

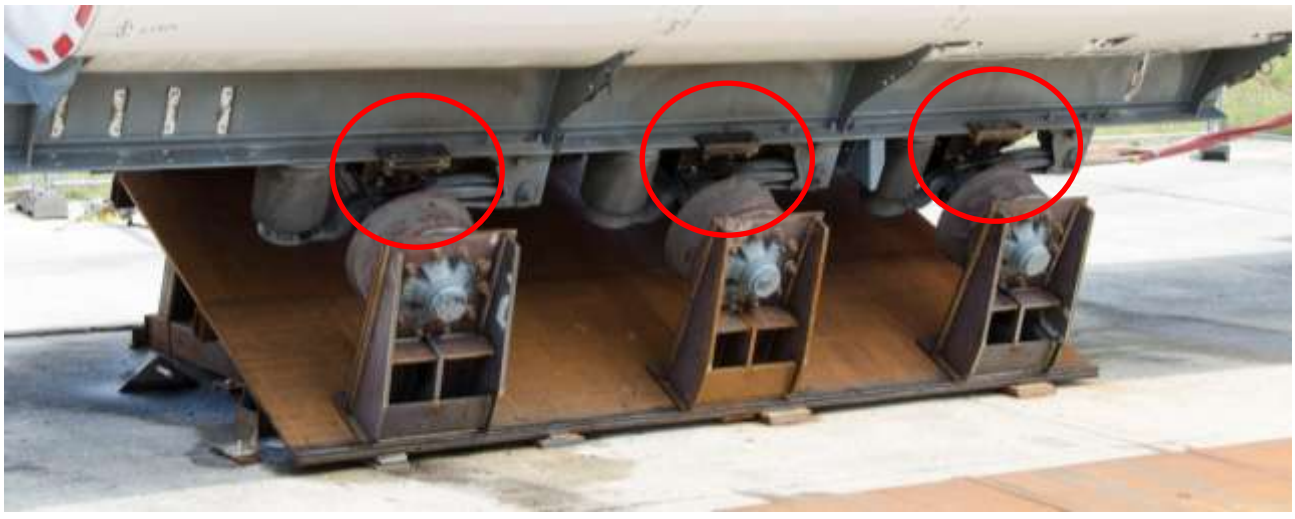

VPS 1406045_009

Figure 6 Chassis rail showing the brackets blocking the suspension

These brackets were fitted to ensure that:

- winching the tanker to the topple position was controlled — any movement between tanker and chassis could cause the tanker to topple prematurely in an unpredictable manner;
- each tanker toppled in a repeatable way — movement of the suspension could vary between tankers. This would cause variations between each test and present difficulties when comparing the results with the predictions; and
- there was no risk the suspension would fail due to the shear forces acting on it when the tanker was in a raised position.

After all the preparation work, including fitting the instrumentation, had been completed in the laboratory, the empty tankers were transferred to the test pad.

However, before the GRW tankers were transferred, each of the six compartments was pneumatically pressure tested by a tanker inspection contractor. One compartment at a time was pressurised to 200 mbar, then sealed; the duration of the test was five minutes. For GRW tanker J2580 the pressure drops in the compartments after five minutes are shown in Table 3, and for GRW tanker J3910 the pressure drops in the compartments after five minutes are shown in Table 4.

Table 3 Pneumatic pressure test – GRW tanker J2580

Compartment No.	1	2	3	4	5	6
Pressure drop after 5 minutes (mbar)	3	0	7	0	0	1

Table 4 Pneumatic pressure test – GRW tanker J3910

Compartment No.	1	2	3	4	5	6
Pressure drop 5 minutes (mbar)	2	3	3	3	3	4

All compartments were within 5 mbar pressure drop (the pass/fail criteria set by the inspector) except for compartment 3 for GRW tanker J2580, which gave 7 mbar. The inspector noted that this was due to a minor leak at the sequential valve into the vapour recovery system. However, this leak corrected itself in the tests on the 'emergency pressure relief valves' (EPRVs) mentioned below. Therefore, it was the inspector's opinion that this did not constitute a leak failure.

Pneumatic pressure tests were repeated after the topple tests (discussed in Section 9.6).

The pressure relief valves were also tested. All of them opened at pressures between 278 and 310 mbar, and re-sealed at pressures between 240 and 281 mbar. This was within acceptable limits for a petroleum tanker.

5.5 WINCHING METHODS

In early discussions, winching the tanker using a recovery vehicle or a Tirfor winch were considered. These ideas were soon eliminated because neither would provide sufficiently fine control of the winching process. If the tanker had been pulled over too quickly, it might have fallen in an uneven way. This may have presented difficulties when comparing the measurements with the predictions from the model.

The method chosen was to winch the tanker using two chain hoists attached to anchor brackets bolted into the concrete pad. Chain hoists have a high gear ratio so the load can be applied in a more controlled way. However, as chain hoists are not specifically designed to be used as winches, HSL investigated this matter and confirmed that was no risk of the chain hoists being unable to support the load, or reductions in the safe working load. Recommendations were made to check the hoist remained lubricated as some hoists have an oil breather which may leak oil when used in the horizontal position: this was not an issue for the chain blocks that HSL chose. The two chains hoists and winching lines are shown in Figures 7 and 8.

The winches were shackled, via textile slings, to steel brackets that had been bolted into the concrete; these brackets had been proof loaded to 5 tonnes. At the other end, the slings were placed over the top of the tanker, then 'choked' onto the 5th wheel assembly at the front, and around the middle or rear axle at the back. Flat, textile webslings (300 mm wide) were used around the tanker body to spread the winching load and prevent high stresses on the tanker body and comb: these are shown in Figures 7 and 8.

Each winch had a load cell in the line so the *Winch Master* (standing between the two load lines) could observe the force in each line and instruct either of the winch operators to haul the 'pull chain' quicker or slower, in order to keep the forces balanced on each line.

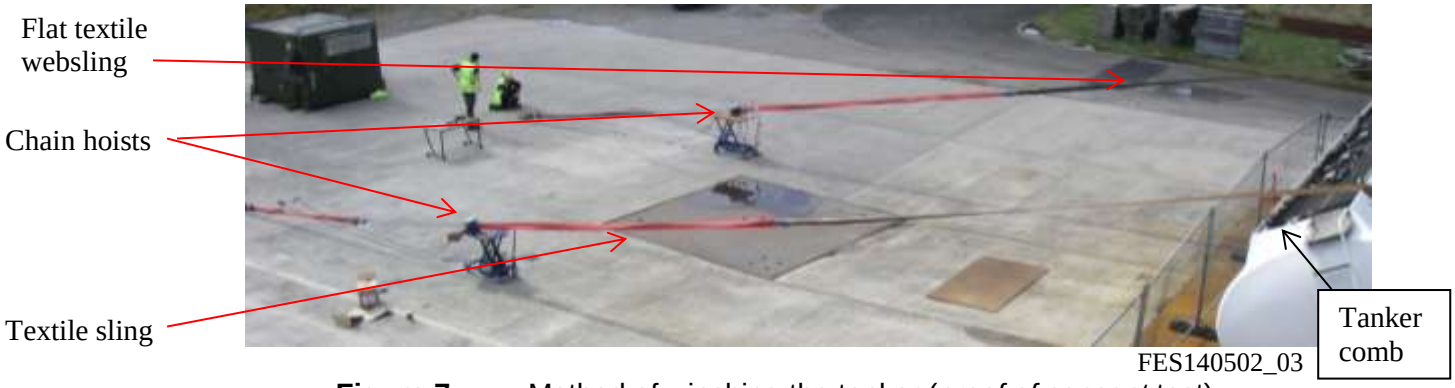

Figure 7 Method of winching the tanker (*proof of concept* test)

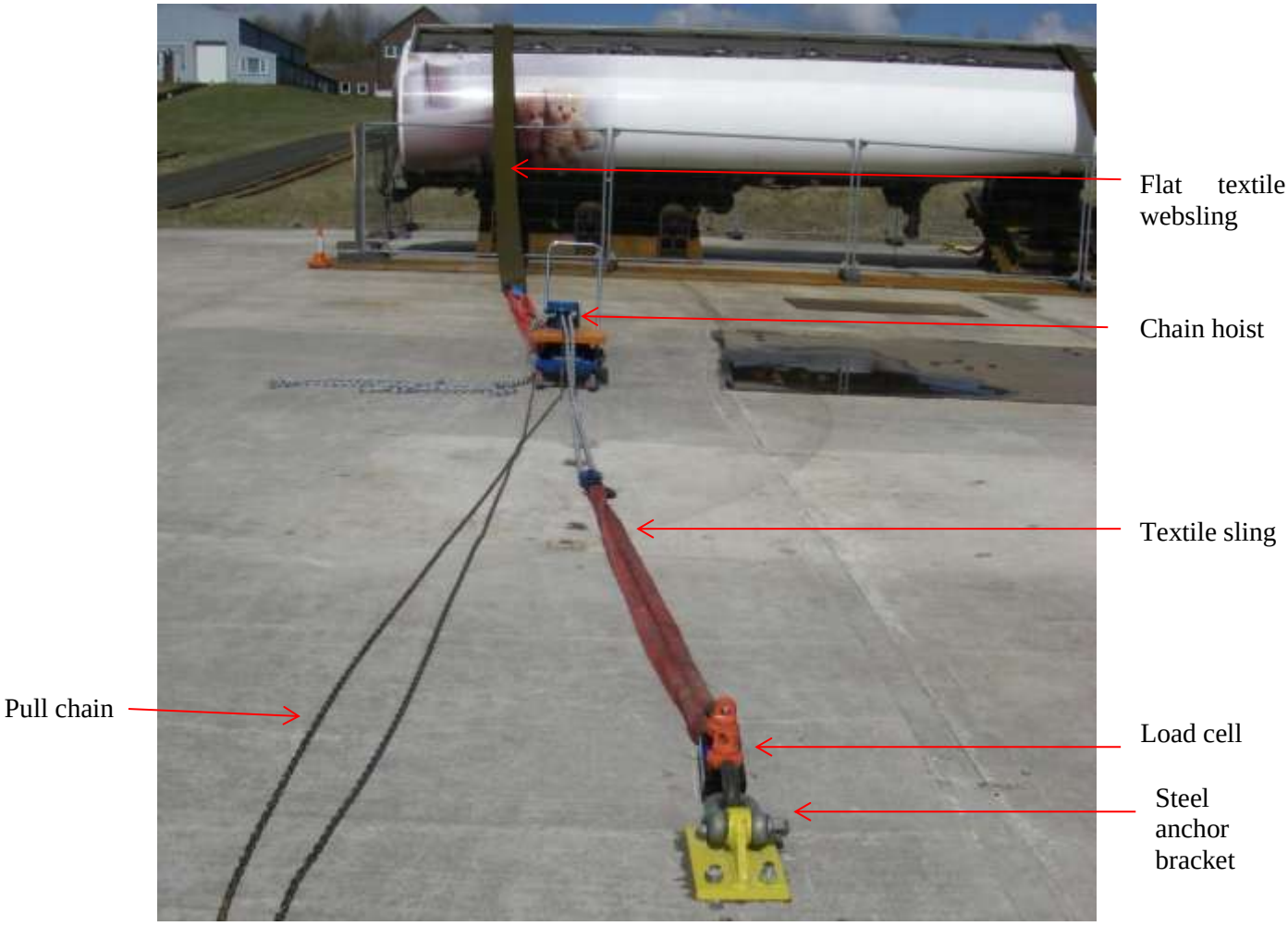

FES140502_04

Figure 8 Method of winching the tanker showing chain hoist used as a winch (*proof of concept* test)

5.6 TEST ASSURANCE

The *test officer* maintained a short track sheet to ensure the tests were carried out in a controlled manner, and instrumentation and video operators were prepared. The sheet was signed after each step had been carried out. Maximum load in the winch lines (800 kgf – 900 kgf on each line) was reached once the upper (near-side) wheels had lifted a short distance from the ramp. As the winches continued to rotate the tanker, the load required on the winch lines began to decrease. This is due to the horizontal distance between the tanker's centre of gravity and the pivot line reducing as the tanker begins to rotate. So the turning force (moment) required to continue to rotate the tanker reduces. At the point of instability, the winch lines went slack as the tanker toppled.

6 PRE TEST INTERNAL FILLET WELD SURVEYS ON GRW TANKERS J2580 AND J3910

Before the tests on the GRW tankers, HSL carried out fillet weld surveys inside the tanks.

6.1 GRW TANKER J2580

For this tanker, there was an initial general visual survey of the locations of the fillet welds, with fillet weld positions plotted on diagrams. After the topple test, to provide more exact fillet weld location information, detailed mapping was conducted following the approach used for J3910 (section 6.2). The more detailed maps are used in Figure 9 and Appendix 1. The fillet weld locations for both sections of compartment 1 are shown in Figure 9. The fillet weld locations for all of the bands are given in Appendix 1.

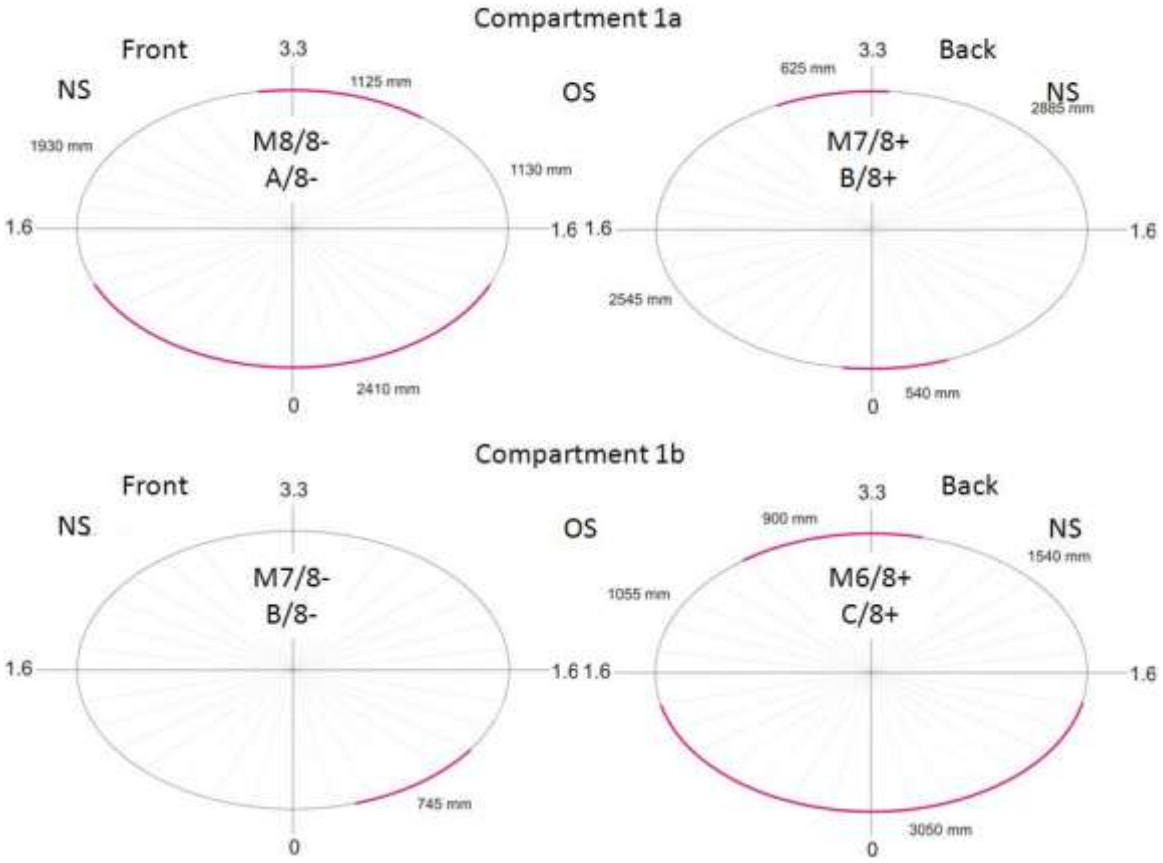

Figure 9 Fillet weld locations for compartment 1 of GRW tanker J2580

OS = offside
NS = nearside
band descriptions are given in Section 6.1 and Figure 10

The two maps on the left in Figure 9 were obtained by looking towards the front of the tanker from within the compartment; the two maps on the right were obtained by looking towards the rear.

Two band numbering systems are used in Figure 9. DfT's consortium numbered the bands A/y to H/y with band A at the front, Band H at the rear (for an 8-banded tanker) and y the number of

bands on the tanker. A contractor numbered the bands Mx where x = the band number, starting from 1 at the rear. For example, A/8 and M8 both refer to the front band on an eight-banded tanker. The suffix '+' refers to the fillet weld on the front side of the band and the suffix '-' refers to the fillet weld on the rear side of the band. For 8-banded GRW tankers such as J2580 and J3910 all divisions between compartments comprise bulkheads, except band B/8 in compartment C1 which is a baffle and, therefore, has an opening in the middle. The front and rear ends of the tanker are also classed as bulkheads. Figure 10 shows this band and compartment numbering.

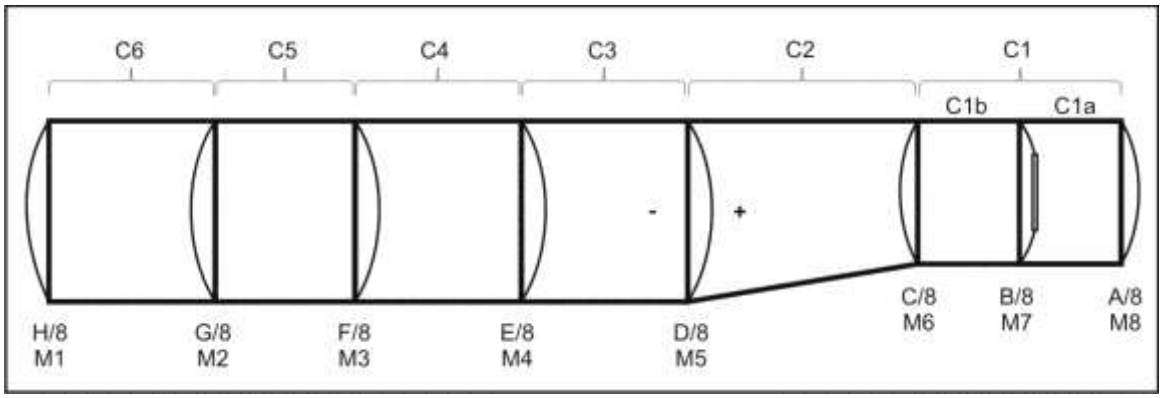

Figure 10 Band and compartment numbers - GRW tankers J2580 and J3910

6.2 GRW TANKER J3910

A detailed internal survey was carried out of the fillet welds in the compartments of GRW tanker J3910 prior to testing. All compartments except C1a were photographed. As compartment C1 is in two sections, with the baffle separating them, the manway only allows access to compartment C1b and the welds in compartment C1a were assessed visually through the hole in the baffle. For compartments C2 to C6, the circumference of the tanker was marked out in 0.2 m intervals before photographs were taken: an example photograph is shown in Figure 11.

A map of the location of the fillet welds was then produced from the photographs. An example of a fillet weld map is shown in Figure 12. The numbers shown in Figure 12 denote the distance in metres around the circumference from the bottom dead centre to the top. Fillet welds were observed at locations marked in magenta. The survey also involved checking the alignment of the main welds. Where no fillet weld was present, a 1 mm feeler gauge was offered to the gap between the nose of the extruded band and the tanker shell. Any areas where the feeler gauge could fit between the shell and the extrusion were marked in blue on the fillet weld maps (as in Figure 12). A cross section of the extrusion showing the position of the feeler gauge, the main circumferential welds, and the fillet weld is shown in Figure 13. The full set of filet weld maps is included in Appendix 1.

Figure 11 Example of a photograph inside compartment 4 showing location indications and fillet welds

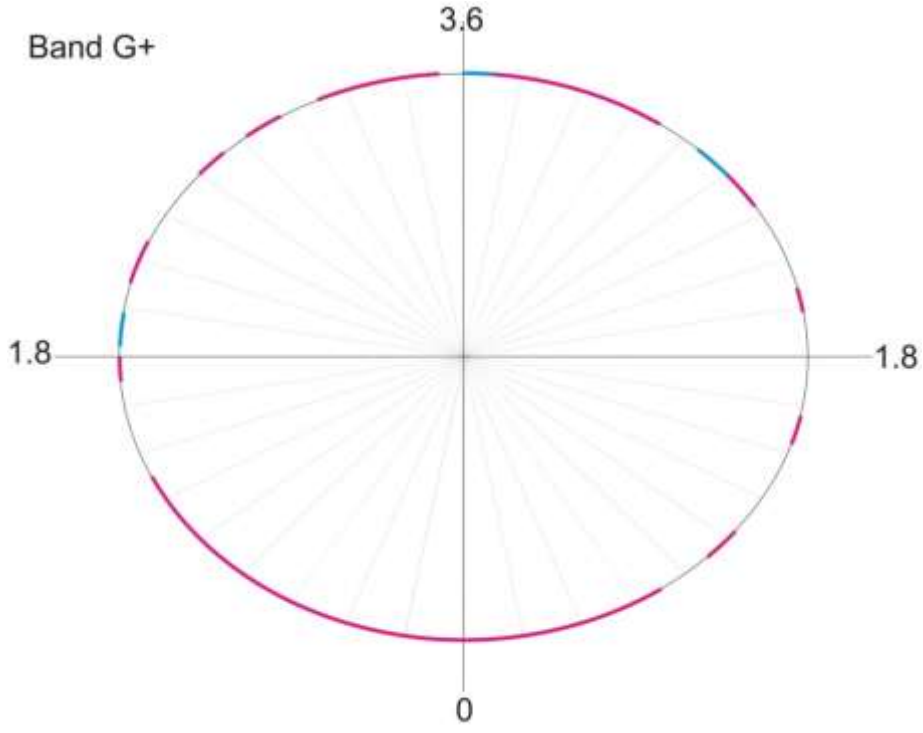

Figure 12 Example of a fillet weld map – GRW tanker J3910

fillet welds- magenta
misalignment - blue

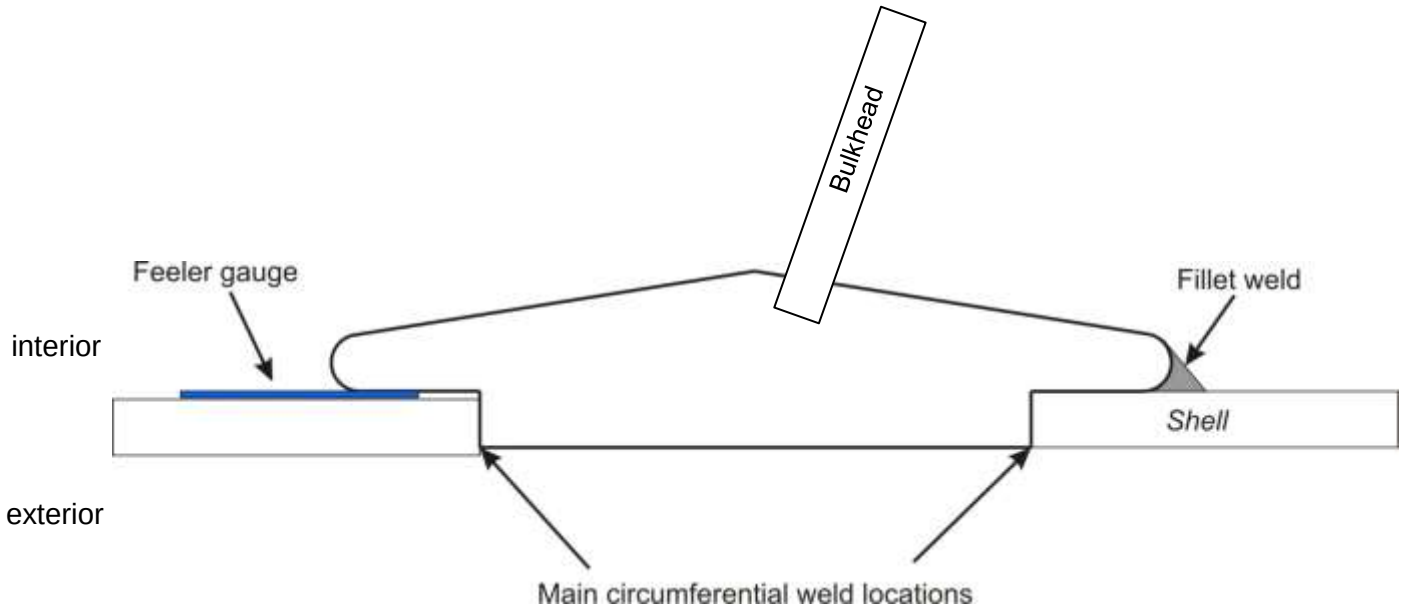

Figure 13 Cross section of the extrusion and misalignment assessment

GRW drawings supplied to HSL indicated fillet welds on the bottom half (between the 3 o'clock and 9 o'clock positions) on bands C/8, D/8 and E/8. It is not clear from the drawings if the fillet welds should be present on both sides of these bands (for example, on C+ and C-), or on one side only (for example, only C+).

One notable difference between the application of fillet welds on GRW tankers J2580 and J3910 was that, on the latter, where a long length of fillet weld is not present, a series of short weld sections was apparent. This 'stitching' took the form of fillet weld sections approximately 70 mm in length with 140 mm gaps (Figure 11). The location of the fillet welds relative to the strain gauge positions on the two tankers is shown in Table 5.

Table 5 Location of fillet welds relative to strain gauge locations

Band	J2580	J3910	Notes
B-	No gauges installed	Gauges 1 & 2 between fillets	See Figure 14
C+	Gauges 5 & 6 adjacent	Gauges 5 & 6 adjacent	Gauge 5 did not measure correctly during J3910 test
E-	No gauges installed	Gauges 7 & 8 adjacent	Gauges 7 and 8 did not measure correctly during J3910 test
F+	Gauges 11 & 12 adjacent	Gauges 11 & 12 adjacent	

Figure 14 shows a strain gauge location with respect to fillet welds for GRW tanker J3910, band B.

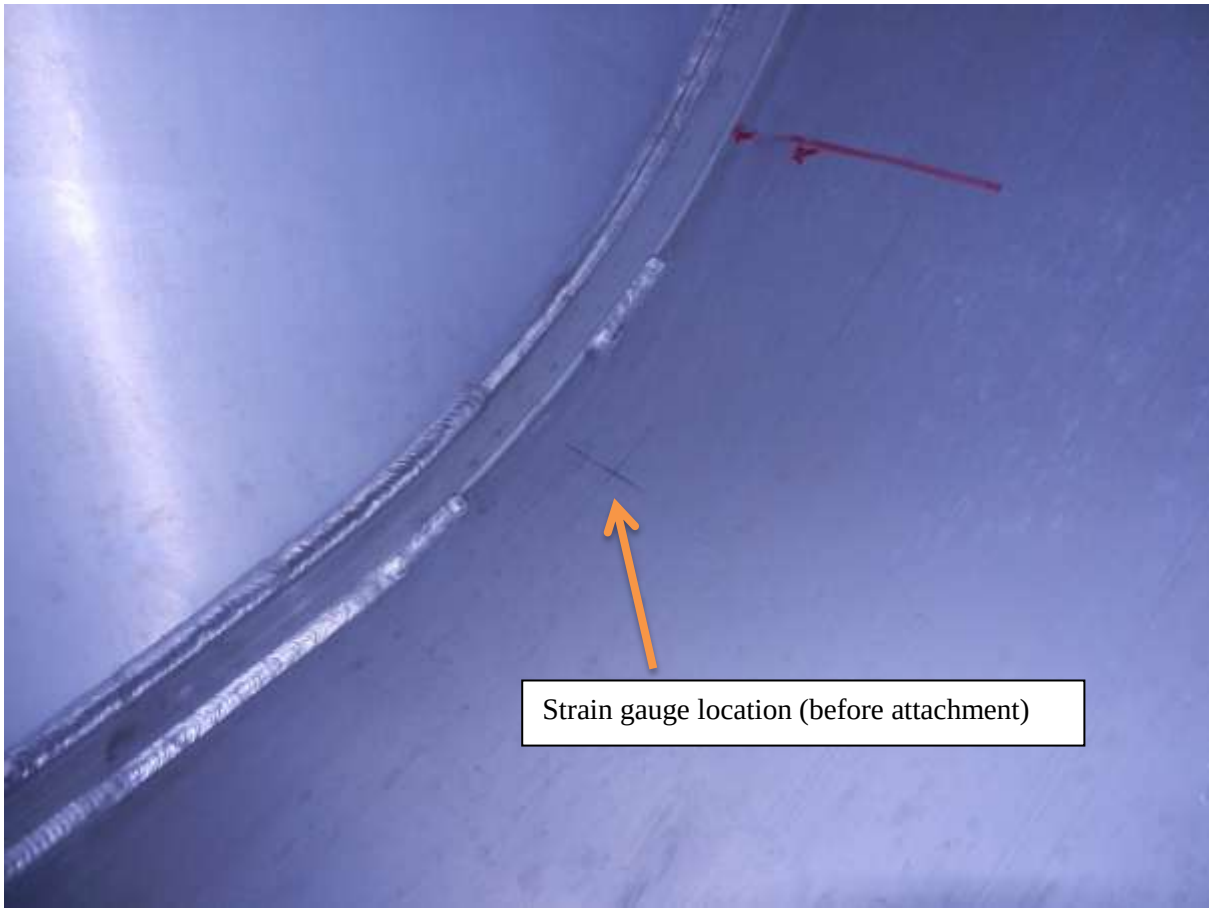

Figure 14 Strain gauge location near to welds (GRW tanker J3910, Band B)

7 TANKER FILLING – WEIGHT CONTROL

7.1 PROOF OF CONCEPT TEST

For the *proof of concept* test, HSL aimed to fill the tanker to its rated volumetric capacity (95% full)[vii]. However, as filling was carried out with the tanker at an angle on the ramp, water started to overflow through the vapour recovery system before this was achieved: the maximum fill was close to 90.5% of maximum volume. The tanker was filled from a fire hydrant and the water flow into each compartment was measured using a calibrated water meter. The volume of water in each compartment is given in Table 6; the number in brackets shows the order of filling the compartments.

Table 6 *Proof of concept* tanker – filling volumes (litres)[viii]

	C1 (front)	**C2**	**C3**	**C4**	**C5**	**C6**	**C7**	**C8 (rear)**	**TOTAL**
Maximum Capacity	5 248	5 262	5 226	5 225	5 217	5 246	5 341	5 218	41 983
Volume of water	4 720 (3)	4 730 (8)	4 740 (4)	4 765 (6)	4 740 (7)	4 750 (2)	4 795 (5)	4 750 (1)	37 990

Maximum capacity taken from the tanker chassis plate, 0% ullage

C1, C2… – compartment 1, compartment 2…

7.2 GRW TANKER J2580

For the GRW tankers, DfT and its consortium agreed to fill the tankers to maximum mass, *not* volume. The identification plate on the chassis stated that the maximum gross weight was 37 000 kg, and the unladen mass was 5 620 kg; this gave a petroleum mass of 37 000 – 5 620 = 31 380 kg. To achieve this mass with water, each compartment needed to be filled to 70.3% of maximum capacity (i.e. 31 376 litres as in Table 7 below).

As for the *proof of concept* test, the tanker was filled from a fire hydrant, and the water flow into each compartment was measured using the same calibrated water meter. The volume of water in each compartment is shown in Table 7; the number in brackets shows the order of filling the compartments.

[vii] *As water is denser than fuel, this means the tanker would be over its maximum rated mass*

[viii] *Comp 8 : 5 000, but it overflowed via the vapour recovery, estimated loss - 250*
Comp 6 : 4 750, filled until water came out of the vapour recovery, estimate minimal loss
Comp 1 : 4 720, filled until water came out of the vapour recovery, estimate minimal loss
Comp 3 : 4 740, filled until water came out of the vapour recovery, estimate minimal loss
Comp 7 : 5 045, but it overflowed via the vapour recovery, estimated loss - 250
Comp 4 : 4 765, filled until water came out of the vapour recovery, estimate minimal loss
Comp 5 : 4 740, filled until water came out of the vapour recovery, estimate minimal loss
Comp 2 : 4 730, filled until water came out of the vapour recovery, estimate minimal loss

Table 7 GRW tanker J2580 – filling volumes (litres)

	C1 (front)	**C2**	**C3**	**C4**	**C5**	**C6 (rear)**	**TOTAL**
Maximum Capacity	8 300	7 470	7 490	7 490	6 370	7 490	44 610
Water Volume	5 838 (2)	5 254 (4)	5 268 (6)	5 268 (5)	4 480 (3)	5 268 (1)	31 376

Maximum capacity taken from the tanker chassis plate, 0% ullage

7.3 GRW TANKER J3910

This tanker was similar in mass and volume to GRW J2580 with the same information on the chassis plate giving the same maximum petroleum mass of 31 380 kg and the same water fill of 70.3% of maximum capacity. Again the tanker was filled from a fire hydrant, and the water flow into each compartment was measured using the same calibrated water meter. The volume of water in each compartment is shown in Table 8; the number in brackets shows the order of filling the compartments.

Table 8 GRW tanker J3910 – filling volumes (litres)

	C1 (front)	**C2**	**C 3**	**C4**	**C5**	**C6** (rear)	**TOTAL**
Maximum Capacity	8 300	7 470	7 490	7 490	6 370	7 490	44 610
Water Volume	5 838 (3)	5 254 (5)	5 268 (1)	5 268 (6)	4 480 (4)	5 268 (2)	31 376

Maximum capacity taken from the tanker chassis plate, 0% ullage

8 INSTRUMENTATION AND VIDEO

8.1 DATA LOGGING EQUIPMENT

The aim of the *proof of concept* test was to ensure the lifting and winching methods were effective, and to obtain some basic data by testing the logging system. One tri-axial accelerometer was used, and the data logger (Graphtec GL-7000) was set to record unfiltered transducer data at 50 000 samples per second (50 ks/s — i.e. one recording every 0.02 millisecond). The logger was triggered manually before the tanker started to topple, and a synchronisation pulse was provided by the high speed video operator.

The test on the GRW J2580 tanker was the first to use the full data acquisition system (accelerometers, pressure transducers, strain gauges) to obtain measurements for comparison with the finite element model. Measurements were made in two compartments (C1b and C4). Two, independent Graphtec GL-7000 loggers, powered through a UPS (uninterruptable power supply), were used. The loggers were set to acquire data at a rate of 50 ks/s (the same as the *proof of concept* test). Each logger was specific to one compartment in the tanker, with the rear accelerometer on the same logger as C4 and the front accelerometer on the same logger as C1b.

The compartments were fitted with pressure transducers and strain gauges on the interior side with additional strain gauges attached to the exterior side at the equivalent position to the strain gauges on the interior (strain gauge pairs). This allowed both bending and membrane stresses to be obtained[ix]. All strain gauges and pressure transducers were located on the impact side (offside) of the tanker.

Cables from the gauges and transducers on the interior side in a compartment were passed through a set of cable glands mounted on a specially designed baffle that was attached to the manway cover on top of the tanker, where the tanker level probe is normally fitted.

The data was stored on the loggers as binary .GBD files. These were converted and exported to comma separated values (.csv) files. Further analysis was done by importing these files into data analysis software packages.

8.1.1 Strain Gauges

The gauges used were Vishay CEA-06-250UT-350 and CEA-06-250UW-350 for GRW J2580, and CEA-13-250UT-350 and CEA-13-250UW-350 for GRW J3910. As variations in the surface temperature of the tanker were insignificant during the tests, no temperature compensation was used. The gauge pairs were installed as follows:

<u>GRW J2580 compartments 1b and 4 (Figure 15)</u>

- two pairs near the rear bulkhead weld (band C/8 & F/8)— measuring longitudinal strain;
- two pairs near the midpoint of the compartment — measuring longitudinal; strain

[ix] *When the radius of curvature of a shell is large (greater than a factor of ten) in relation to the thickness of the shell, as it is with the tankers, the shell is often referred to as a membrane. If it is exposed to internal pressure alone, as in a pressure vessel, then the stress in the membrane can be considered to be uniform across the thickness. All the stress is parallel to the membrane wall, and bending stress is insignificant. Although the tanker shell is a membrane in the sense that the radius of curvature of the tanker shell is much greater than ten times the wall thickness, because it is being exposed to an impact event rather than a uniform (or uniformly varying) pressure that it would experience during service, the stresses across the wall thickness are not uniform. However the* ***average*** *membrane strain, and the* ***average*** *bending strain, can be obtained from the strain gauge pairs.*

- two pairs near the midpoint of the compartment — measuring hoop strain.

GRW J3910 compartments 1b and 4 (Figure 16)

- two pairs near the rear bulkhead weld (band F/8 & C/8) — measuring longitudinal strain;
- two pairs near the midpoint of the compartment — one measuring longitudinal strain, one measuring hoop strain;
- two pairs near the front bulkhead weld — measuring longitudinal strain.

All gauges were connected, as quarter-bridge, to bridge completion modules on the logger with a three-wire compensation configuration. Gauges were calibrated with shunt resistors at a local junction box before the test. In total there were twenty four (24) strain gauges on each tanker. Table 9 shows the strain gauge numbering system for GRW J2580. Figure 15 shows the strain gauge locations on GRW J2580.

Table 9 Strain gauge numbering system – GRW tanker J2580

compartment 1b	**compartment 4**
1a to 6a – outer skin	7a to 12a – outer skin
1b to 6b – inner skin	7b to 12b – inner skin
hoop (circumferential) strain gauges – 1a and 1b, and 2a and 2b	hoop (circumferential) strain gauges – 7a and 7b, and 8a and 8b
longitudinal strain gauges – 3a and 3b to 6a and 6b	longitudinal strain gauges – 9a and 9b to 12a and 12b

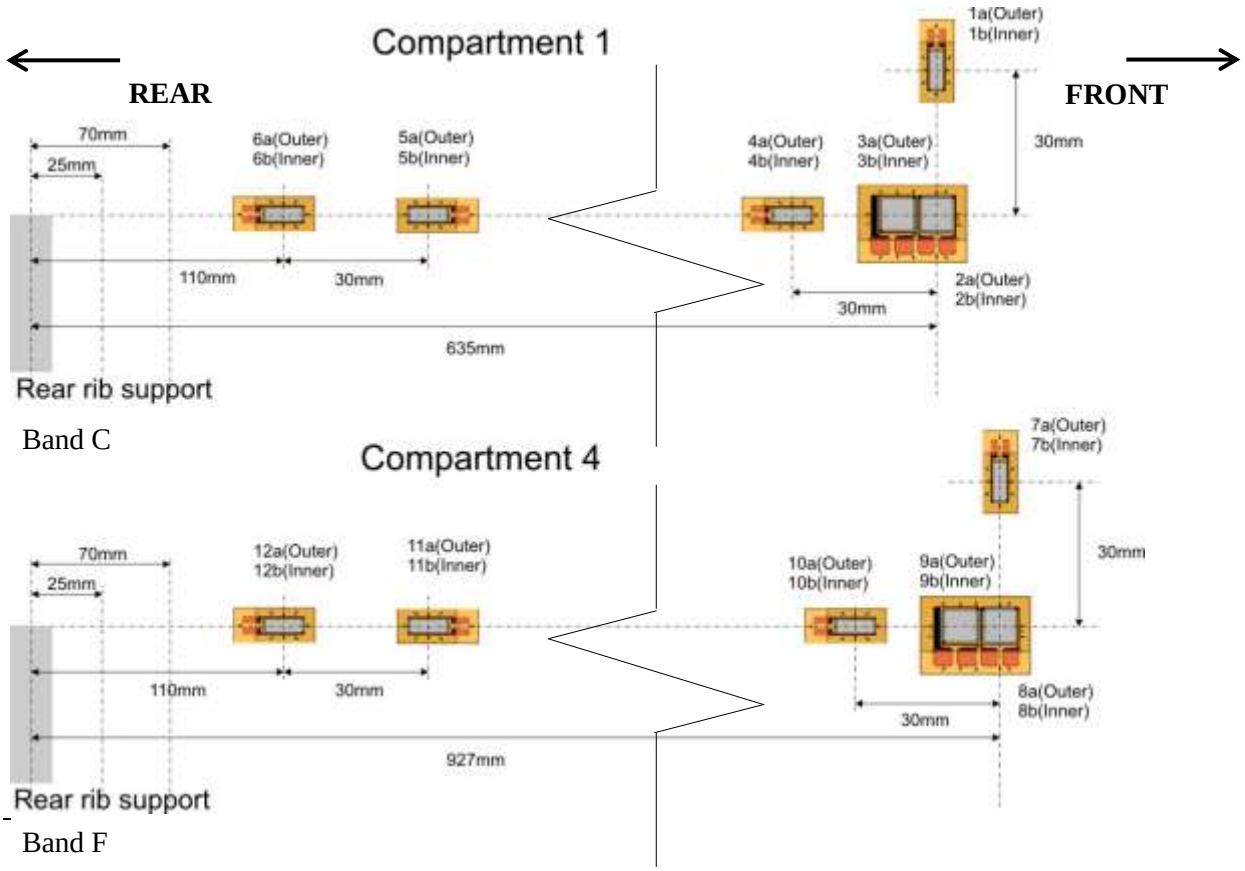

Figure 15 Strain gauge locations (not to scale) GRW tanker J2580

All gauges were installed on the impact side. The longitudinal line passing through the centre of all gauges (except gauges 1a and 1b, and 7a and 7b) was level with the top of the tank supports (i.e. the saddle): this is the 8 o' clock position shown in Figures 19 and 20 (29^{o} below the horizontal centreline of the tanker).

The centre-line of the bulkhead at the rear of each compartment was in the same position as the rear rib support.

Table 10 shows the strain gauge numbering system for GRW tanker J3910.

Table 10 Strain gauge numbering system – GRW tanker J3910

compartment 1	**compartment 4**
1a to 6a – outer skin	7a to 12a – outer skin
1b to 6b – inner skin	7b to 12b – inner skin
hoop (circumferential) strain gauges – 3a and 3b	hoop (circumferential) strain gauges – 9a and 9b
longitudinal strain gauges – 1a and 1b, 2a and 2b, 4a and 4b, 5a and 5b, 6a and 6b	longitudinal strain gauges – 7a and 7b, 8a and 8b, 10a and 10b, 11a and 11b, 12a and 12b

Figure 16 shows the strain gauge locations on GRW J3910.

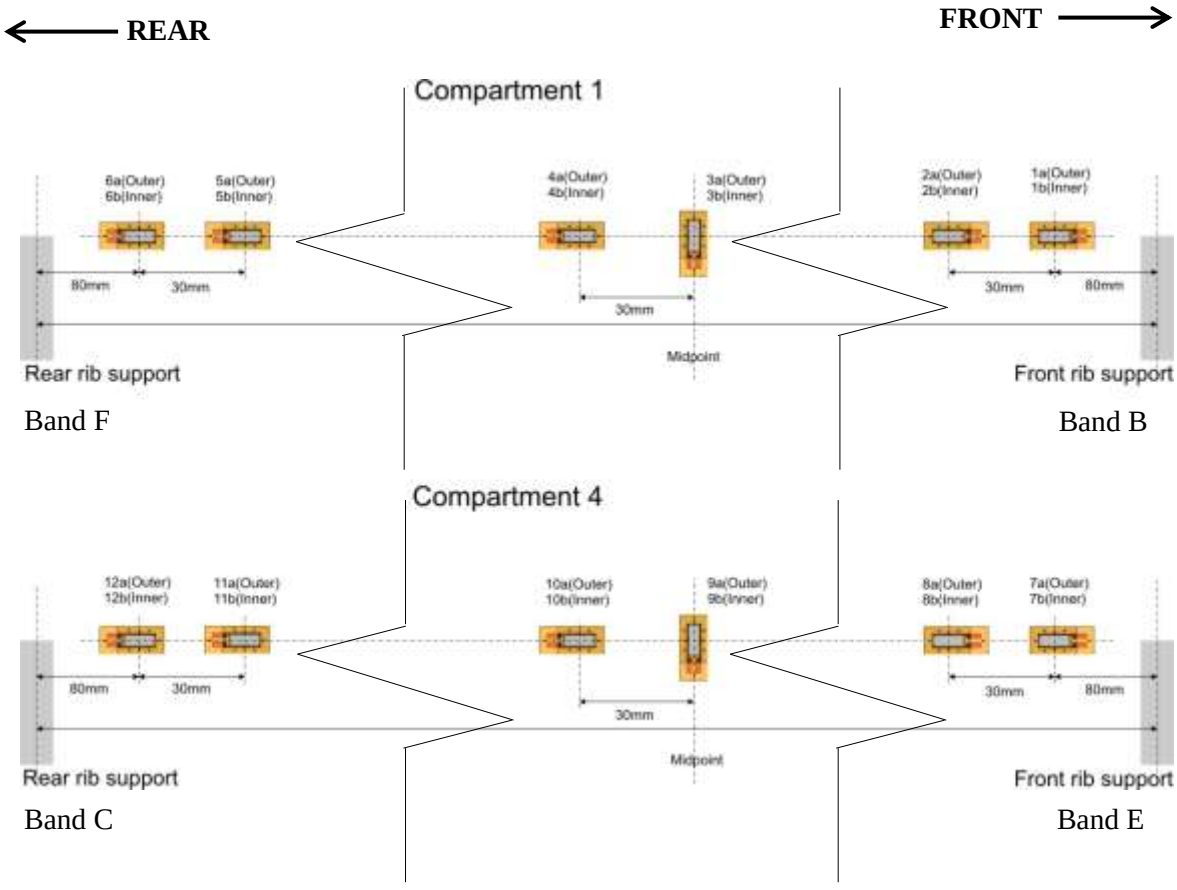

Figure 16 Strain gauge locations (not to scale) GRW tanker J3910

All gauges were installed along the same longitudinal line as for J2580.

Figure 17 shows a typical variation in strain that may occur across the thickness of the tanker shell during the test.

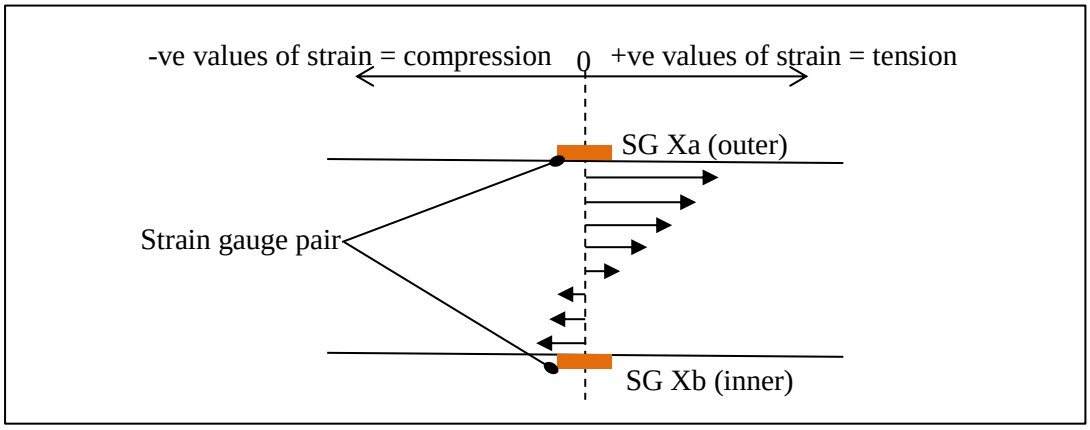

SG = strain gauge

Figure 17 Strain across the thickness of the tanker shell

For *membrane strain* the time-varying strains measured in each pair are added, then divided by two to obtain the *average membrane strain*

$$\frac{Xa_{(t)}+Xb_{(t)}}{2} \qquad (1)$$

Where

$Xa_{(t)}$ is the time varying strain measured by the *outer* strain gauge X

$Xb_{(t)}$ is the time varying strain measured by the *inner* strain gauge X

This is the average strain parallel to the tanker shell.

For *bending strain*, the time-varying strain values of each pair are subtracted, then divided by two, which gives the *average bending strain*

$$\frac{Xa_{(t)}-Xb_{(t)}}{2} \qquad (2)$$

If the membrane strain is positive, then the average state at the measuring point is in tension; if the membrane strain is negative, then the average state at the measuring point is in compression.

If the bending strain is positive, then the tanker shell is flexing outwards (hogging); if the bending strain is negative, then the tanker shell is flexing inwards (sagging).

The example in Figure 17 shows the tanker shell mainly in bending, but with an average tensile loading. Therefore, the *average bending strain* will be greater than the *average membrane strain* as the inner surface of the shell has gone into compression. As the analysis accounts for the direction as well as magnitude of the strain, the difference between the two measured values will be greater than the sum of the two values so equation (2) will give a greater value than equation (1).

8.1.2 Pressure transducers

Fourteen pressure transducers, seven in each compartment, were placed at approximately 6, 7, 8, 9, 10, 11, 12 o'clock positions on the impact side; the transducers were positioned at the mid-point between the front and rear bulkheads in each compartment. The type of transducer used was a 34.5 bar (with 138 bar over-range) Omega PX709GW-500SGV. The pressure transducers are the sealed-gauge type, which means the readings are relative to a 1 bar internal reference. Each was supported by two cable conduit connectors that were glued to the inside surface of the tanker using waterproof epoxy glue. All pressure transducers were installed with their longitudinal axes horizontal. The outputs were connected to transducer input modules on the Graphtec data loggers. Figure 18 shows a pressure transducer in position (the tape was removed after the glue had set).

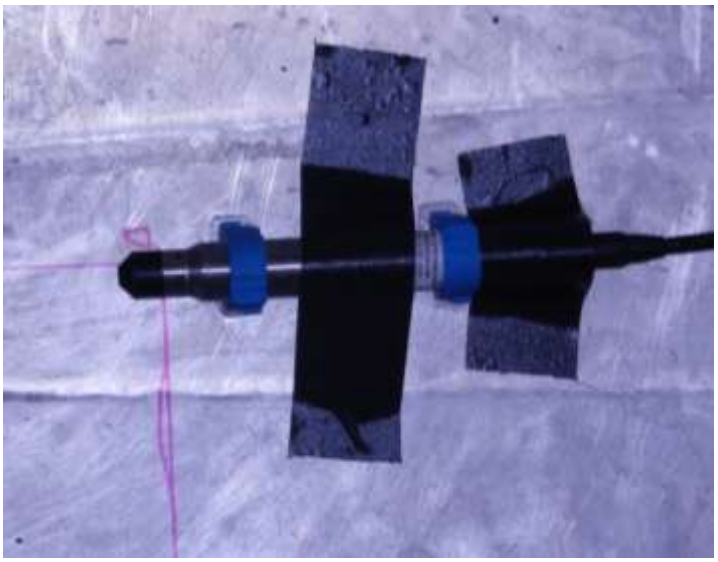

FES 140601_02

Figure 18 Pressure transducer fitted to the inside of a GRW tanker

The pressure transducers were installed in identical positions for both GRW tankers.

Figures 19 and 20 show the positions of the pressure transducers in compartments 1 and 4, respectively.

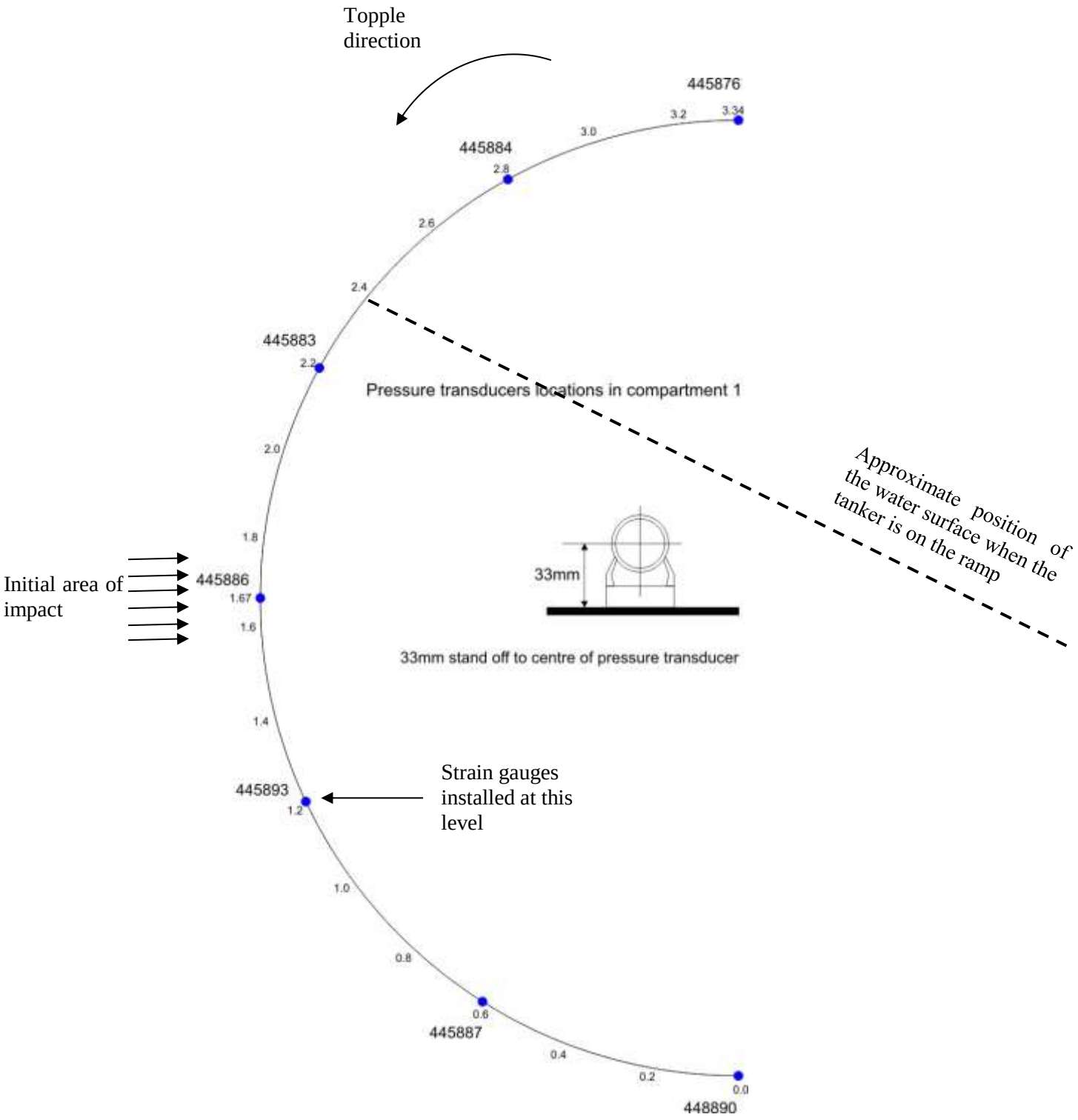

- Position of the pressure transducers

Numbers on the circumference are distances in metres around the tanker surface from 'bottom dead centre' (BDC)

Pressure transducer numbers are 44----

Figure 19 Pressure transducer locations (tanker in the upright position) – compartment 1 (GRW J2580 and J3910 – offside, viewed from the front)

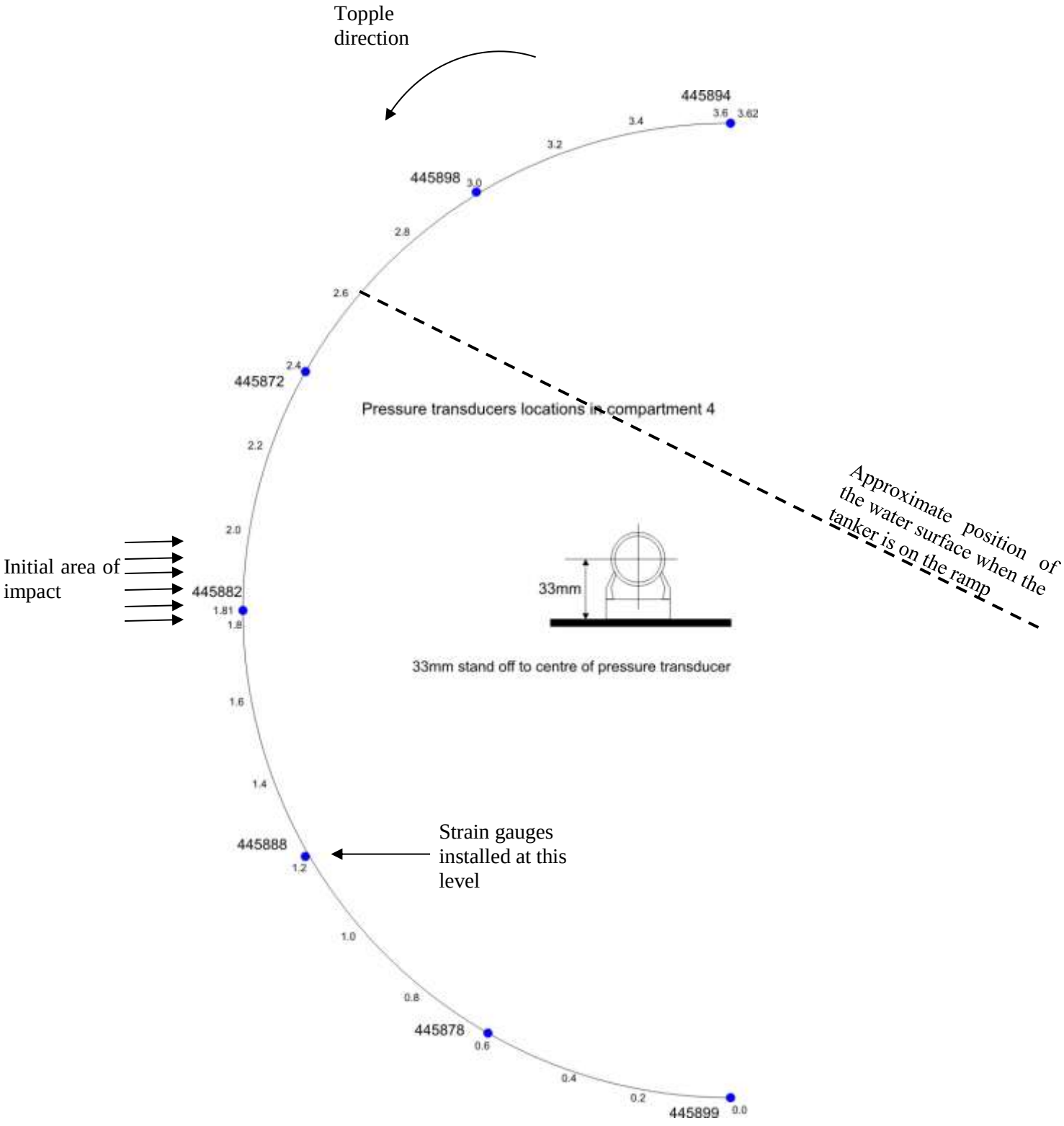

Figure 20 Pressure transducer locations (tanker in the upright position) – compartment 4 (GRW J2580 and J3910 – offside, viewed from the front)

In Figures 19 and 20, a dotted line has been added to show the approximate position of the water surface when the tanker is resting on the 27° ramps (i.e. tilted over to the left in this figure so the line is horizontal). When placed on the ramp, the depth between the water surface and the lower-most transducers (445888, 445878 and 445899 in Figure 20) is about 1.2 m; so the static pressure acting on these gauges above atmospheric pressure, and prior to winching, will be

Static pressure $= \rho g h$ N/m^2

Where ρ = density of water = 1 000 kg/m^3
g = acceleration due to gravity = 9.81 m/s^2
h = head of water = 1.2m (approx.)

So static pressure = 1 000 x 9.81 x 1.2 = 11 772 N/m^2 which is approximately 12 000 N/m^2
or in bar
Static pressure = 12 000 x 10^{-5} bar = 0.12 bar (1.74 psi)

As the tanker is toppling, the head of water will increase on the transducers fitted at higher positions on the tanker body as they become submerged. Also the head of water above the transducers at the greatest depth prior to toppling will also change slightly. This will cause small increases and decreases in static pressure (depending in the gauge location) as the tanker starts to rotate. *However*, in addition to these effects, as the tanker rotates, the water and the pressure transducers are moving together. As the tanker starts to topple, the water will exert less and less pressure on the transducers until, at the point of free fall, the water exerts no additional pressure on the transducers. So at the moment before the tanker impacts, the transducers can be assumed to be measuring atmospheric pressure alone (i.e. zero-gauge pressure). This is shown in Figure 28 (Section 9.2.4).

8.1.3 Accelerometers

For the *proof of concept* test, one tri-axial accelerometer block was located at the centre point of the front bulkhead of the tanker; the block comprised of

- +/- 25g in the x-axis (horizontal axis at impact),
- +/- 25g in the y-axis (vertical axis at impact),
- +/- 25g in the z-axis (longitudinal axis).

For subsequent tests, two tri-axial accelerometer blocks were located at the centre of the front *and* rear bulkheads of the tanker. Measurements in the z-axis were not made as the measurement on the *proof of concept* test was dominated by free vibration (ringing), and very little information directly related to the impact event itself could be deduced.

On GRW J2580, the accelerometers at the front and rear were arranged as follows (front and rear of the tanker):

- One +/- 20g in the x-axis (horizontal axis at impact); and
- One +/- 50g and one +/- 20g in the y-axis (vertical axis at impact).

On GRW J3910, the accelerometers at the front and rear were arranged as follows:

- One +/- 50g in the y-axis (vertical axis at impact).

The accelerometer types were *Measurement Specialities* 4000A-020-060 and 4000A-050-060, connected to transducer input modules on the Graphtec loggers.

8.1.4 Measurement Grids

Grids comprising a 5 by 5 array of circles (inside diameter 19 mm, outside diameter 25 mm, centre-to-centre 28 mm) were added above the likely impact zone either side of the welds which enclose bulkheads C1b and C4. These grids were intended to provide indication of the deformation close to the welds in the compartments with strain gauges.

8.1.5 Summary of the Locations of all the Instrumentation

Figure 21 shows the approximate positions of all the pressure transducers, accelerometers, strain gauges and measurement grids.

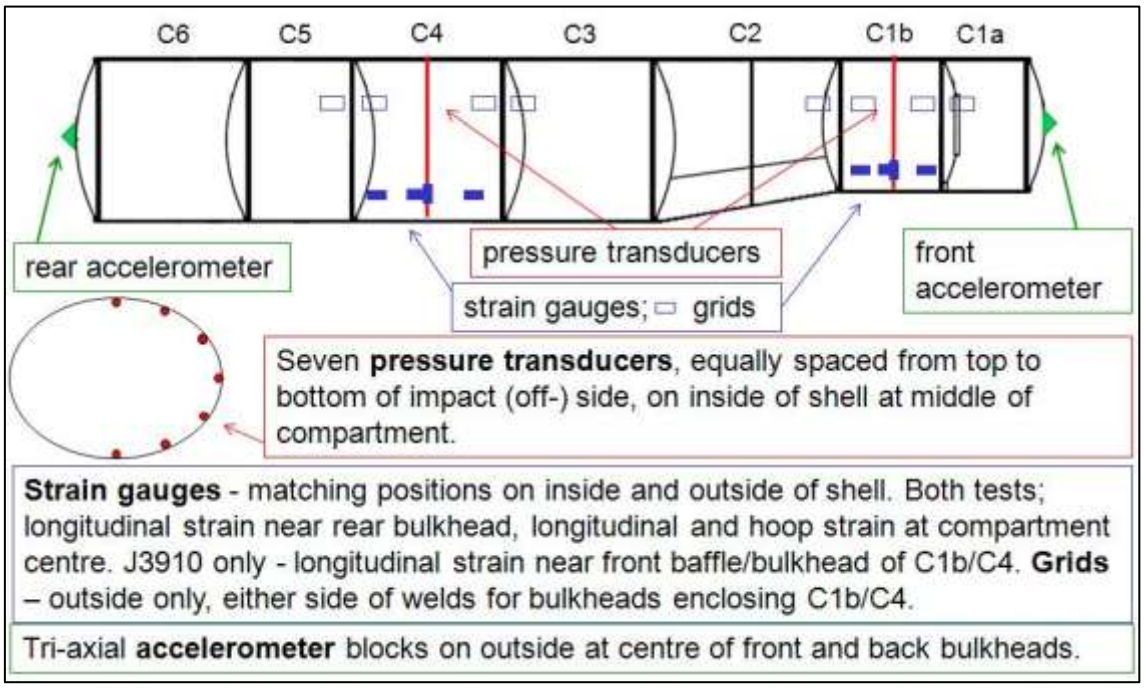

Figure 21 Location of instrumentation on the GRW tankers

8.2 VIDEO METHODS

For the *proof of concept test*, nine video cameras, ranging from standard speed (25 frames per second) to high speed (1 000 frames per second) were used to record the test.
For the GRW tankers, thirteen video cameras ranging from standard speed (25 frames per second) to high speed (1 000 frames per second) were used to record the tests, together with time lapse and stills cameras.

The high speed video images were analysed to obtain the impact velocity and deceleration during impact at the front and rear of the tanker. Targets were placed at each end of the tanker that could be seen on the high speed video. The distance between each target was known; this provided a calibration scale for the high speed video images. The movement of these targets was followed through each consecutive frame of the high speed video. The distance travelled by the targets was divided by the time taken: this gave the linear velocity.

The rotational velocity was then calculated from this using the equation

$$\omega = \frac{v}{r} \text{ rads/sec} \qquad (3)$$

where

v is the impact velocity obtained from the high speed video (m/s)
r is the distance from the pivot point to the target (m)

A frame from the high speed video, showing the targets at the front end of the tanker, is shown in Figure 22.

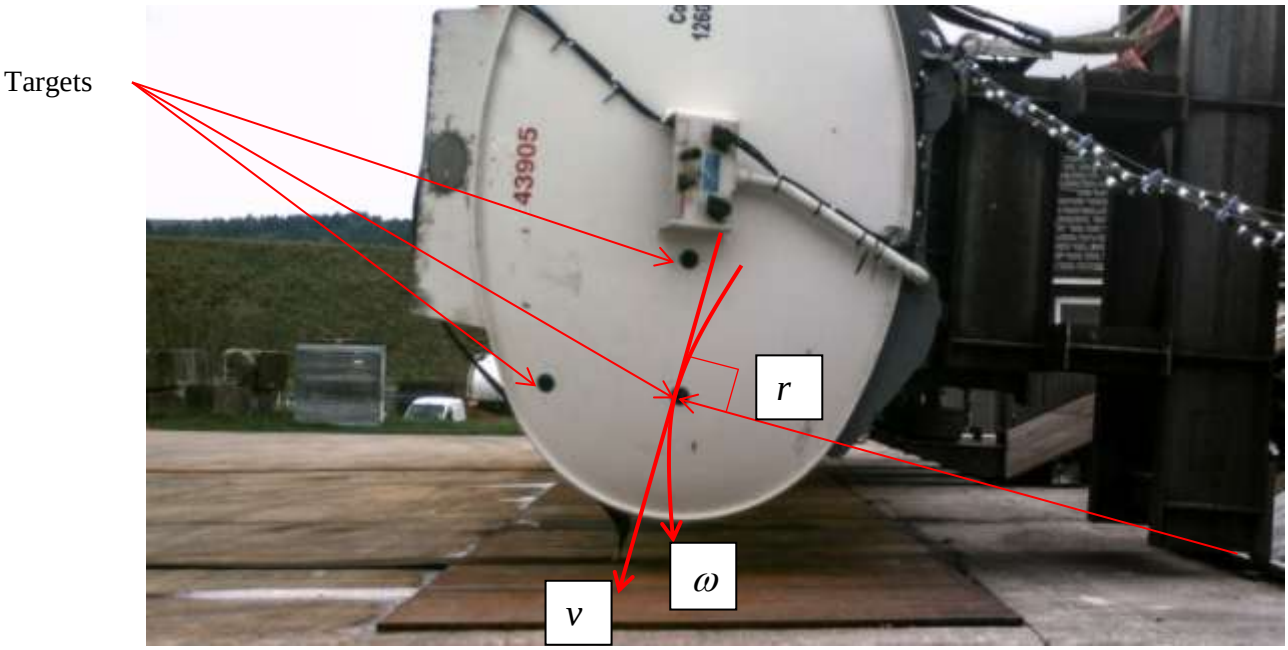

Figure 22 Frame from the high speed video during the topple test on GRW J2580 – showing the targets used to obtain the impact velocity

8.3 LASER SCANNING OF THE TANKER AND WELDS

8.3.1 Laser scanning the tankers

For accurate information on the deformation of the tanker due to the testing (which was to be compared with the numerical model) all tankers were laser scanned at the following times:

- On arrival at HSL.
- After being lifted onto the ramps
- After the topple test (lying on its side)
- After being lifted back onto its wheels

The laser scanner was a Leica Scanstation C10, serial number 1260769. It was last serviced on 18/11/2013, which included a calibration. Its user manual states:

Accuracy of single measurement
Position:* 6 mm
Distance:* 4 mm
Angle (horizontal/vertical): 60 μrad / 60 μrad (12” / 12”)

Modelled surface
precision/noise:** 2 mm
Target acquisition* 2 mm std. deviation
Dual-axis compensator Selectable on/off, resolution 1", dynamic range +/- 5', accuracy 1.5"

* At 1 m – 50 m range, one sigma
** Subject to modelling methodology for modelled surface

The laser scanner works on the 'time of flight' of a pulsed laser. The laser turns on and off 50 000 times a second, the time for each pulse to be reflected back to the scanner is used to calculate the distance to the surface which the pulse has reflected off.

8.3.2 Laser scanning the welds caps for GRW tanker J3910

A contractor surveyed the circumferential weld cap dimensions for tanker GRW J3910 with a higher resolution laser scanner. The circumferential weld locations on the extrusion are shown in Figure 23. The weld cap data consists of cap height, cap width, cap spacing and misalignment measurements taken in circumferential strips from both sides of each band on the tanker (like a set of ribs) as illustrated in Figure 23. All circumferential weld caps were surveyed and the data has been passed to TWI for analysis in WP2. The measurements are given in Appendix 2 for information.

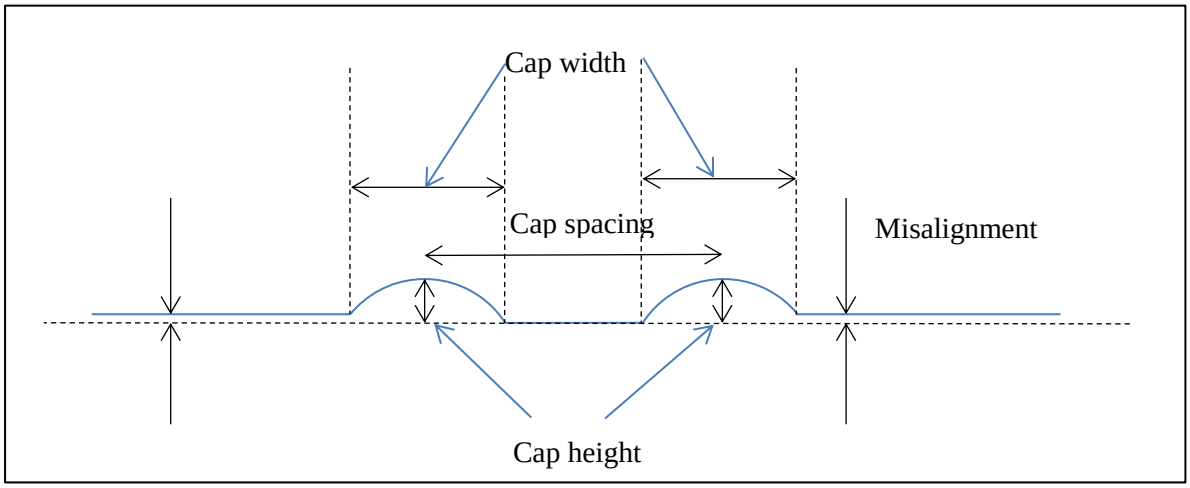

Figure 23 Profile of the circumferential weld caps

8.4 GRW J3910 AND J2580 - LASER SCANS OF THE DAMAGE PROFILE

After the GRW tankers were lifted upright following the test, parameters describing the deform profile along the length of the tanker was calculated using the laser scan data and used to validate HSL's FE model (HSL report ES/14/39/06). Some measurements are included in the damage assessment in Section 9.6 of this report.

9 RESULTS AND DISCUSSION

All raw data was analysed to calibrate the transducer outputs, for example voltages, into scientific units.

9.1 PROOF OF CONCEPT TEST

9.1.1 Instrumentation

The measurements from the accelerometers were recorded successfully; the peak values are shown in Table 11. Measurements above the accelerometer's dynamic range (i.e. above 25 g) are unreliable. The value in the z-axis had overloaded (i.e. the +ve and –ve peaks of the signal were cropped). By assessing the signal, it was likely the peak value was above 100g.

Table 11 Measured acceleration (unfiltered values) – *proof of concept* test

Axis	Peak acceleration (g)
x (horizontal axis at impact)	22
y (vertical axis at impact)	33
z (longitudinal axis)	74

After the data was obtained, it was processed in two ways:

- the time history was filtered using a 25 Hz low pass filter; and
- the data was averaged using a 1 000-point moving average[x] to smooth out the impulses.

When the y-axis acceleration was filtered at 25 Hz, most of the negative components disappeared leaving a 10 millisecond (ms) pulse at 11 g. The results for the 1 000-point moving average also gave a similar result (a 12 ms pulse at 12 g). The z-axis measurement shows a lot of high frequency components due to vibration (ringing) in the tanker body after impact. As the tanker response was causing the measurement system to overload, the ability to analyse the data was limited.

The z-axis acceleration contributed little value to the validation exercise; so the loss of data on this axis was not significant, and HSL chose not to measure on this axis in subsequent tests. To try and reduce the high frequency response causing an over-load on the other two axes, a thin resilient strip was placed between the accelerometer and tanker for measurements on the GRW tankers.

9.1.2 Impact behaviour

The overall impact duration was a few seconds for all the tests, with most deformation occurring in the first 100 ms. Analysing the high speed video, the *proof of concept* tanker was found to have

[x] *A 1 000-point moving average means that 1 000 adjacent sample points are averaged together, a step forward of one data point is then made, and a new 1 000-point average is calculated. This process is then repeated at one sample step at a time until the whole data set has gone through this averaging (smoothing) process. In other data analyses, 799- and 19-point moving averages were made. This is the same method as for the 1 000-point moving average (i.e. take an average, move one data point forward then take another average), but a different number of data points are averaged together each time. This is a standard technique commonly used with time series data to smooth out short-term fluctuations and highlight longer-term trends or cycles.*

impacted reasonably uniformly along its length, with front and rear hitting the ground within a few milliseconds of each other. The impact speed at the rear of the tanker was 4.25 m/s.

After first impact, the proof of concept tanker continued to roll forward, away from the ramps, until at 130 to 140 degrees the comb along the top of the tanker hit the ground, after which the tanker rolled back before coming to rest on its side (at 0 degrees).

9.2 GRW TANKER J2580

9.2.1 Impact behaviour

The overall impact duration was a few seconds for all the tests, with most deformation occurring in the first 100 ms. Analysing the high speed video (Section 9.2.6) provided the information that GRW tanker J2580 impacted with speeds of 4.50 m/s (1.82 rad/s) at the front and 4.10 m/s (1.86 rad/s) at the rear of the tanker, and the rear hitting the ground first, less than 1 ms before the front of the tanker.

After first impact, GRW tanker J2580 slid forward and also rolled forward 10 to 15 degrees, then slid and rolled back before coming to rest on its side (at 0 degrees).

9.2.2 Presentation of strain and pressure gauge data

All strain gauge and pressure transducer measurements were averaged using a 19-point moving average through the data samples. As the data from these transducers did not show the same high frequency components as the accelerometers, there was no need to smooth the data as much. Therefore a smaller number of points were averaged together than the 1 000 points described in Section 9.1.

All the strain gauge and pressure measurements are from zero on the timebase. The authors decided to make the zero point the moment that the *first* gauge or transducer started to respond to the impact. The rear accelerometer responded sooner to the impact than the front accelerometer (less than 1 millisecond (ms)). This was due to the rear of the tanker impacting the pad slightly before the front of the tanker. The strain gauges responded about 3 ms after the rear accelerometer, and the pressure transducers responded about 4 ms after the rear accelerometer.

9.2.3 Strain Gauge Measurements

Figure 24 shows the measurements for compartments 1 and 4 from all the strain gauges: strain is measured in micro strain ($\mu\varepsilon$ which is extension/original length multiplied by 10^6).

The time-base is referenced to zero at the initial impact. The impact event is relatively short (about 0.1 seconds). The non-zero values of strain after this are caused by:

- changes in load on the tanker wall due to water displacement in the tanker (sloshing);
- plastic deformation in the tanker wall; and
- the rocking movement of the tanker as it settled after impact.

A secondary impact, caused by the tanker rolling back until the 5th wheel assembly and steel wheels impacted the ground, could be seen in the strain measurements about 1.5 seconds after the initial impact (not shown in Figure 24).

Figure 25 shows the same measurement on a much shorter time-base to focus on the initial impact event. In each compartment the circumferential strain gauges were close to each other and midway between bulkheads (Figure 15), so they were measuring at two points in a stress field where little spatial variation was expected. For compartment 1b, by comparing SG 1a with SG 2a (top left graph) and comparing SG 1b with SG 2b (top right graph) in Figure 25, the curves are

seen to be similar, as expected. This similarity can also be seen in the results for the circumferential gauges at the equivalent positions in compartment 4 (SG 7 and SG 8 in the lower graphs of Figure 25).

However, the curves do show significant peaks and troughs, which are more pronounced for the circumferential strain gauges (SG 1, SG 2 and SG 7, SG 8). The high speed video for the offside of the tanker as it rolled towards the camera captured free travelling flexural waves propagating away from the impact line around the circumference of the tanker. These waves would be expected to have a greater effect on the circumferential strain gauges than the longitudinal strain gauges, which is in agreement with the test data.

Little difference would be expected for the longitudinal strain gauges at SG 3 and SG 4 midway between bulkheads in compartment 1b as there should be little variation in the stress field between these points. Comparing the measurements for SG 3a with SG 4a (top left graph) and SG 3b with SG 4b (top right graph) in Figure 25, the curves are very close to each other. This similarity can also be seen in compartment 4 (SG 9 and SG 10 in the lower graphs in Figure 25).

These measurements are considered further in HSL report ES/14/39/06.

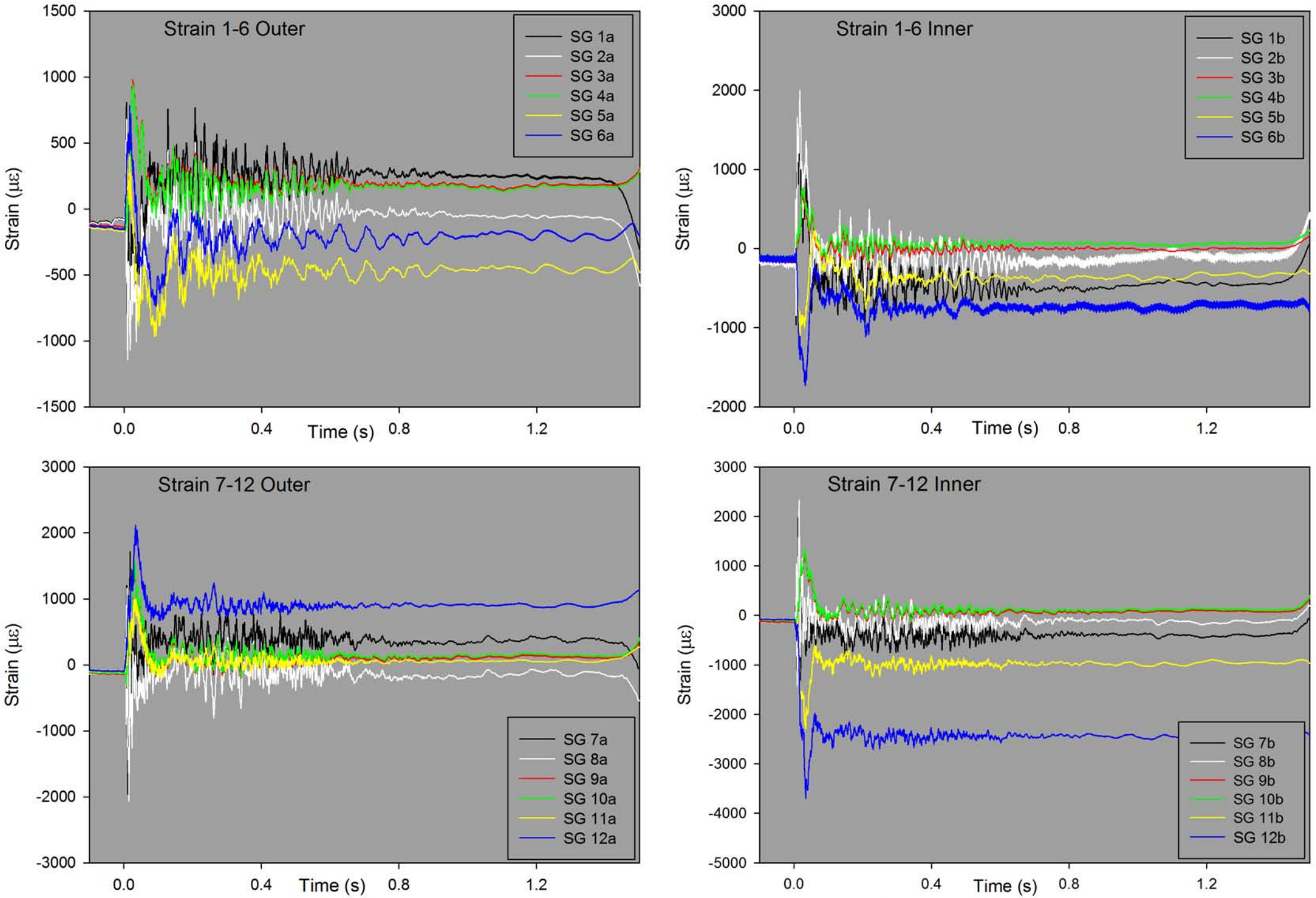

Figure 24 GRW J2580 strain measurements - all gauges (full time history)

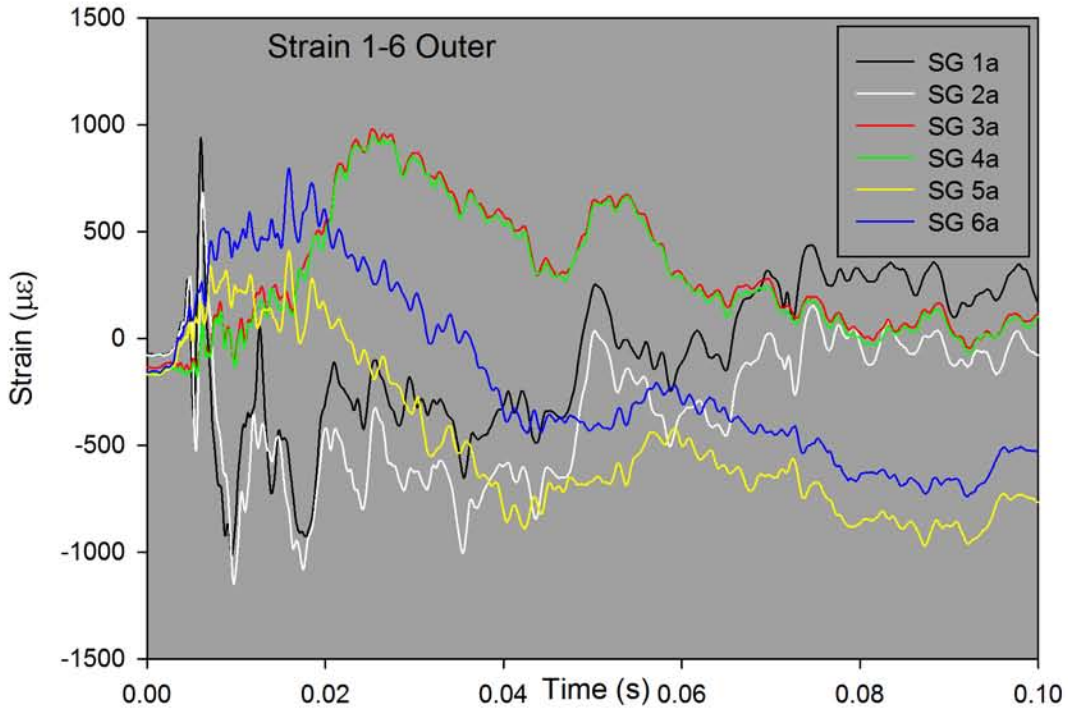

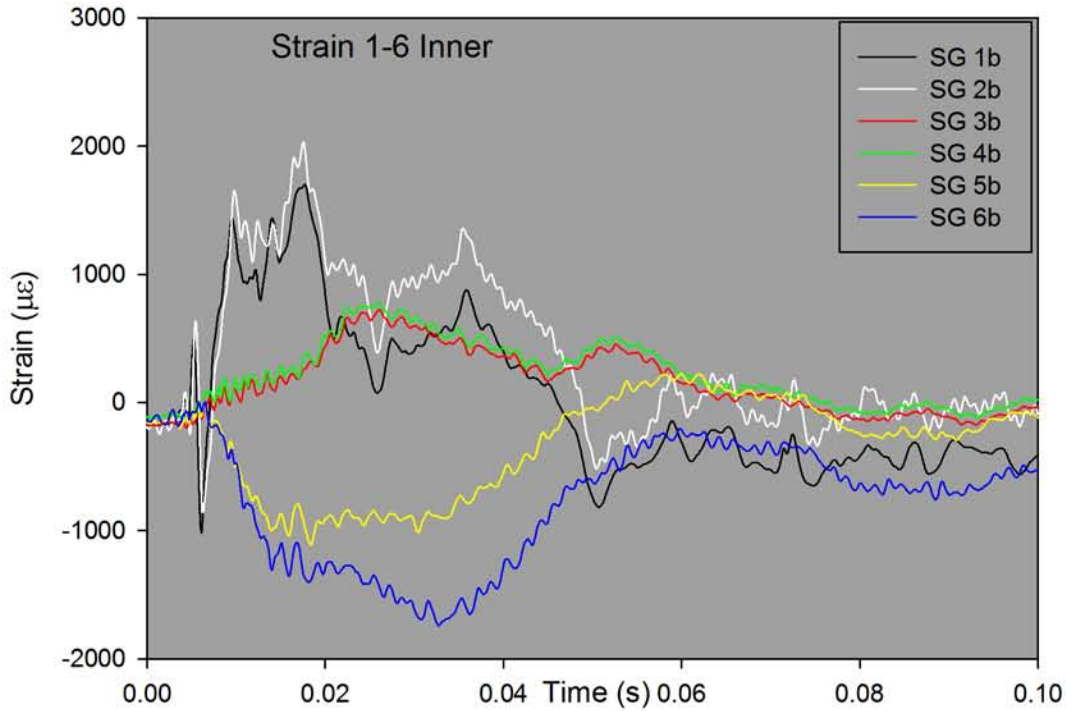

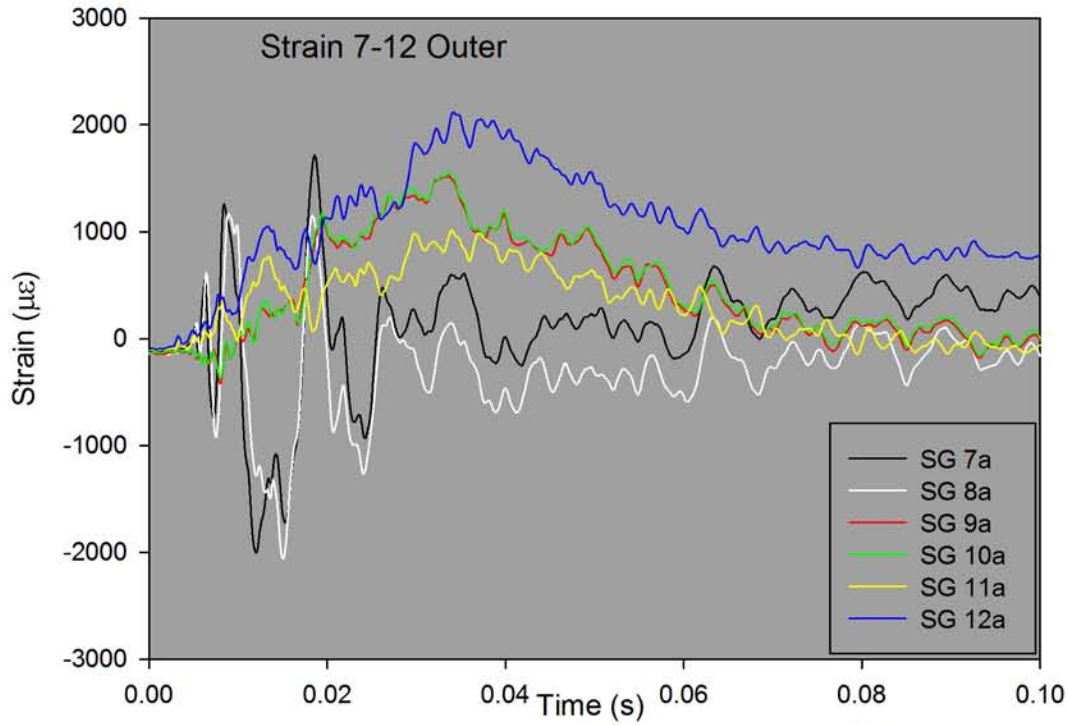

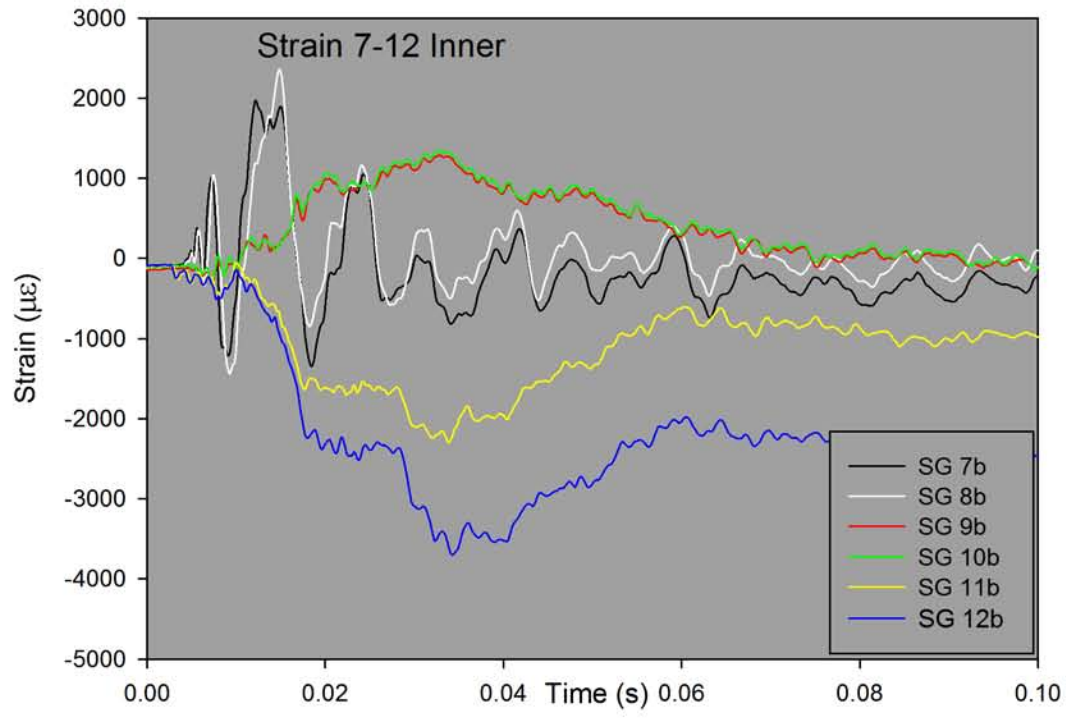

Figure 25 GRW J2580 strain measurements - all gauges (impact event only)

Figures 26 (SG pairs 2, 4 and 6) and 27 (SG pairs 8, 10 and 12) show the *average membrane strain* and the *average bending strain* for compartments 1b and 4; these values have been obtained from equations (1) and (2) in Section 8.1.1.

SG 2 measured strain in the circumferential direction (hoop strain). As the *average bending strain* was negative, the wall was flexing inwards at this point (sagging). The *average membrane strain* was positive, so the average state was tension, which means that the inner surface must have been in tension.

SG 4 and SG 6 measured strain in the longitudinal direction. SG 6 was much closer to the band than SG 4; so the strain at this point was likely to be more strongly influenced by the boundary conditions at the welds between shell, extrusion and bulkhead. For SG 4, the *average bending strain* was close to zero, which suggests there was little flexure in the wall at this point. The *average membrane strain* was positive, which means the average state was tension.

The strain measurements in the longitudinal direction from SG 6 (top graph in Figure 26) show a positive *average bending strain*, and negative *average membrane strain*. A positive bending strain means the wall was flexing outwards (hogging) at this point. A negative *average membrane strain* means the average state was compression, which means that the inner surface must have been in compression.

SG 8 measured circumferential (hoop) strain. As the *average bending strain* was fluctuating between positive and negative values, this suggests this point on the tanker was flexing in and out during the impact event: this was probably due to the influence of the free travelling flexural waves discussed earlier. As the *average membrane strain* fluctuated about zero, the average state was varying between tensile and compressive strain.

SG 10 and SG 12 measured strain in the longitudinal direction. SG 12 was much closer to the band than SG 10; so, as for SG 6, the strain at this point was likely to be more influenced by the boundary conditions at the welds between shell, extrusion and bulkhead. For SG 10, the *average bending strain* was close to zero, which suggests there was little flexure in the wall at this point. The *average membrane strain* was positive, which means that the average state was tension.

The strain measurements in the longitudinal direction from SG 12 (top graph in Figure 27) show a positive *average bending strain*, and negative *average membrane strain*. A positive bending strain means the wall was flexing outwards (hogging) at this point. A negative *average membrane strain* means that the average state was compression, so the inner surface must also have been in compression. These results are similar to those for SG 6, which was in a similar position in compartment 1b.

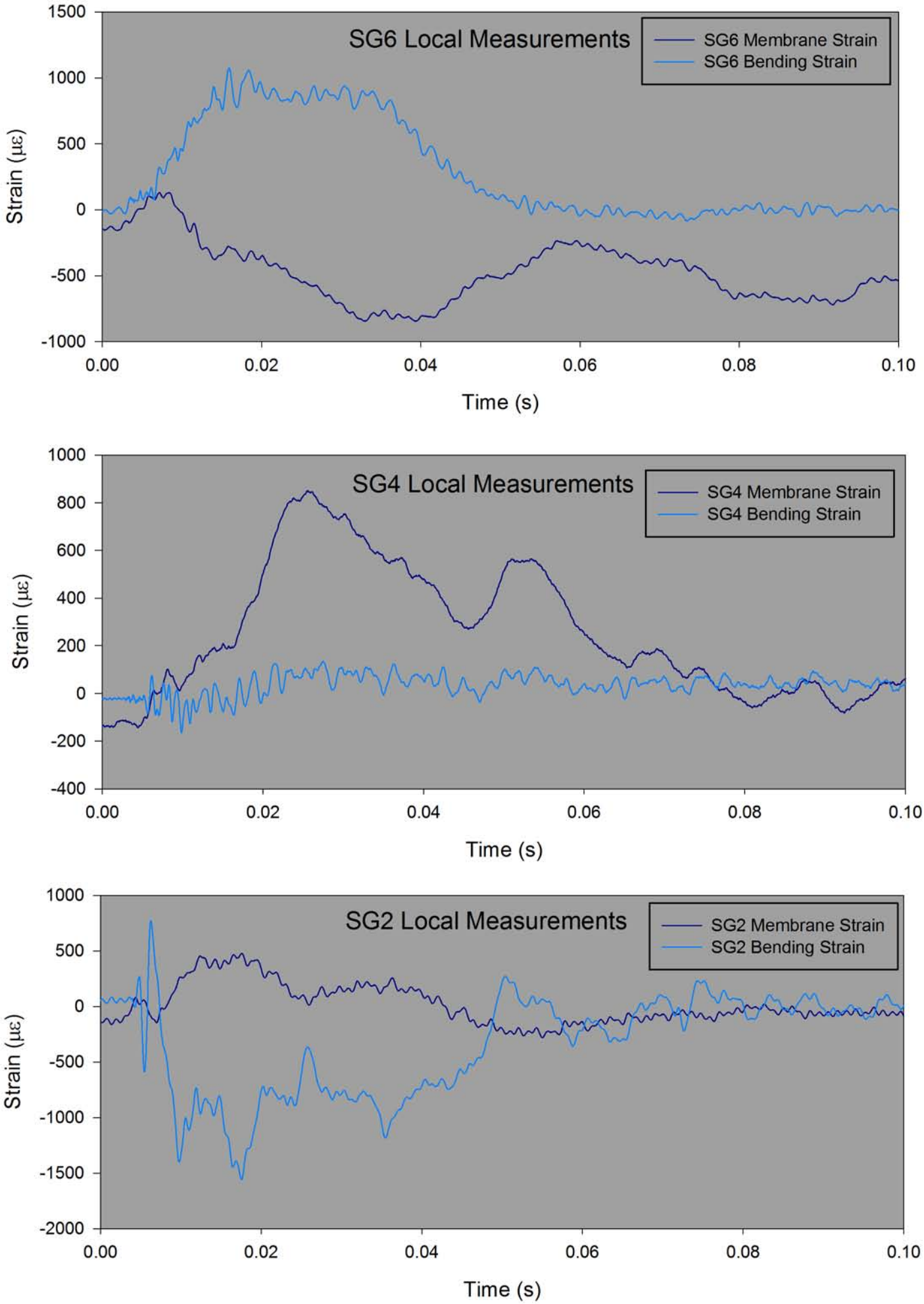

Figure 26 GRW J2580 membrane and bending strain from three strain gauge pairs - compartment 1

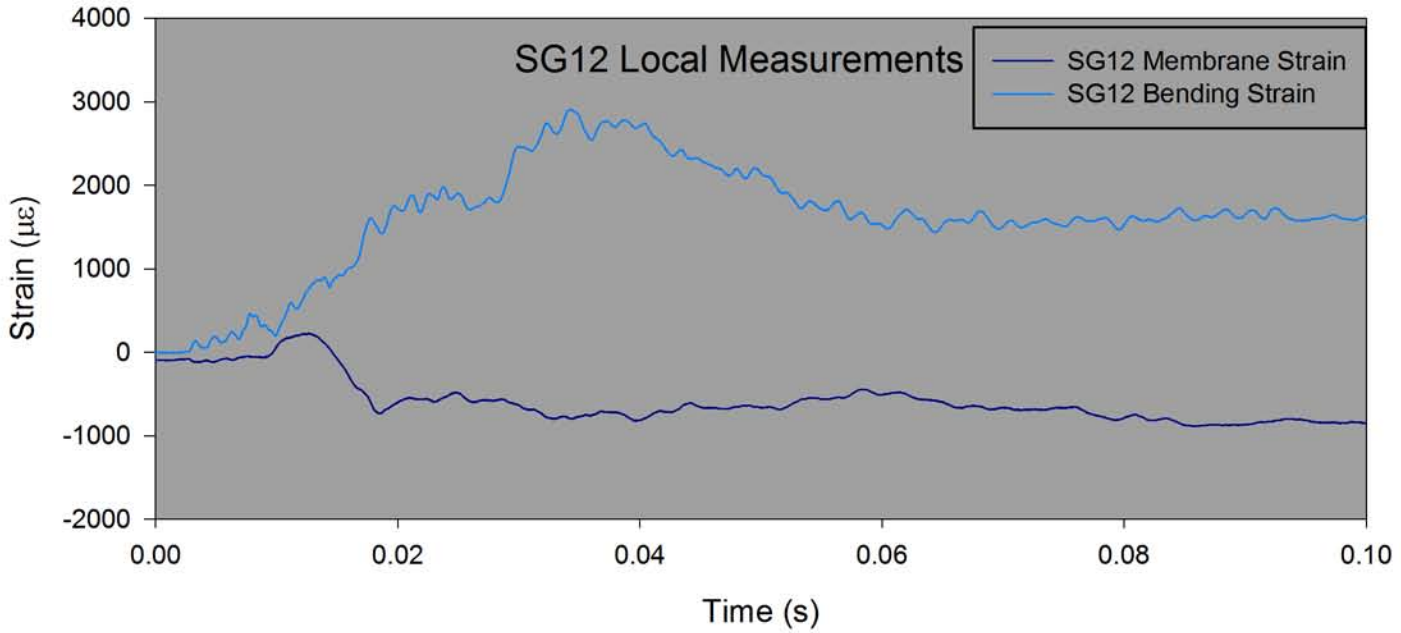

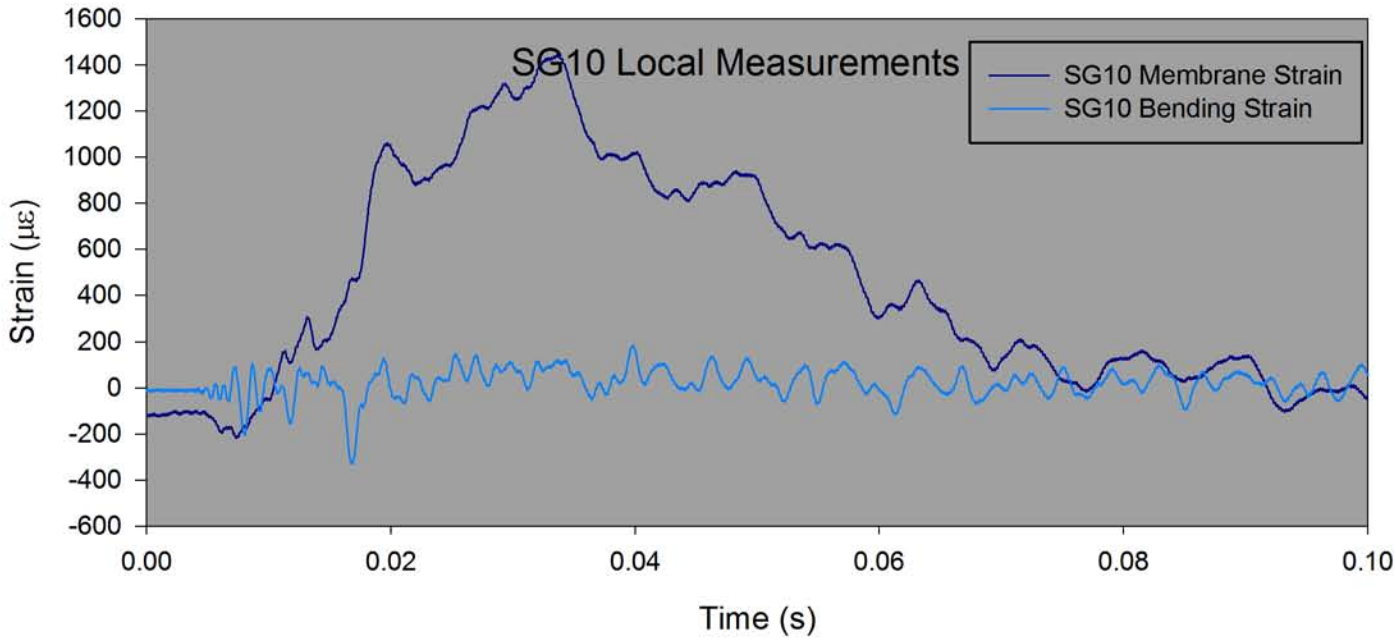

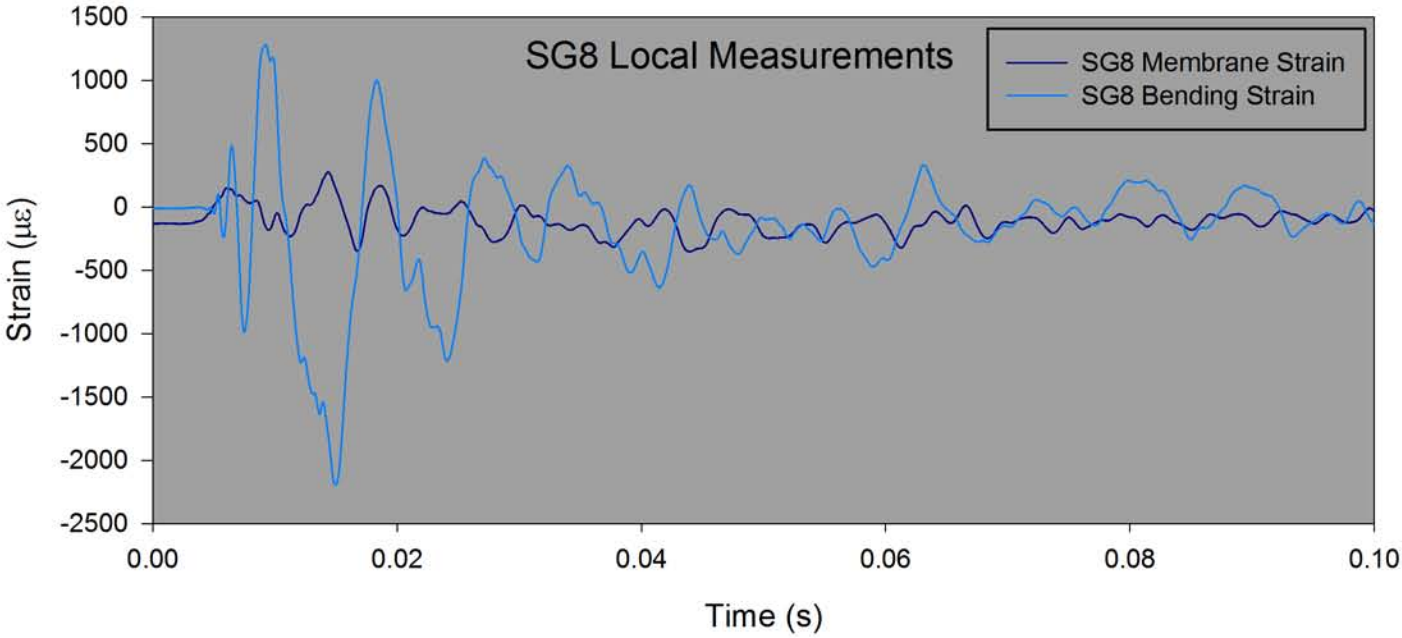

Figure 27 GRW J2580 membrane and bending strain from three strain gauge pairs - compartment 4

9.2.4 Pressure Measurements

All pressure measurements were *gauge* measurements; so measurements close to zero were measuring the ambient air pressure. As mentioned in Section 8.1.2, the static pressure at the measuring points due to the head of water reduce as the tanker topples. Figure 28 shows the pressure measured by each transducer before and during the tanker topple. Considering compartment 4, as expected, gauges 445899, 445878 and 445888 gave the highest static pressure as they were at the deepest level in the water. Transducers 445894 and 445898 were reading close to zero as they were above the water level prior to topple. As explained in Section 8.1.2, as the tanker begins to topple the pressure at each gauge reduces until the moment of impact - by this time *all* transducers were measuring less than 0.05 bar (0.725 psi). So, assuming the transducers were measuring atmospheric pressure at the point of impact is reasonable.

Figure 29 shows the measurements from the pressure transducers for compartments 1b and 4 throughout the test. With the tanker in the upright position, HSL have ordered the transducer numbers in the graph legends from the transducer at the 6 o'clock position at the top, to the transducer at the 12 o'clock position at the bottom. The pressure changes directly resulting from the impact occurred in a very short time period immediately after the impact.

Figure 30 shows the same measurements over a much shorter time period after the impact. The highest pressures were measured for the transducers closest to the impact point (around the 9 o'clock position) as expected. The transducers at the 6 o'clock and 12 o'clock positions gave little deviation from ambient pressure. The fact that the curves were showing some frequency modulation (sinusoidal short waves being carried on a longer, low frequency wave) suggests that many of the transducers were measuring acoustic waves as well as changes in water pressure.

The maximum pressure was measured on the transducers in the 9 o'clock position (transducer 445886 for compartment 1b, and 445882 for compartment 4). These transducers measured transient peaks around 7.2 bar (105 psi) at the moment of impact. About 0.03 seconds after impact, all transducers were measuring pressures below the solid red line at 2 bar (29 psi), and about 0.05 seconds after impact (compartment 1) and 0.07 seconds after impact (compartment 4) all transducers were reading close to ambient pressure.

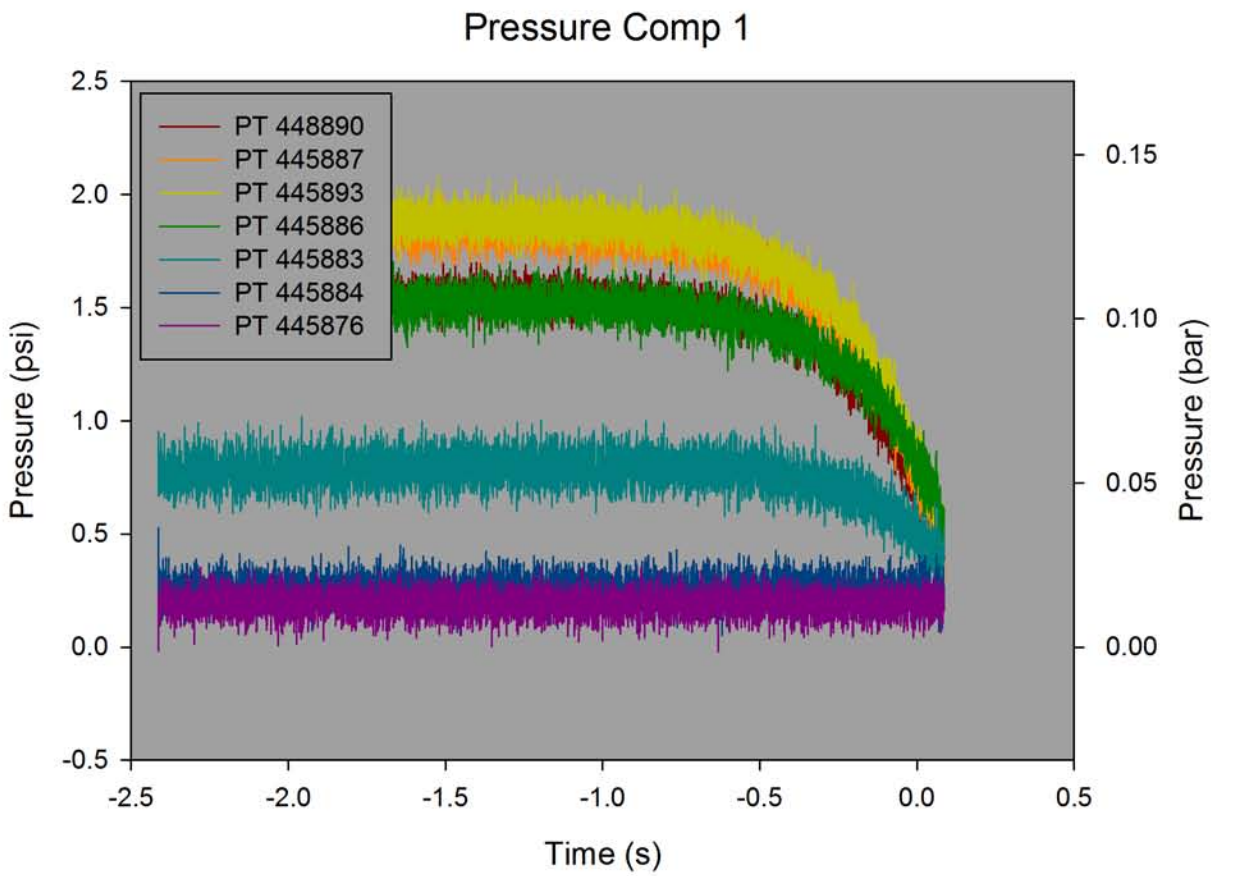

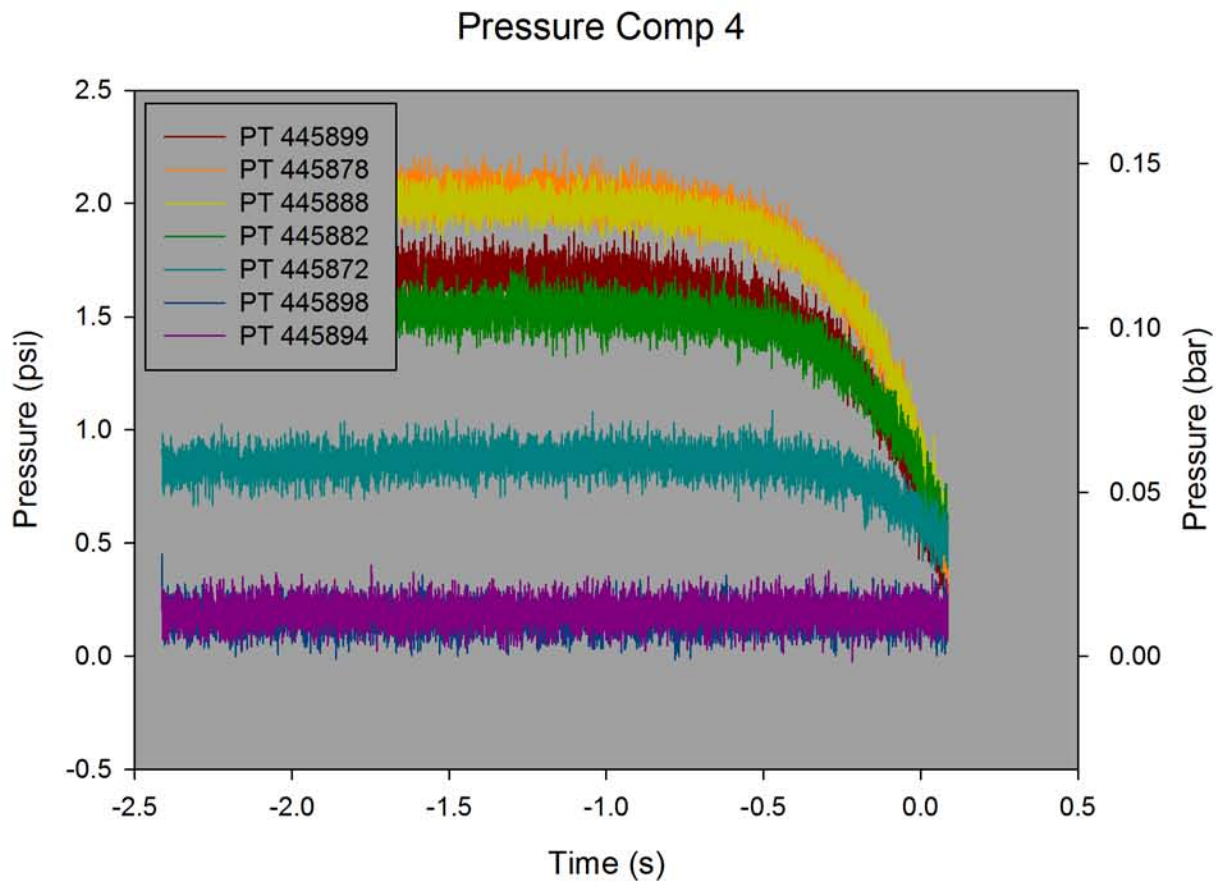

Figure 28 GRW J2580 pressure measurements - all transducers (during topple)

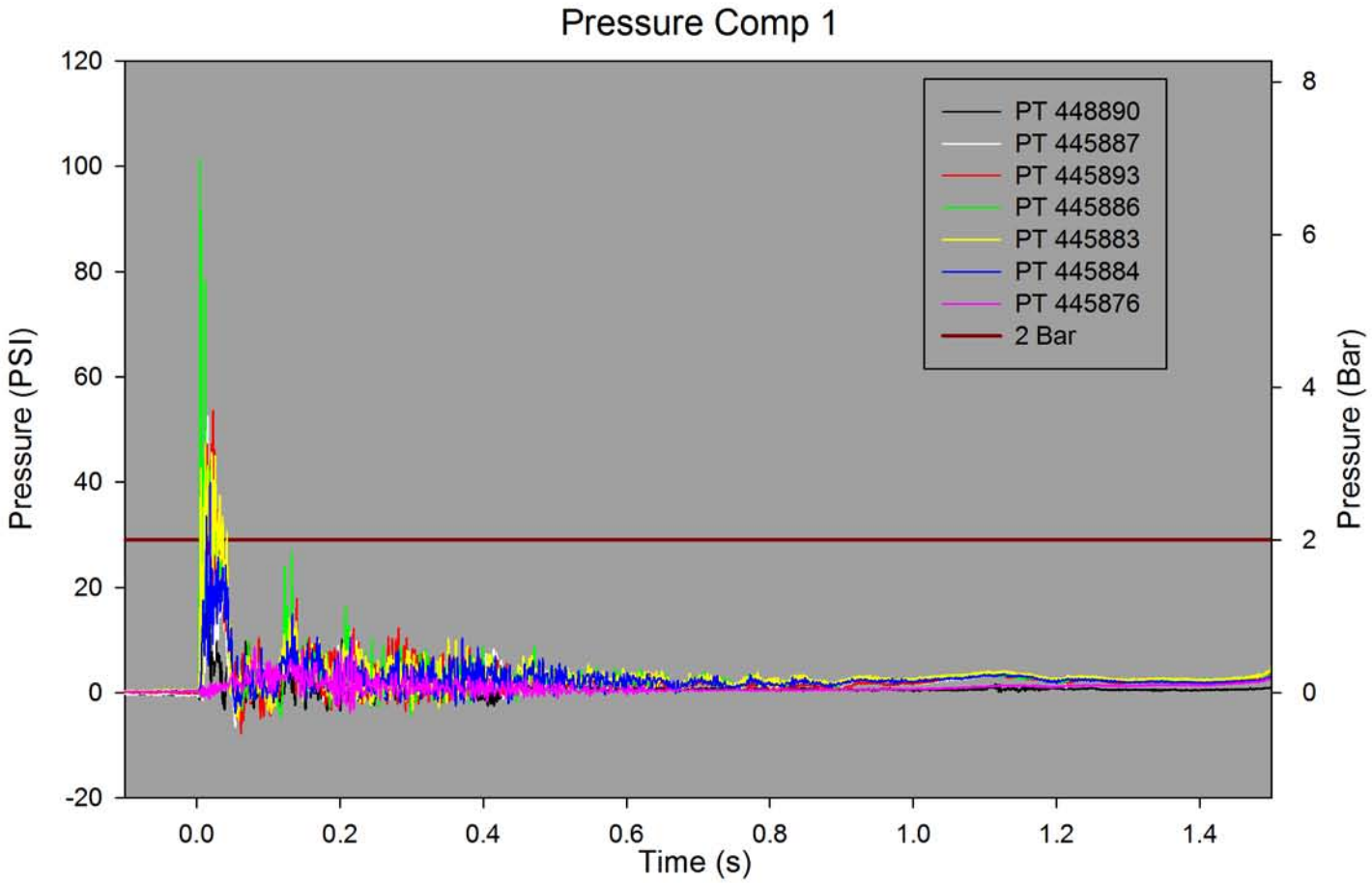

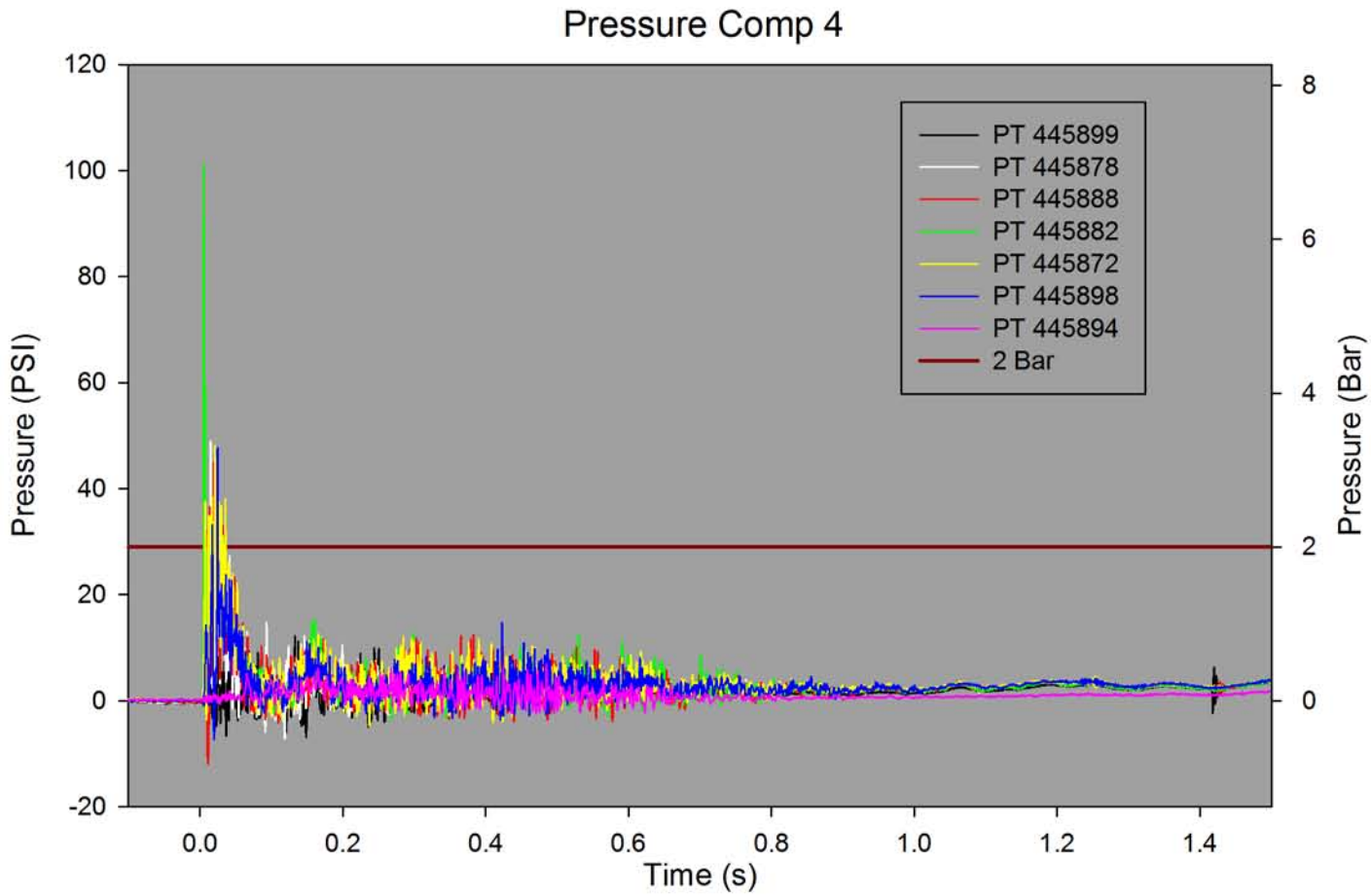

Figure 29 GRW J2580 pressure measurements - all transducers (full time history)

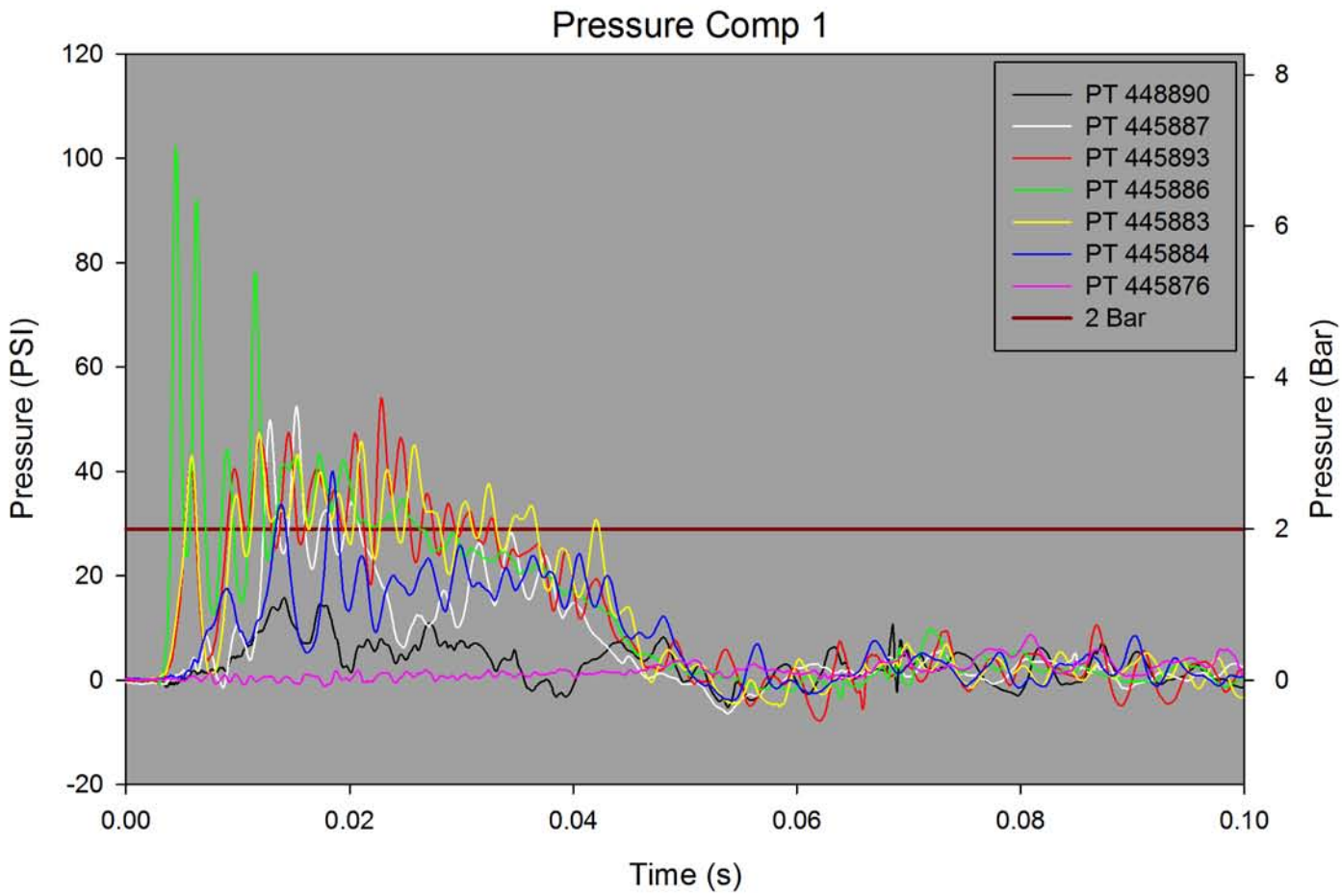

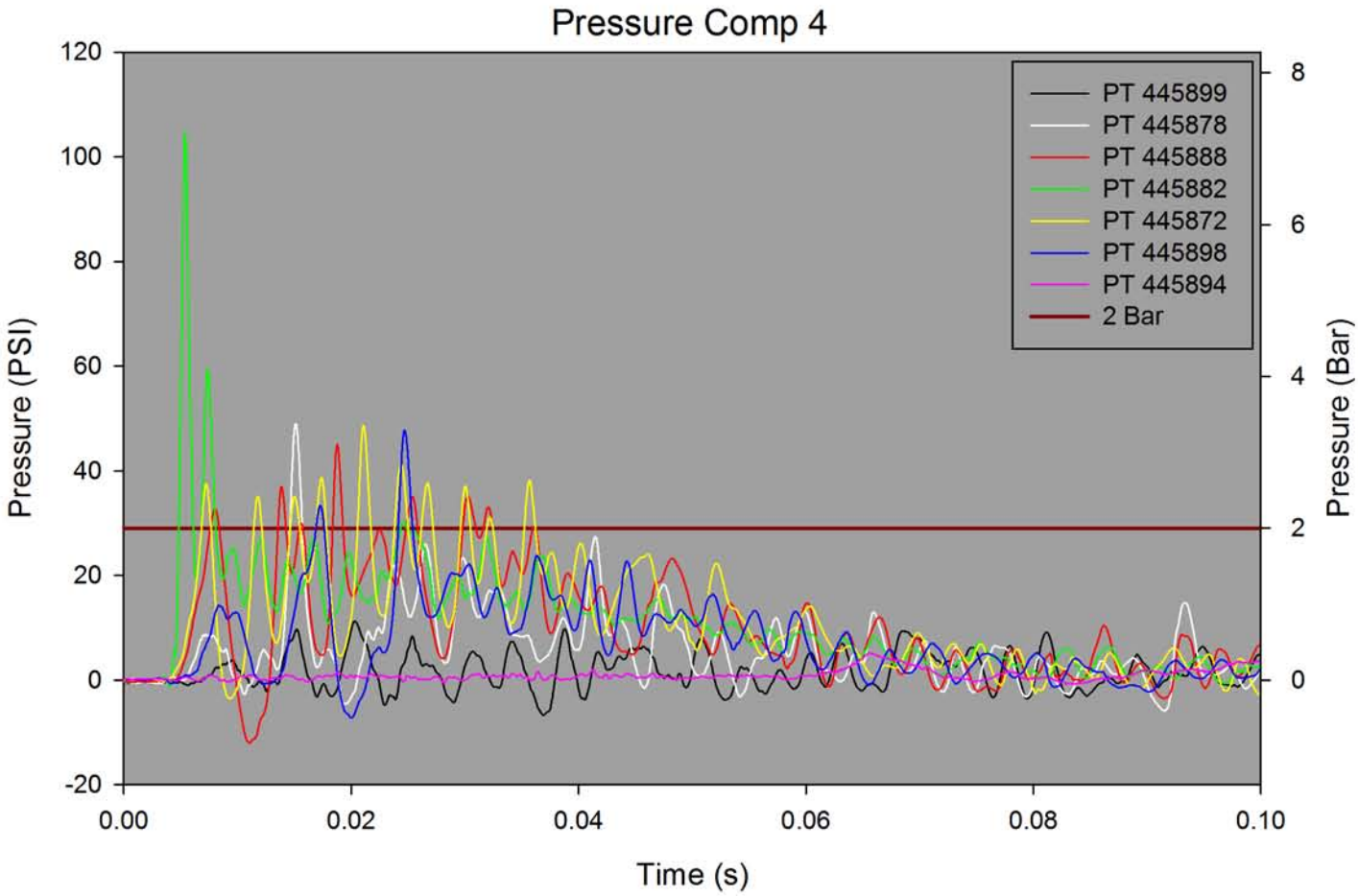

Figure 30 GRW J2580 pressure measurements - all transducers (impact event only)

9.2.5 Acceleration Measurements

As in the *proof of concept test* the accelerometer signals showed significant ringing, causing the accelerometers to overload and again the positive and negative peaks of the signal were 'cropped'. Therefore, the resilient strip between the mounting block and the tanker, to act as a mechanical filter, was still allowing some high frequency vibration (ringing) to affect the measurement. Filtering the signal through a low pass filter may not have provided reliable data as some digital filters cannot cope with cropped peaks and troughs effectively. The data was simply smoothed to reduce the effect of the rapid changes in signal amplitude due to the vibration: for these measurements a 799-point moving average was selected. Although carrying out a moving point average on 'clipped' data can introduce some errors to the average value, as the signal has not been clipped too much the measurements can still be used for comparative purposes as explained by the second footnote in the next paragraph. These results were then compared with the acceleration calculated from analysing the high speed video (HSV).

The results are shown in Figure 31 for the y-axis accelerometer[xi] and high speed video at the front of the tanker, and Figure 32 for the y-axis accelerometer and high speed video at the rear of the tanker. The smoothed data from the accelerometers and high speed video showed good agreement with each other up to the maximum deceleration, given the cropped accelerometer data[xii]. After this, the tanker movement, in response to the impact, would have included some rotation about a longitudinal axis within the tanker body. This probably explains why there are differences between the two measurements as the accelerometer and the targets are not at exactly the same position on the tanker body.

9.2.6 Impact Velocity Measurements

The impact velocities obtained from the high speed video using the *image pro plus* software were as follows:

- 4.5 m/s at the front of the tanker; and
- 4.1 m/s at the back of the tanker

The radius (r) (see Figure 22) at the front of the tanker is 2.47 m, and the radius at the rear is 2.20 m. Using equation (3) in Section 8.2

$$\omega = \frac{v}{r} \text{ rads/sec}$$

The rotational velocity at the front was

$$\omega = \frac{4.5}{2.47} = 1.82 \text{ rads/sec}$$

and the rotational velocity at the rear was

$$\omega = \frac{4.1}{2.20} = 1.86 \text{ rads/sec.}$$

[xi] *i.e. the accelerometer that is in the vertical position at impact*

[xii] *Figure 31 and 32 show the 'raw' acceleration signal has been clipped more on the negative peaks than the positive peaks; so the moving point averaging process is ignoring more data points on the negative side than the positive side. This means the average values are weighted towards the positive (i.e. the calculated average is higher than the true average). However, as these data have not been 'clipped' too much, and as a large number of points have been used in the moving point average, the missing data points do not have a significant effect on increasing the average value.*

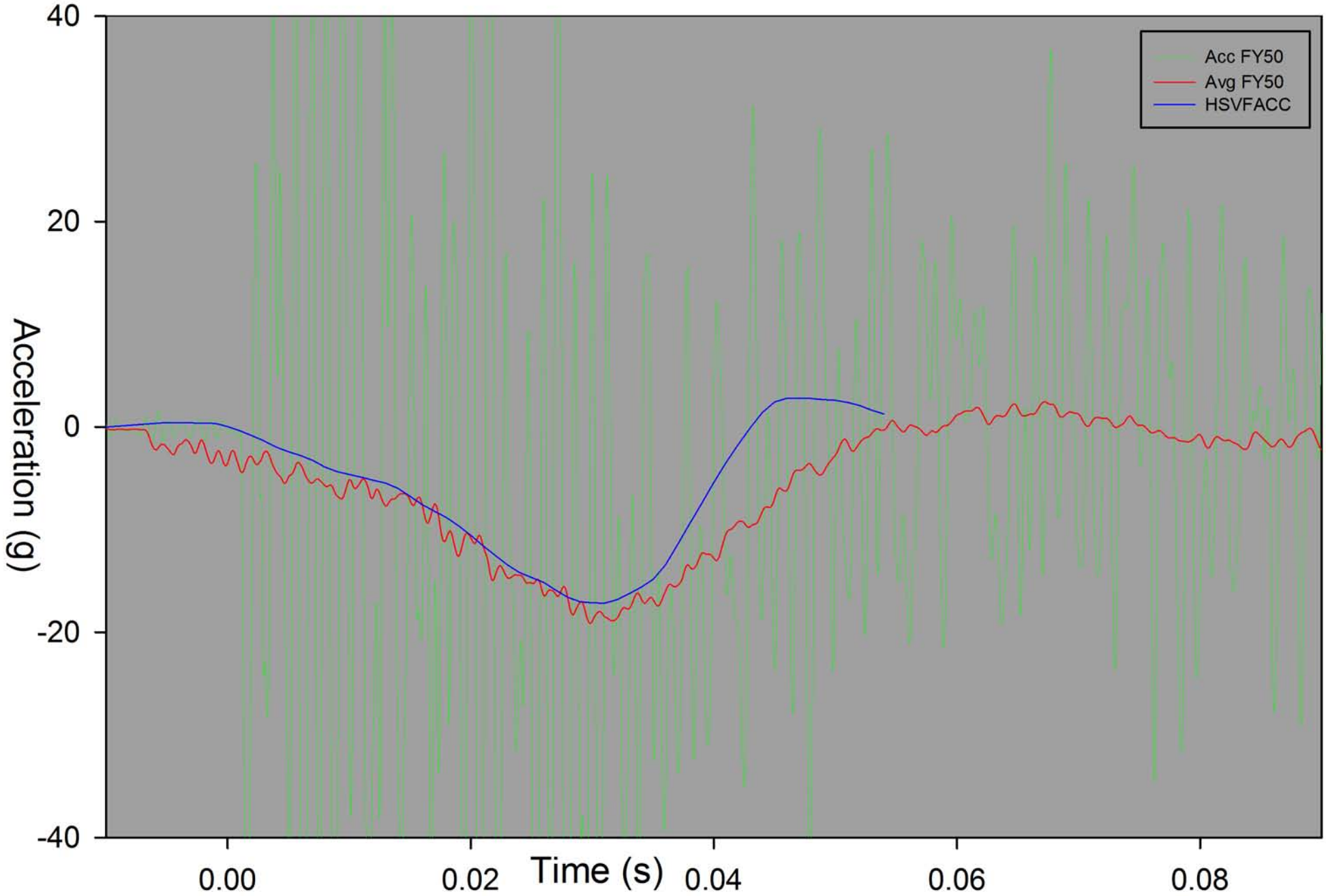

Figure 31 GRW J2580 acceleration measurements - accelerometer and HSV - front

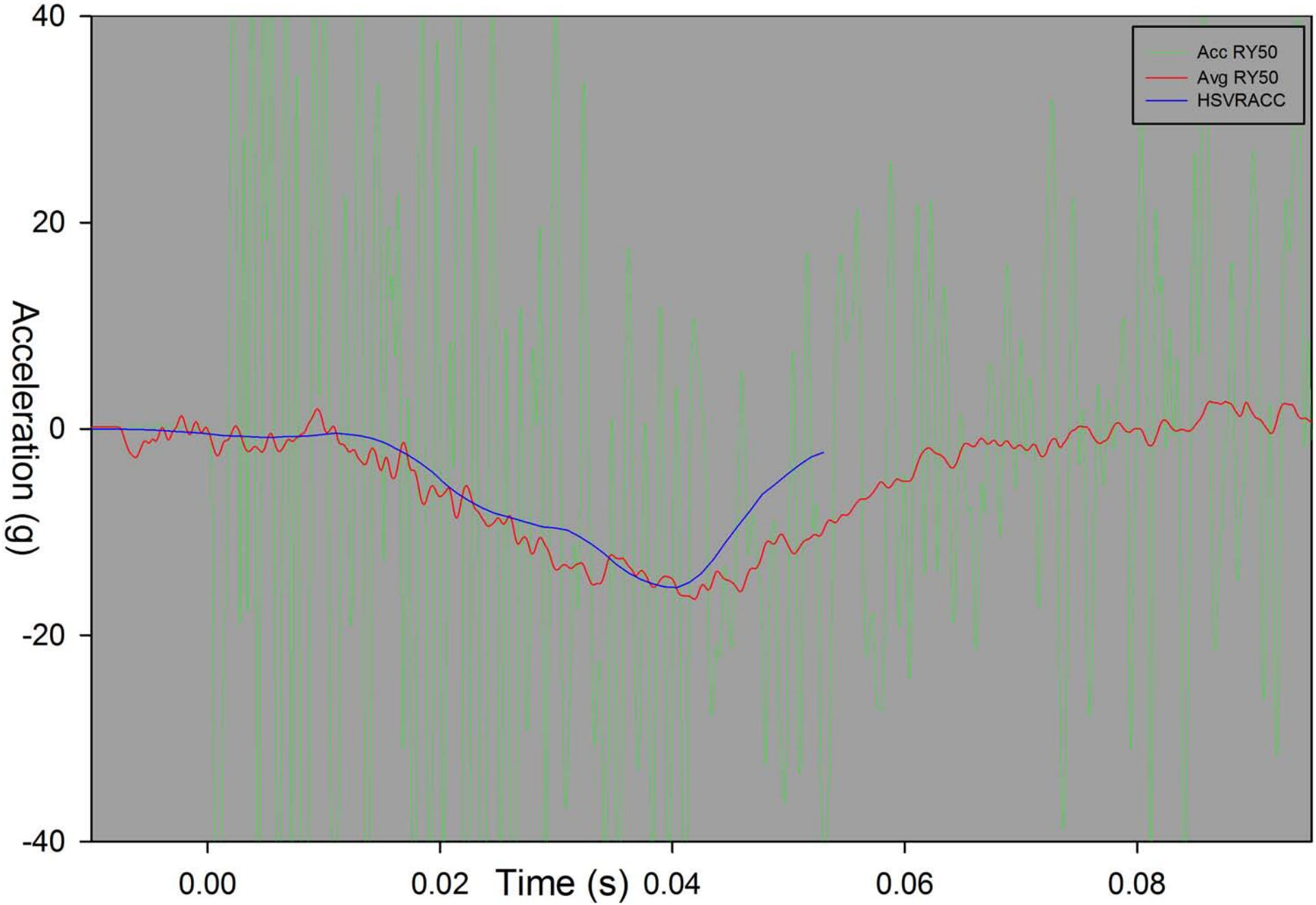

Figure 32 GRW J2580 acceleration measurements - accelerometer and HSV - rear

9.3 GRW TANKER J3910

9.3.1 Impact behaviour

The overall impact duration was a few seconds for all the tests, with most deformation occurring in the first 100 ms. For GRW tanker J3910, analysis of high speed video (Section 9.3.6) gave impact speeds of 4.55 m/s (1.84 rad/s) at the front and 4.25 m/s (1.93 rad/s) at the rear of the tanker, and the rear hitting the ground first, less than 7 ms before front of the tanker. After first impact, GRW tanker J3910 slid forward and also rolled forward 10 to 15 degrees, then rolled back but hardly slid back before coming to rest on its side (at 0 degrees).

9.3.2 Presentation of strain and pressure gauge data

As for GRW tanker J2580, all strain gauge and pressure transducer measurements have been averaged using a 19-point moving average through the data samples. Also, the zero point was the moment that the *first* gauge or transducer started to respond to the impact. The rear accelerometer responded about 6 to 8 ms before the front accelerometer, the strain gauges responded about 4 to 8 ms after the rear accelerometer, and the pressure transducers responded about 4 to 8 ms after the rear accelerometer. Again this was due to the rear of the tanker impacting the pad slightly before the front of the tanker.

9.3.3 Strain Gauge Measurements

During filling, the signals from three of the internal strain gauges were lost when the gauges came into contact with the water; these gauges were:

- one of two longitudinal gauges located at the rear of compartment 1b (SG 5b); and
- both longitudinal gauges located at the front of compartment 4 (SG 7b and SG 8b).

However, the signals from these gauges appeared to recover and show the impact occurring, and the curve trends during impact were similar to the other gauges. However, the magnitudes did not appear to be reliable. Data from these gauges are included in the report for completeness, but cannot be reliably compared with the data from the FE model. Figure 33 shows the measurements from all the strain gauges. For the inner strain gauges, SG 5b,7b and 8b (denoted by (i)), the data are unreliable for the reasons explained above.

The initial impact was shown by the sharp peak at zero on the time-base. The impact event was relatively short (about 0.1 seconds). As for GRW tanker J2580, any non-zero values of strain after this were caused by:

- changes in load on the tanker wall due to water displacement in the tanker (sloshing);
- plastic deformation in the tanker wall; and
- the rocking movement of the tanker as it settles after impact.

Figure 34 shows the same measurement on a much shorter time-base to focus on the initial impact event. Only one circumferential (hoop) strain gauge pair was used in each compartment (compartment 1b – SG 3a and SG 3b; compartment 4 – SG 9a and SG 9b), at the midpoint between the bulkheads. As for GRW tanker J2580, the strain gauges measuring circumferential strain measured significant peaks and troughs. High speed video of the offside of the tanker as it rolled towards the camera captured free travelling flexural waves propagating away from the impact line and around the circumference of the tanker, similar to those for GRW tanker J2580.

SG 1a, close to the front bulkhead, measured a much higher value of tensile strain than the other gauges. SG 1b on the inside measured an almost ‘mirror image’ of negative strain, which shows the tanker wall was flexing outwards significantly at this point. The strain at the same position in compartment 4 (SG 7a) did not show such an increase in tensile strain (7b cannot be compared due to the faulty gauge). The two gauge pairs closest to the rear bulkhead in compartment 4 (SG 11 and 12) measured very high levels of positive (tensile) strain on the outer gauges, and corresponding high levels of negative (compressive) strain on the inside.

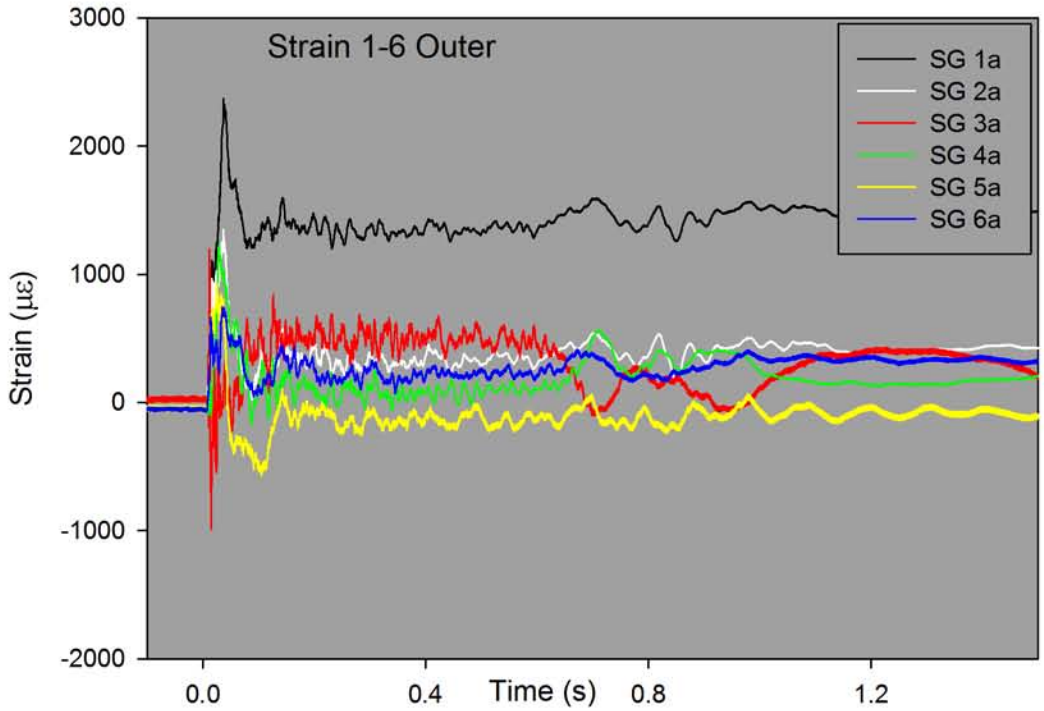

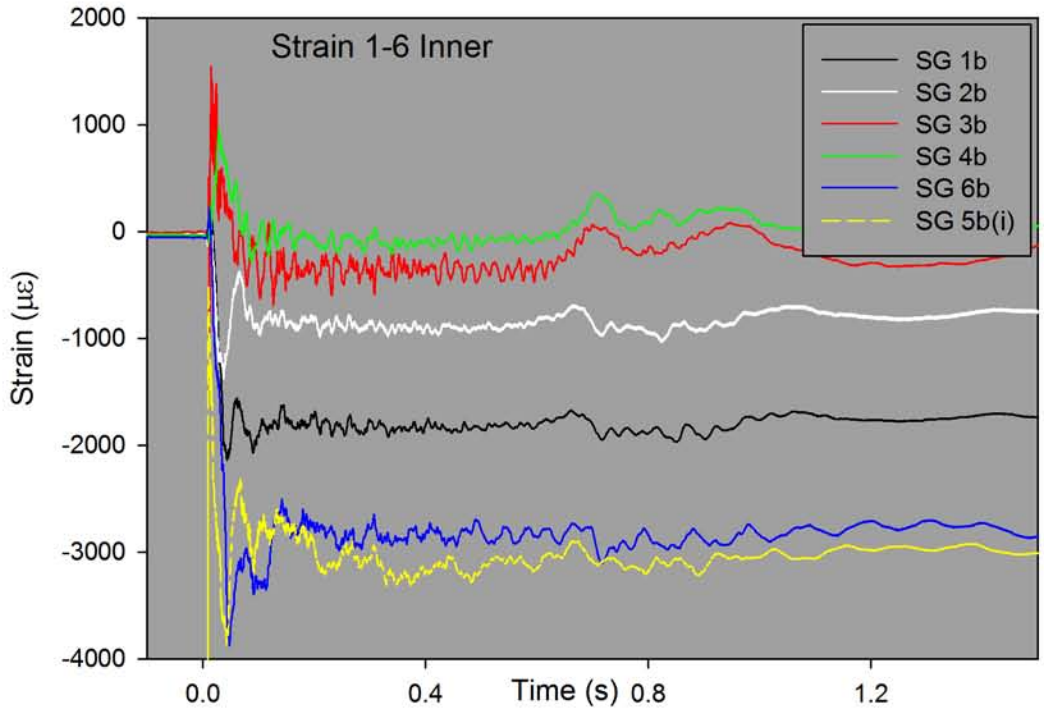

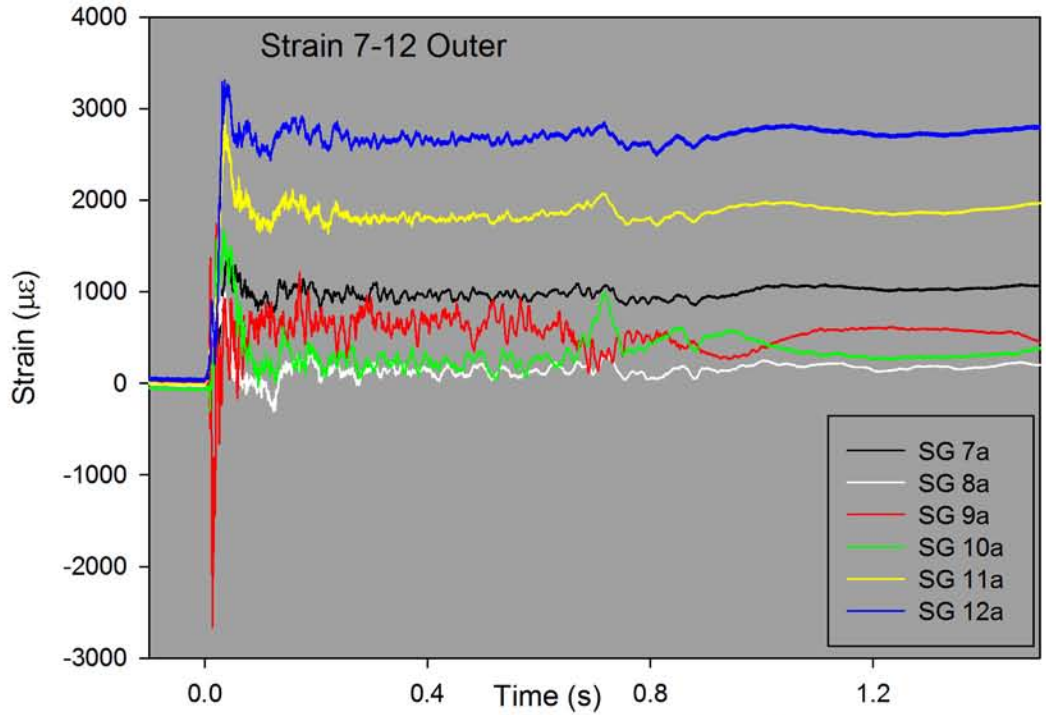

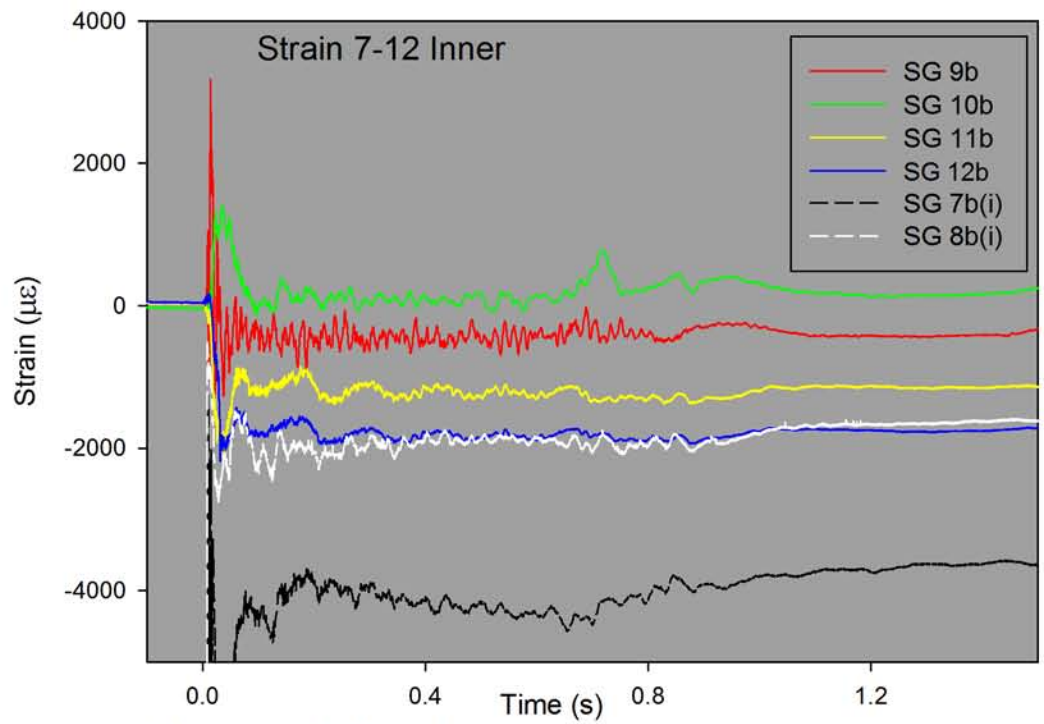

Figure 33 GRW J3910 strain measurements - all gauges (full time history)

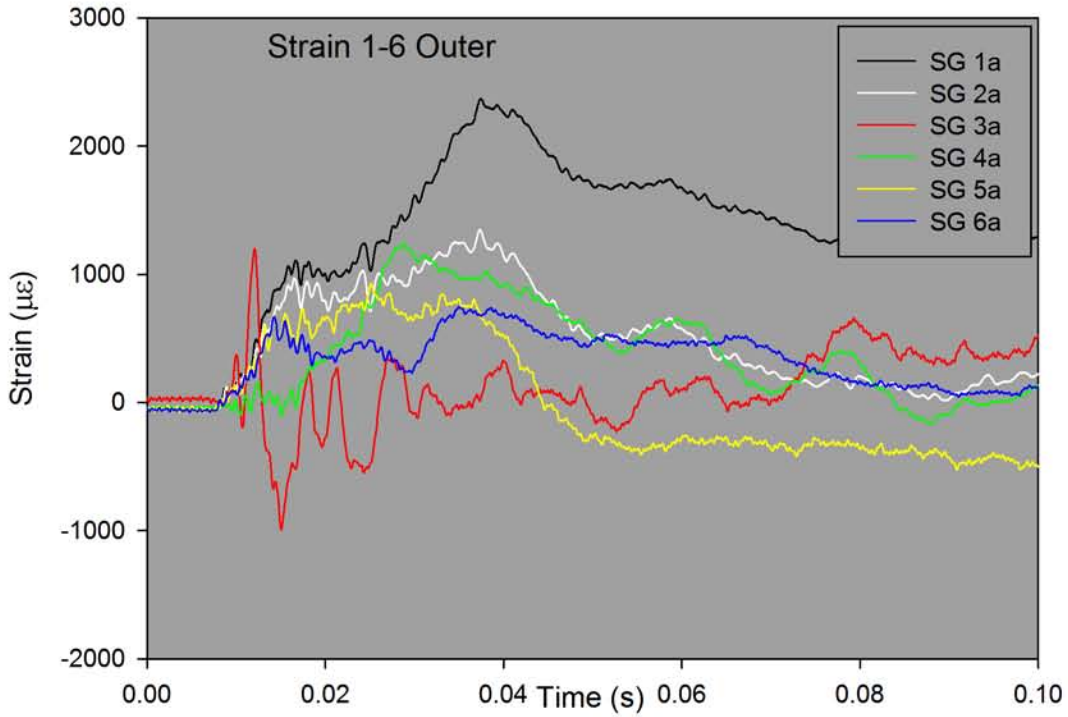

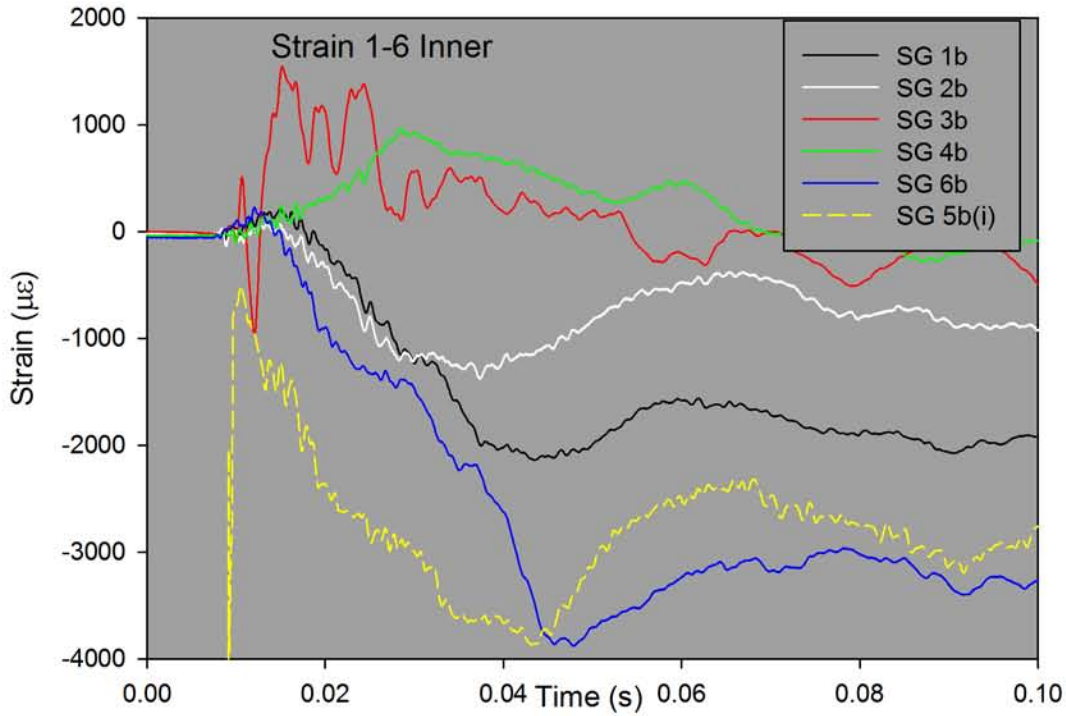

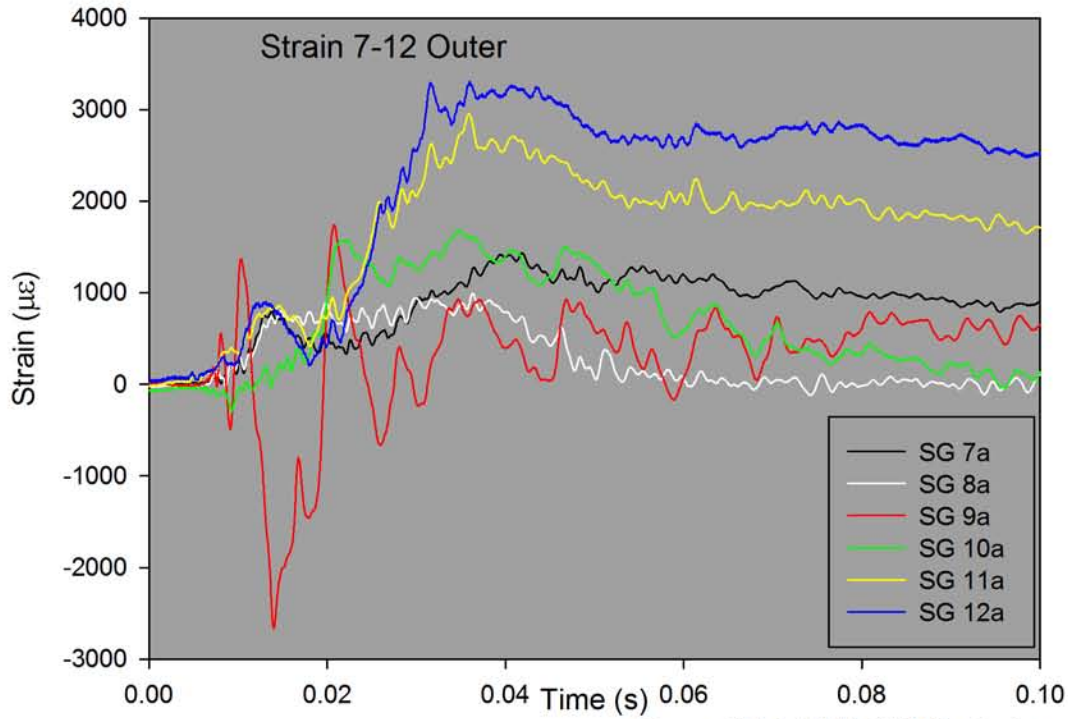

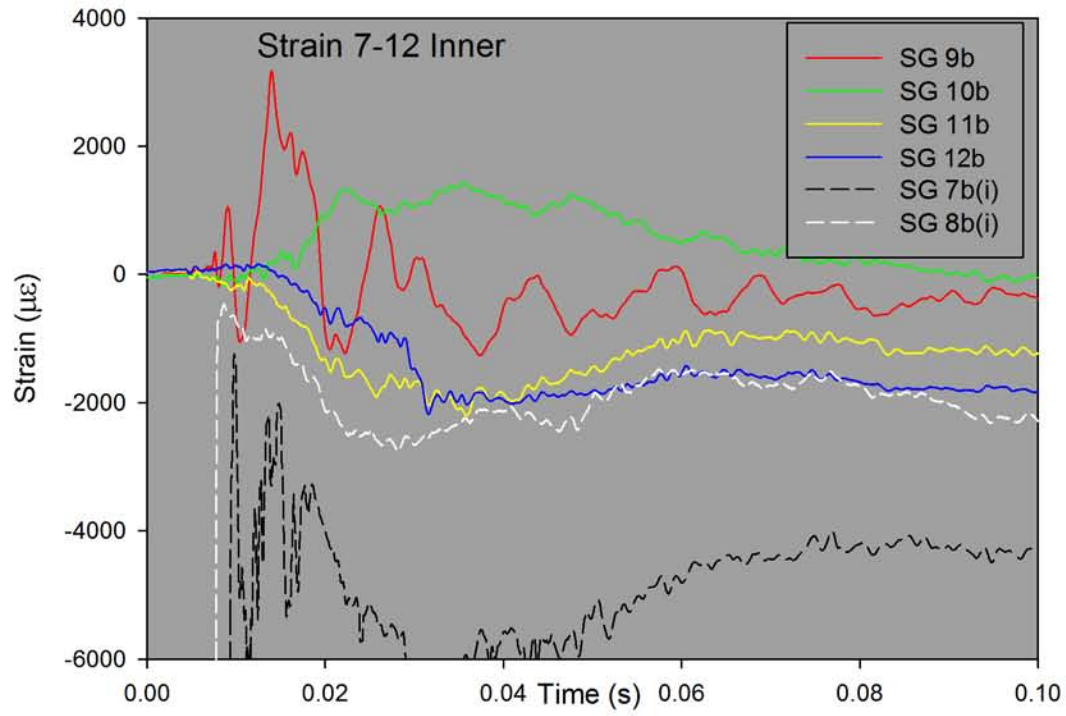

Figure 34 GRW J3910 strain measurements - all gauges (impact event only)

Figures 35 (SG pairs 3, 4 and 6) and 36 (SG pairs 9,10 and 12) show the *average membrane strain* and the *average bending strain* for compartments 1b and 4; these values have been obtained from equations (1) and (2) in Section 8.1.1.

Strain gauge pair (SG) 3 was measuring strain in the circumferential direction (hoop strain). As the *average bending strain* was negative, the wall was flexing inwards at this point (sagging). The *average membrane strain* was positive, so the average state was tension which means that the inner surface must have been in tension.

SG 4 and SG 6 were measuring strain in the longitudinal direction. SG 6 was much closer to the bulkhead than SG 4; so the strain at this point was likely to be more influenced by the boundary conditions at the welds between shell, extrusion and bulkhead. In Figure 35, for SG 4, the *average bending strain* is close to zero, which suggests there was little flexure in the wall at this point. The *average membrane strain* was positive, which means the average state was tension.

The strain measurements in the longitudinal direction from SG 6 (top graph in Figure 35) gave a positive *average bending strain*, and negative *average membrane strain*. A positive bending strain means the wall was flexing outwards (hogging) at this point. A negative *average membrane strain* means the average state was compression, which means that the inner surface must have been in compression.

SG 9 (Figure 36) was measuring strain in the circumferential direction (hoop strain). As the *average bending strain* was varying between positive and negative cycles, this suggests this point on the tanker was flexing in and out during the impact event: this was probably due to the influence of the free travelling flexural waves discussed earlier. As the *average membrane strain* fluctuated about zero, the average state was varying between tensile and compressive strain.

SG 10 and SG 12 were measuring strain in the longitudinal direction. SG 12 was much closer to the bulkhead than SG 10; so again the strain at this point was likely to be more influenced by the boundary conditions at the welds between shell, extrusion and bulkhead. In Figure 36, for SG 10, the *average bending strain* was close to zero, which suggests there was little flexure in the wall at this point. The *average membrane strain* was positive, which means that the average state was tension.

The strain measurements in the longitudinal direction from SG 12 in the top graph of Figure 36 gave a positive *average bending strain*, and a positive *average membrane strain*, but at a much lower value of strain. A positive bending strain means the wall was flexing outwards (hogging) at this point. The results for bending strain are similar to those for SG 6, which was in a similar position in compartment 1b, but whereas the membrane strain was predominantly tensile (positive values) for SG12, the values were predominantly negative for SG 6, which suggests there was greater compression in the wall in compartment 1b at this point.

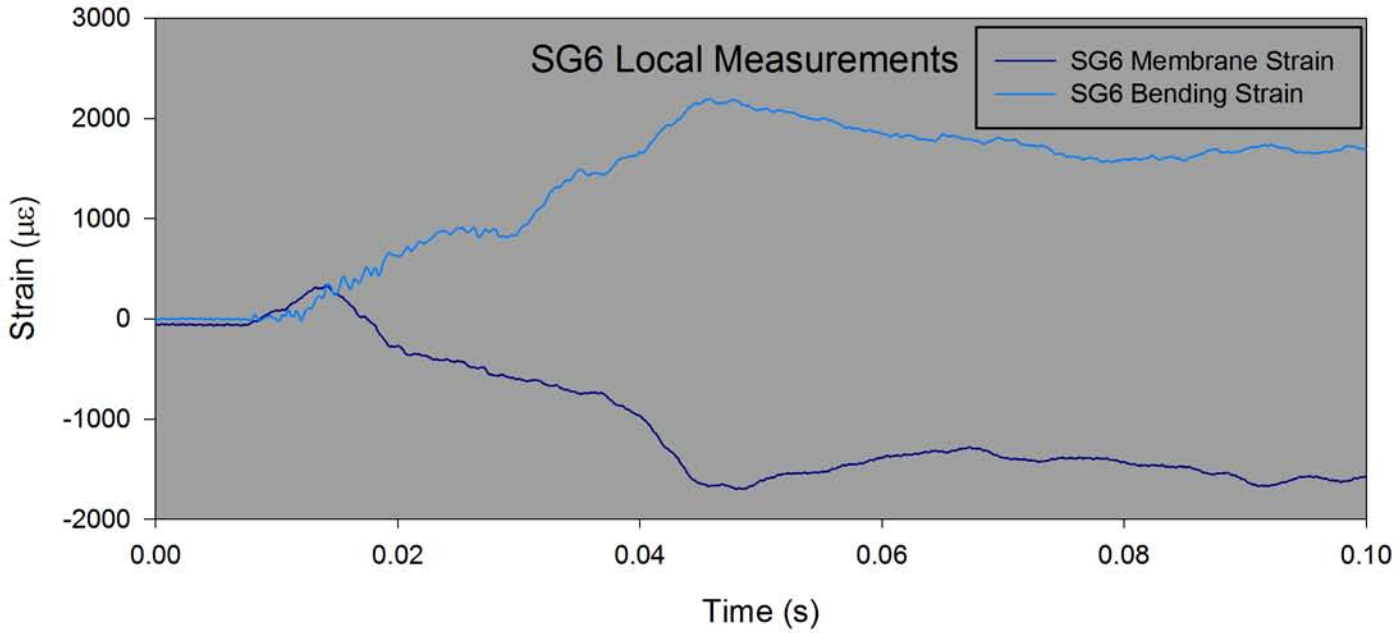

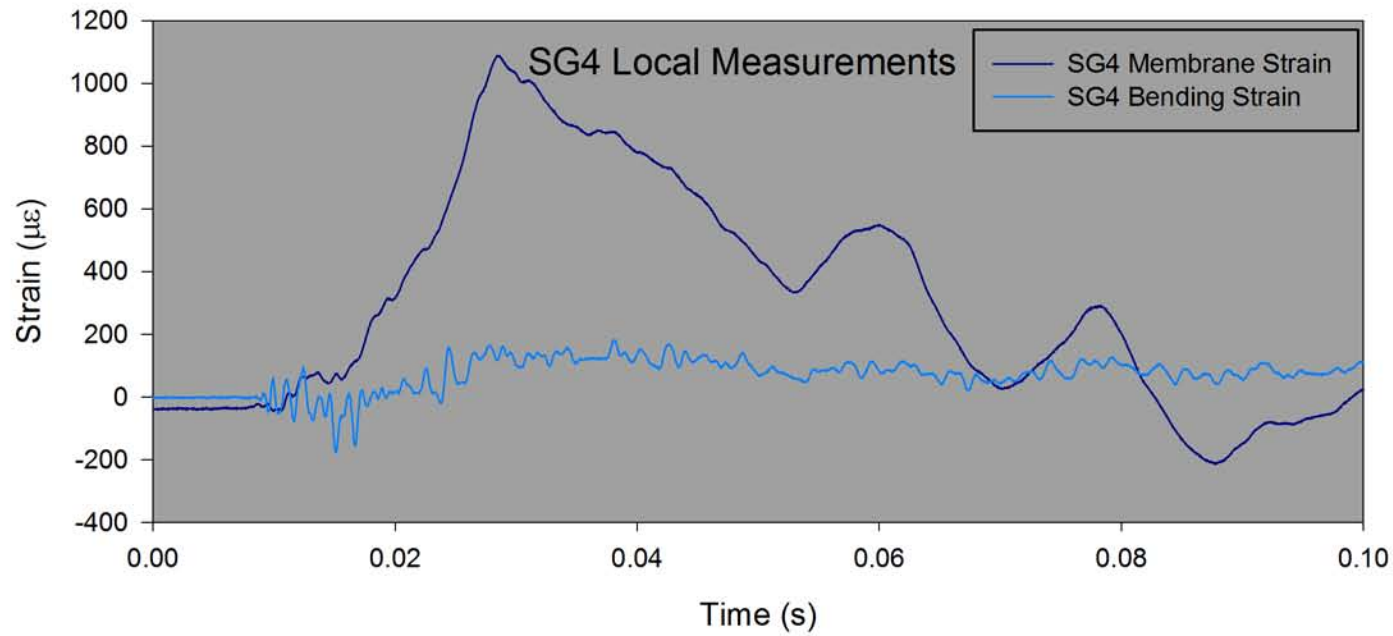

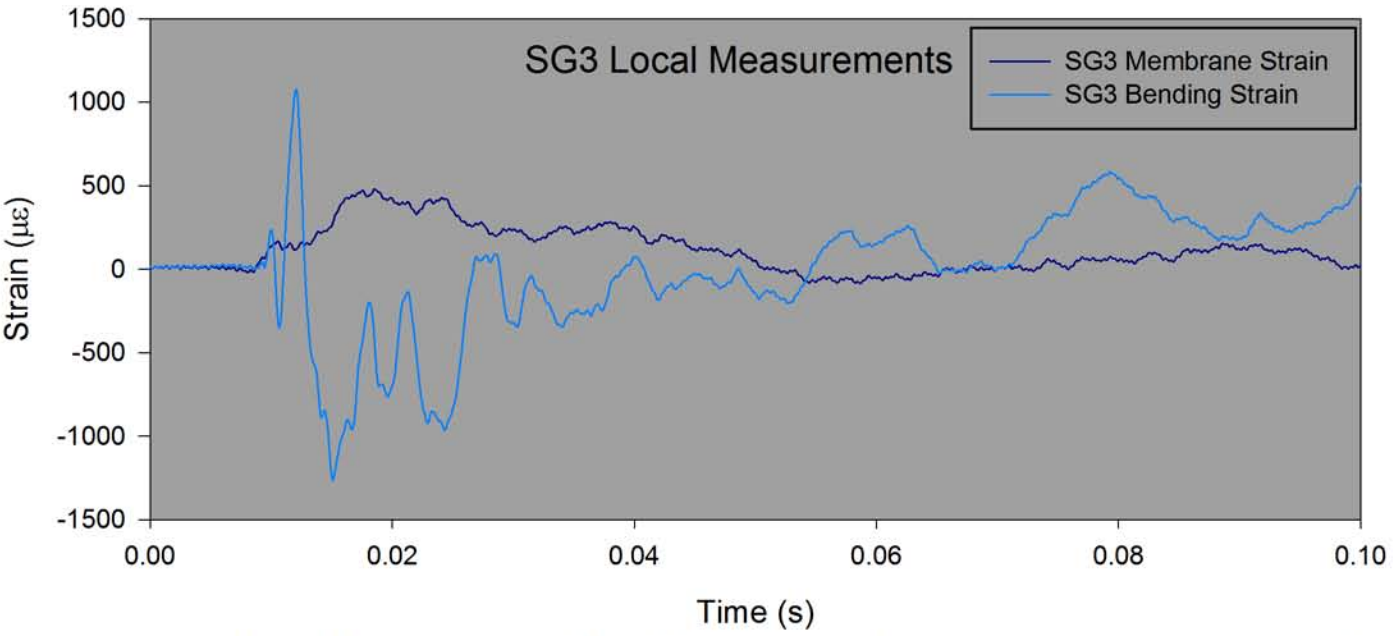

Figure 35 GRW J3910 membrane and bending strain from three strain gauge pairs - compartment 1

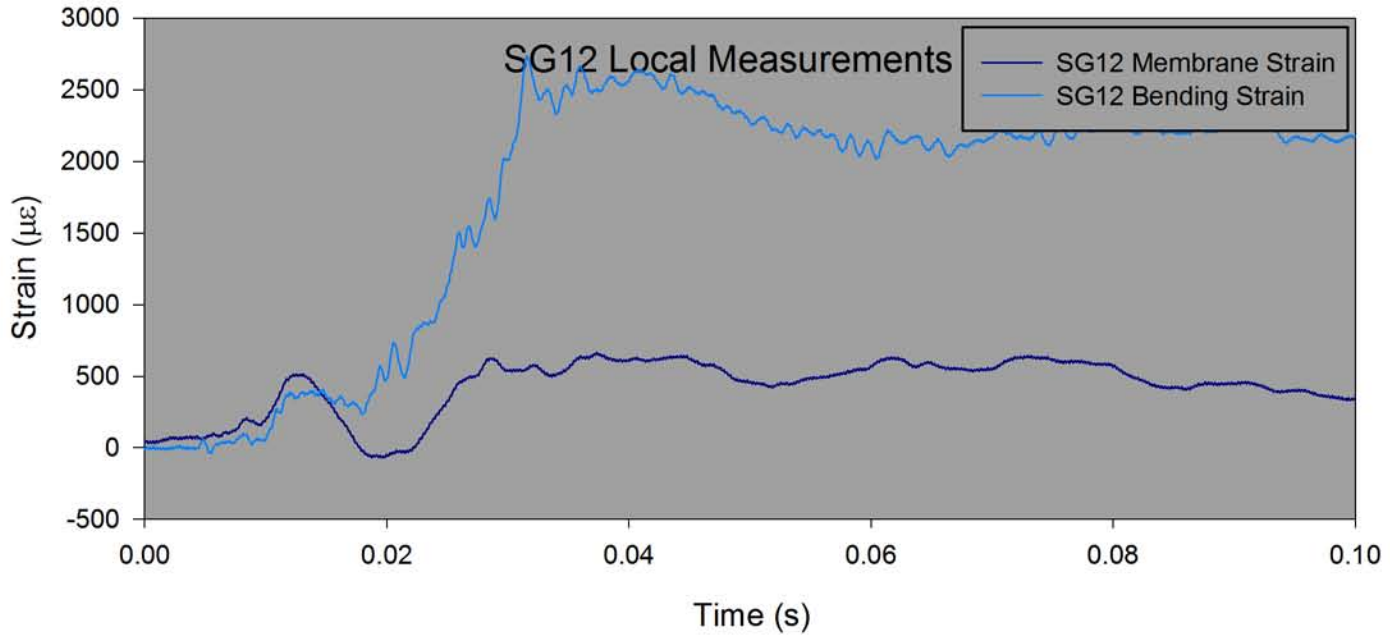

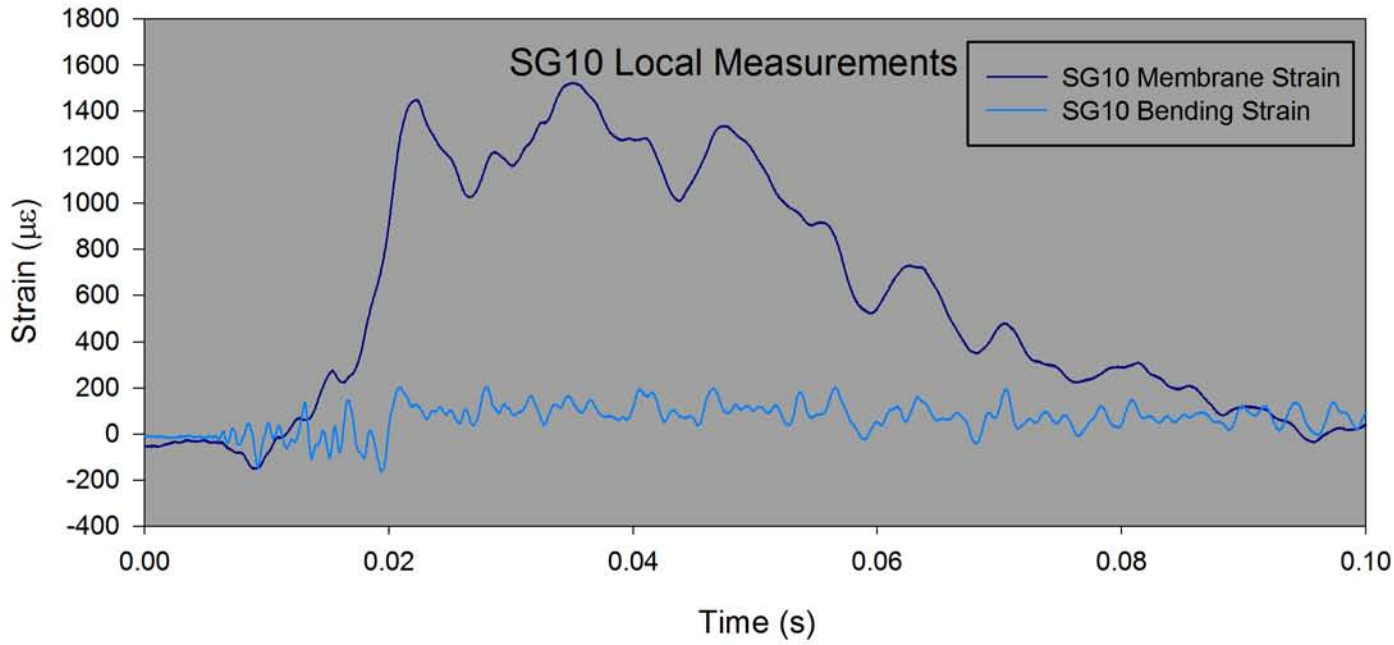

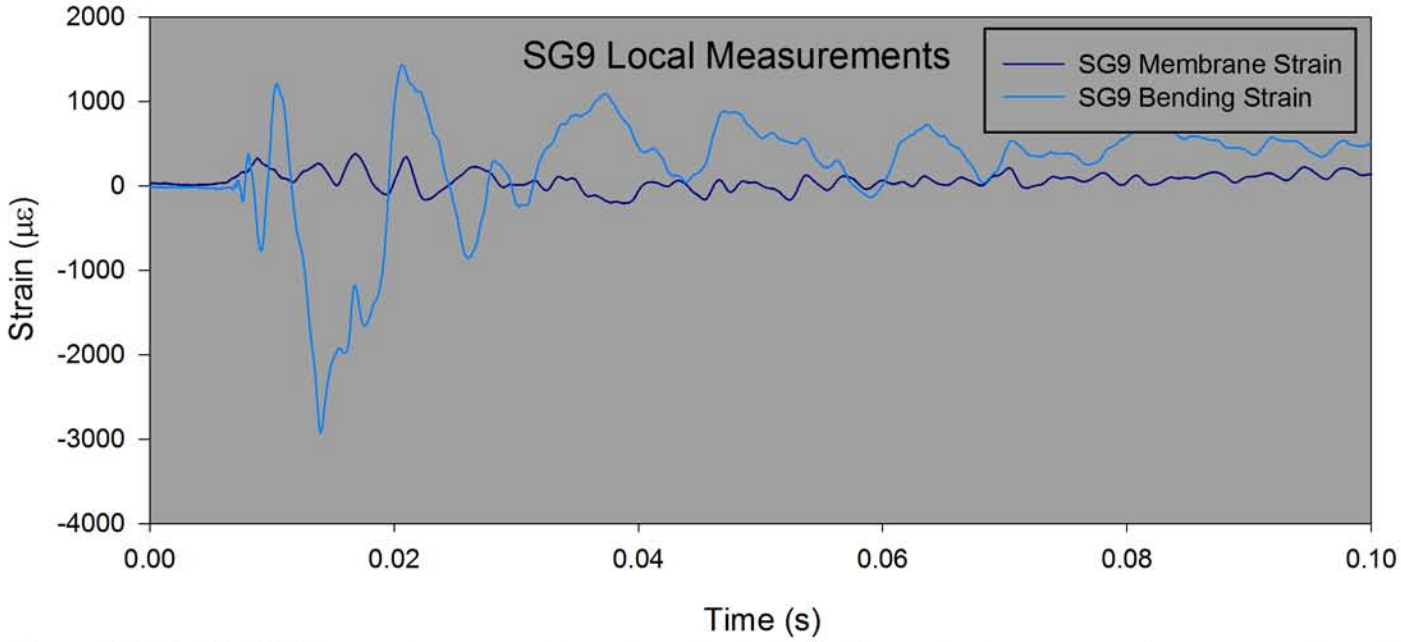

Figure 36 GRW J3910 membrane and bending strain from three strain gauge pairs - compartment 4

9.3.4 Pressure Measurements

Figure 37 shows the measurements from the pressure transducers for compartments 1b and 4. With the tanker in the upright position, as before, HSL have ordered the transducer numbers in the legend from the transducer at the 6 o'clock position at the top, to the transducer at the 12 o'clock position at the bottom. The pressure changes directly resulting from the impact occurred in a very short time period immediately after the impact.

Figure 38 shows the same measurements over a much shorter time period after the impact. The highest pressures were measured for the transducers closest to the impact point (around the 9 o'clock position), as expected. The transducers at the 6 o'clock and 12 o'clock positions show little deviation from 0 bar. As described before, many of the transducers were measuring acoustic waves as well as changes in water pressure.

The maximum pressure was measured on the transducers in the 9 o'clock position (transducer 445886 for compartment 1b, and 445882 for compartment 4). These transducers measured transient peaks around 6.9 bar (100 psi) at the moment of impact. About 0.04 seconds after impact, nearly all transducers were measuring pressures below 2 bar (29 psi), and about 0.05 seconds after impact (compartment 1) and 0.07 seconds after impact (compartment 4) all transducers were reading close to zero pressure.

9.3.5 Acceleration Measurements

As in the *proof of concept test* the accelerometer signals showed significant ringing causing the accelerometers to overload, and again the peaks of the signal were 'cropped'. Therefore, the resilient strip that was placed between the mounting block and the tanker, to act as a mechanical filter, was still allowing high frequency free vibration (ringing) to affect the measurement. Again, as filtering was unsuitable (explained in Section 9.2.5) the data was smoothed to reduce the effect of the rapid changes in signal amplitude due to these vibration components: for these measurements a 799-point moving average was selected, as before. These results were then compared with the acceleration calculated from the high speed video. The results are shown in Figure 39 for the y-axis accelerometer[xiii] and high speed video at the front of the tanker, and Figure 40 for the y-axis accelerometer and high speed video at the rear of the tanker. The accelerations measured from the accelerometer and calculated from the high speed video show good agreement with each other, but with differences after maximum deceleration (reasons for this are explained in Section 9.2.5).

9.3.6 Impact Velocity Measurements

The impact velocities obtained from analysing the high speed video were as follows:

- 4.55 m/s at the front of the tanker; and
- 4.25 m/s at the back of the tanker

Again the radius (r) (see Figure 22) at the front of the tanker is 2.47 m, and 2.20 m at the rear. Using equation (3) in Section 8.2

$\omega = \frac{v}{r}$ rads/sec

The rotational velocity at the front was $\omega = \frac{4.6}{2.47} = 1.84$ rads/sec

The rotational velocity at the rear was $\omega = \frac{4.3}{2.20} = 1.93$ rads/sec.

[xiii] *i.e. the accelerometer that is in the vertical position at impact*

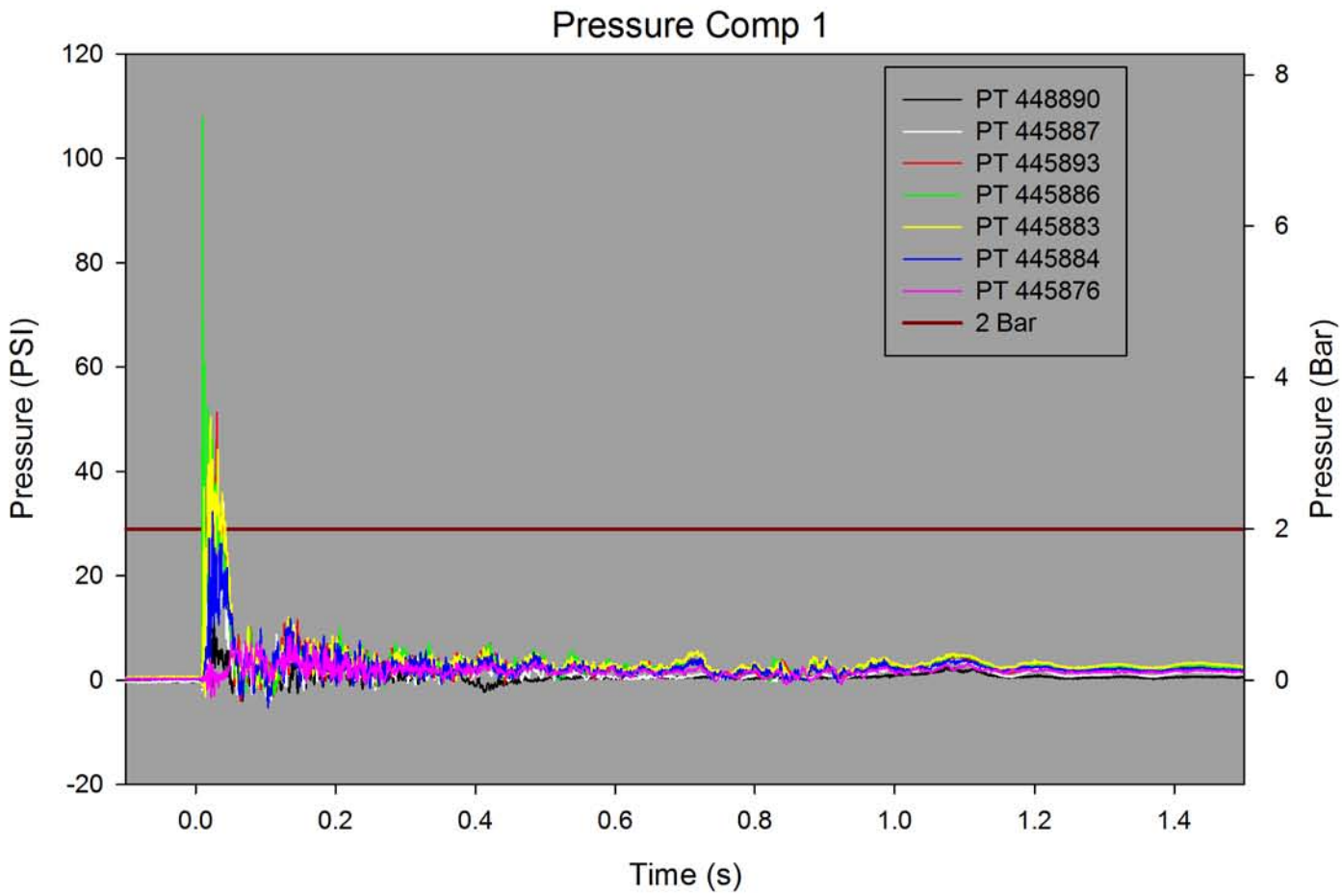

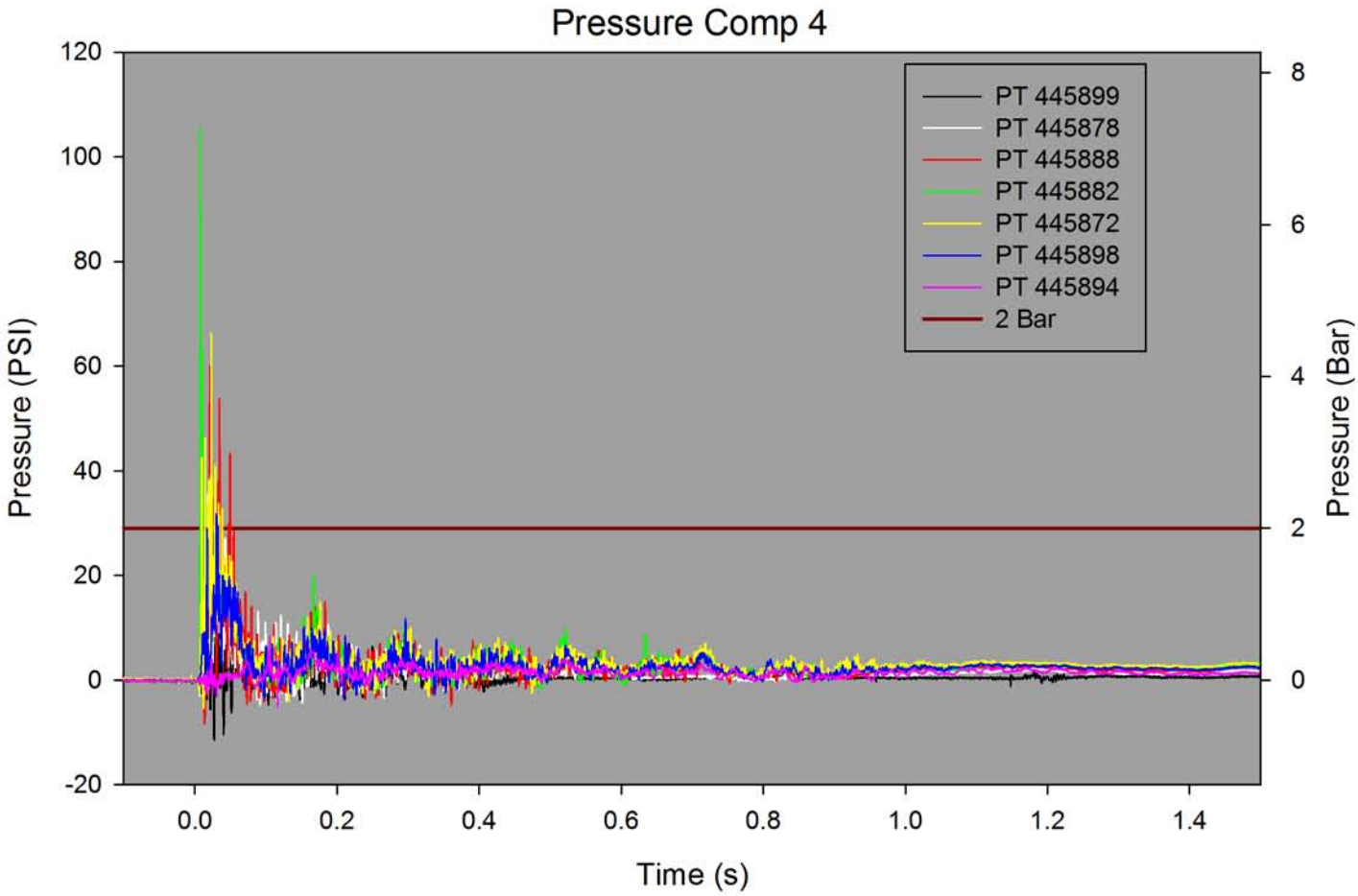

Figure 37 GRW J3910 pressure measurements - all transducers (full time history)

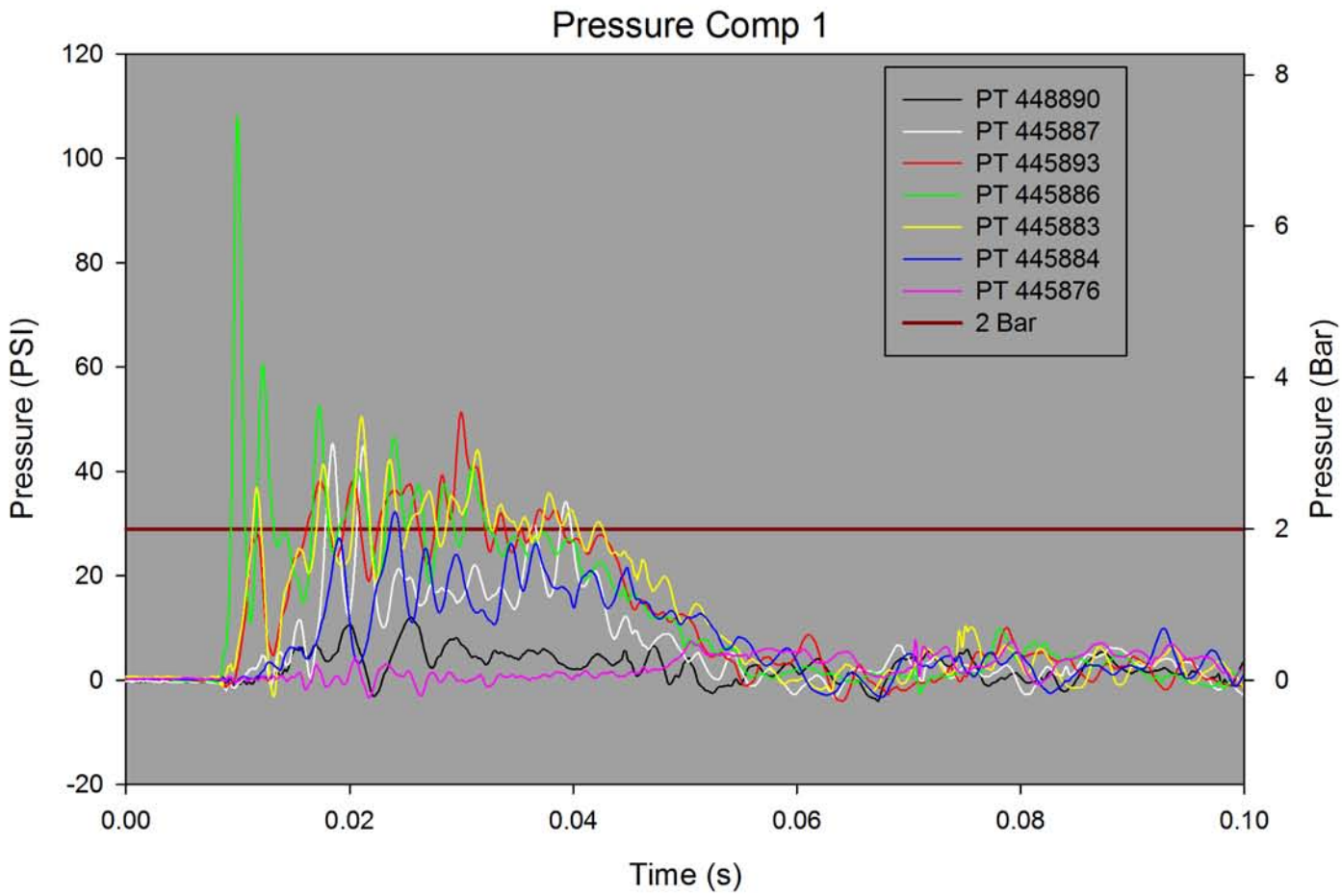

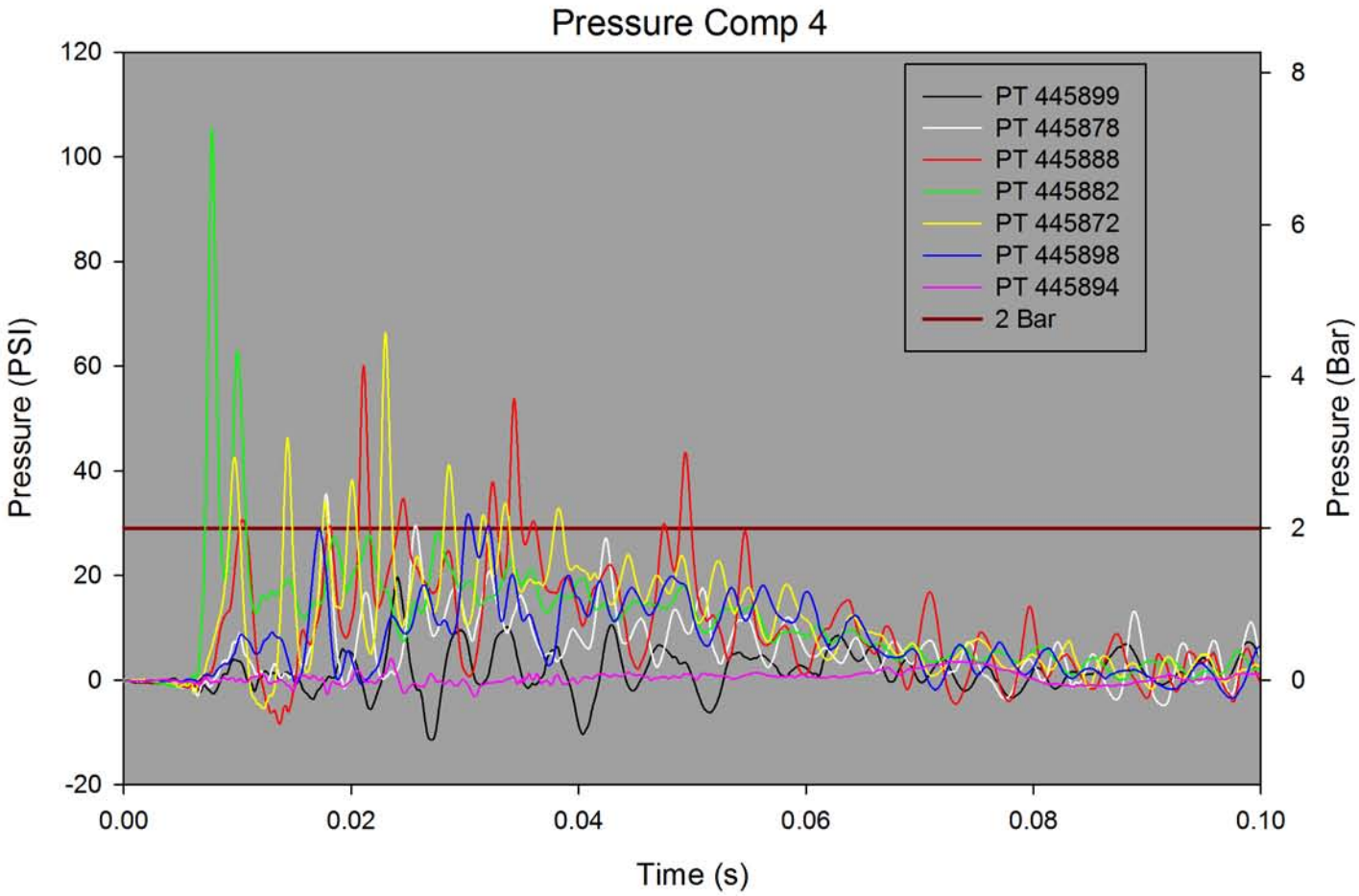

Figure 38 GRW J3910 pressure measurements - all transducers (impact event only)

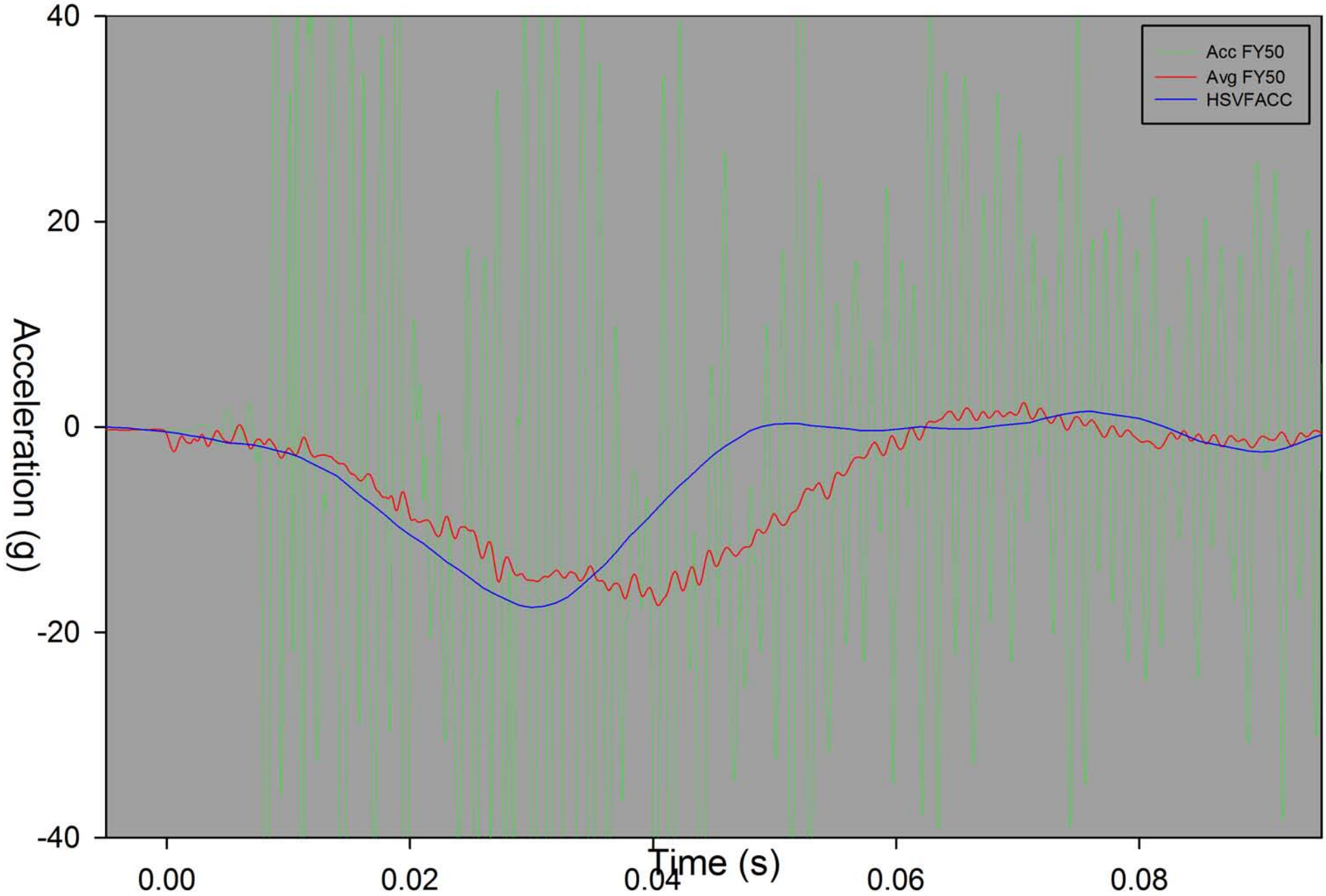

Figure 39 GRW J3910 acceleration measurements - accelerometer and HSV - front

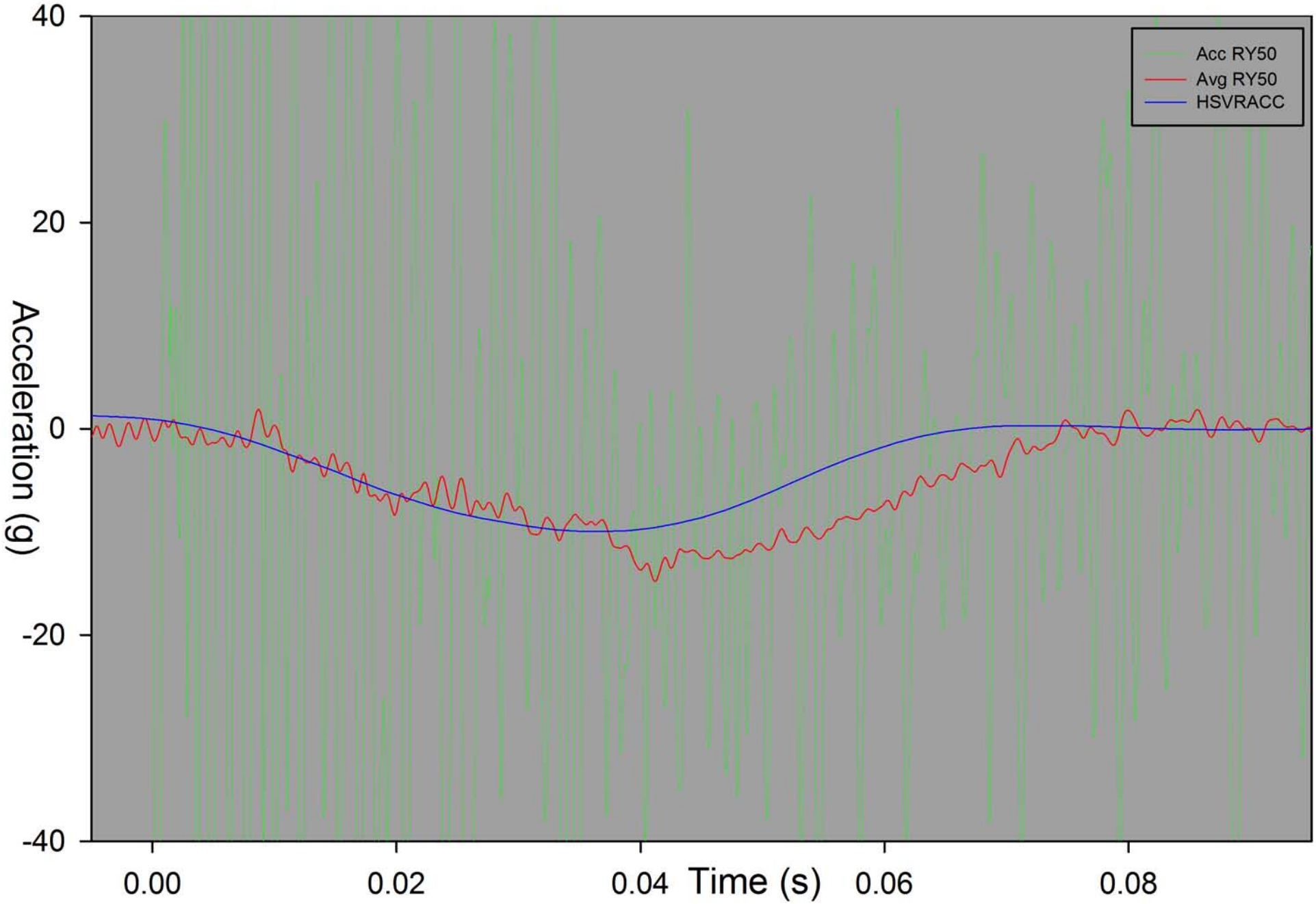

Figure 40 GRW J3910 Acceleration measurements - accelerometer and HSV - rear

9.3.7 Measurement grids after the test

Figure 41 shows the tanker after the tests with the measurement grids highlighted.

VPS 1407033_002

Figure 41 Grid locations on GRW tanker J3910 (after the topple test)

Figures 42 to 45 show close ups of the grids. The distances between the grid circles were measured after the test; the results are included in Appendix 3.

As a baffle forms a partial division between compartment 1a and 1b, *C1 Baffle F* refers to the grid located to the front side of the baffle, *C1 Baffle R* refers to the grid located to the rear side of the baffle. All other locations reference their position relative to the compartment, hence *C1 R* is located to the rear of compartment 1 and *C2 F* is located to the front of compartment 2 etc.

VPS 1407033_034

← tanker rear C1 Baffle R band B/8 C1 Baffle F tanker front →

Figure 42 Grids at compartment 1 baffle - GRW tanker J3910 after topple test

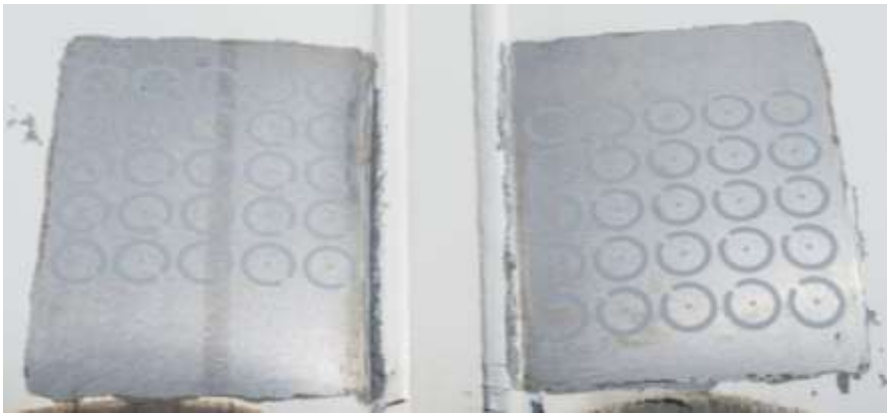

VPS 1407033_032

← tanker rear C2 F band C/8 C1 R tanker front →

Figure 43 Grids at compartments 1 and 2 - GRW tanker J3910 after topple test

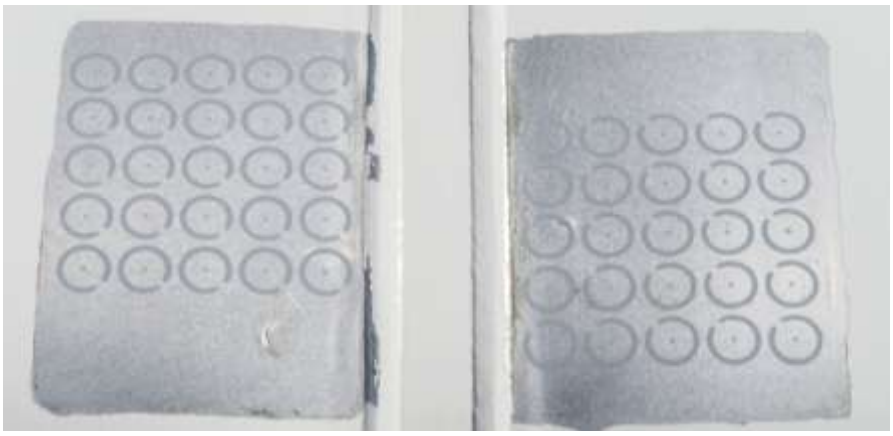

VPS 1407033_030

← tanker rear C4 F band E/8 C3 R tanker front →

Figure 44 Grids at compartments 3 and 4 - GRW tanker J3910 after topple test

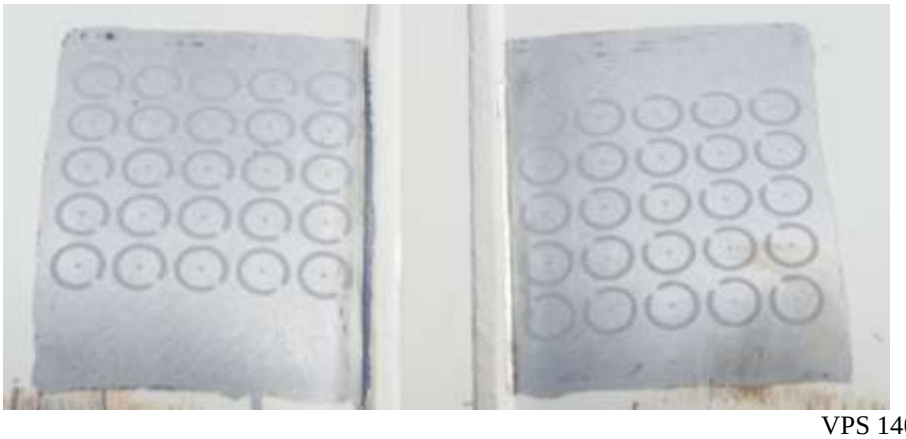

VPS 1407033_028

← tanker rear C5 F band F/8 C4 R tanker front →

Figure 45 Grids at compartments 4 and 5 - GRW tanker J3910 after topple test

9.4 COMPARATIVE MEASUREMENTS BETWEEN GRW TANKERS J2580 AND J3910

This section compares the strain and pressure measurements between the two GRW tankers.

Figure 46 is a combination of the information on strain gauge locations in Figures 15 and 16, and shows which strain gauges were fitted at the same positions on both tankers.

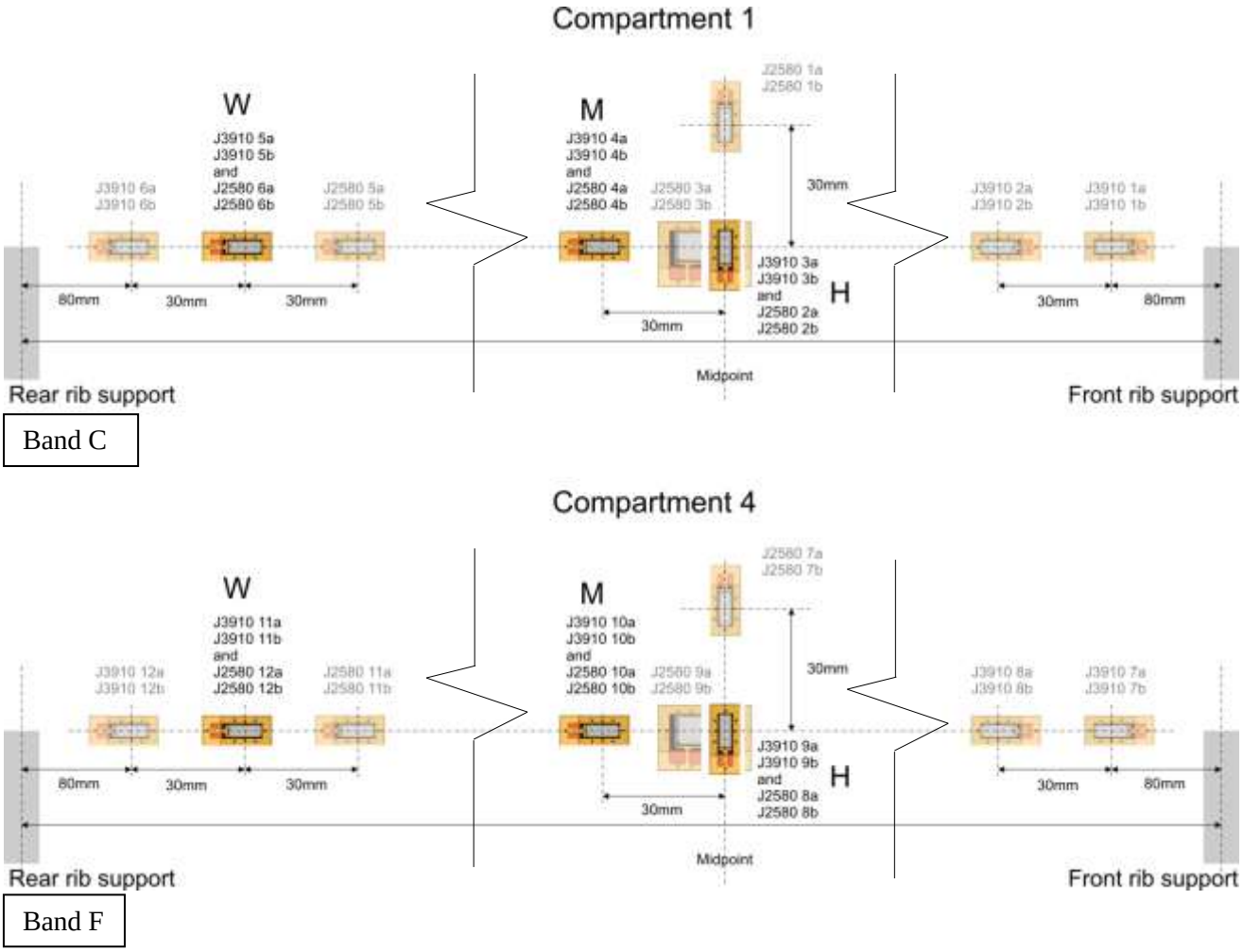

Figure 46 Strain gauge locations (not to scale) on the GRW tankers showing which gauges were in the same position

Gauges that are shown faded are those that were only in that position on one of the tankers, gauges shown in full colour are those that were in the same position on each tanker. **W** refers to the gauges close to the weld at the rear rib support, **M** refers to longitudinal gauges near the midpoint, and **H** refers to circumferential (or hoop) gauges. The strain gauge numbers from Figures 15 and 16 are also shown.

In the measurement time histories, as the zero point (described in Section 9.2.2) is slightly different for the two sets of measurements on the GRW tankers, some of the following strain and pressure curves have been adjusted horizontally along the time base where necessary to ensure the beginning of the impact is at exactly the same point in time for each set of measurements. The time adjustments required were of the order of 2 to 3 milliseconds.

Figure 47 shows the strain gauge measurements for the **H** gauges. **Ha** refers to the outer gauges and **Hb** refers to the inner gauges. The positions of the peaks and troughs in the measurement pairs reasonably agree in a number of cases - however there is some variation between the pairs. In compartment 1b the curves are in quite different positions at 0.02 to 0.05 seconds on the time base but still show a similar trend. The tanker shell in J2580 appears to be experiencing greater compressive strains at the outer gauge, and greater tensile strains at the inner gauge. In compartment 4 the response to the initial impact corresponds well for inner and outer gauges. Although the J3910 gauge shows greater tensile strain at the outer gauge, and greater compressive strain on the inner gauge, these differences are fairly minor.

Figure 48 shows the measurements for the longitudinal **M** strain gauges close to the midpoint of the compartments. For compartment 1b, both pairs show peaks and troughs at similar positions on the timebase, and the gradients of the curves after impact are reasonably similar. For compartment 4, the curves are very similar.

Figure 49 shows the measurements close to the weld **W** at the rear bulkhead. As gauge J3910 5b in compartment 1b was unreliable, the large difference between the two curves at **Wb** in compartment 1 (bottom left hand curves in the figure) is probably due to this, and not due to a difference in response. All other measurement pairs show similar responses in each case, although the results for compartment 4 do show consistently higher tensile strain on the outer gauge, and lower compression strain on the inner gauge, for J3910.

Figure 50 shows the pressure response for compartment 1b. The pressure transducers shown are the three closest to the impact point (see Figure 19). The closest transducer to the impact is 445886, which explains the high initial peak of around 110 psi (7.6 bar). The agreement between the transducer pairs is very good in all three cases with similar amplitudes, and similar periodicity on the timebase.

Figure 51 shows the pressure response for compartment 4. Again, the closest transducer to the impact (445882) measured the highest pressure at impact of around 110 psi (7.6 bar). The agreement between measurement pairs is very good.

As the strain measured at the gauges is changing before, during and after the test, to give an overall picture, Table 12[xiv] shows the strain measured at each gauge at three discrete time segments during the test as follows:

- The point where the tanker begins to topple **(Topple Point)**.
- The moment before the impact (at the point that the first accelerometer starts to measure the impact event) **(Pre Impact)**.
- 10 to 15 seconds after the impact **(Post Impact)**.

The final column for each tanker shows the difference between the topple-point strain, and the post-impact strain. As before all values of strain are in microstrain.

[xiv] *Each measurement channel generated about 770 000 data points (i.e. approximately 15 seconds of data at a sampling rate of 50 kilo samples/second). To reduce this to a practical size, every 100 sequential data points were averaged together to give 100-point averages. To get the 'topple point' data, 100 of these 100-point averages were averaged together: so the 'topple point' measurement for each gauge consists of an average of 10 000 data points. The 'pre impact' data was an average of 60 100-point averages, and the 'post impact' data was an average of 357 100-point averages. The benefit of averaging is to smooth the data and remove the effect of random noise and transients on the measurements. Note that this smoothing technique was employed only for this particular analysis*

Table 12 Strain measurements, in microstrain (με), before, during and after the impact for the GRW tankers J2580 and J3910

J2580						J3910				
Strain gauge no.	**Topple-point**	**Pre-Impact**	**Post-Impact**	**Topple Point – Post Impact**	**Lines show which strain gauges are in identical positions on each tanker**	**Strain gauge no.**	**Topple-point**	**Pre-Impact**	**Post-Impact**	**Topple Point – Post Impact**
1a	-204	-100	-254	-50		1a	159	-47	1 485	1 327
1b	-9	-140	-28	-19		1b	20	-28	-1 854	-1 874
2a	-225	-104	-539	-315		2a	170	-47	417	247
2b	-10	-160	358	368		2b	-68	-23	-847	-779
3a	-84	-124	322	406		3a	-20	26	-45	-26
3b	-106	-162	162	268		3b	65	-8	57	-8
4a	-96	-143	304	400		4a	0	-32	430	430
4b	-43	-99	221	265		4b	15	-29	236	221
5a	-41	-149	-490	-449		5a	79	-43	-87	-165
5b	-67	-152	-288	-221		5b				0
6a	-13	-134	-238	-224		6a	71	-51	335	264
6b	-43	-128	-704	-661		6b	51	-51	-2 905	-2 956
7a	-93	-110	-54	40		7a	71	-5	975	905
7b	-119	-94	-113	6		7b				0
8a	-90	-133	-584	-494		8a	64	-15	151	87
8b	-183	-128	208	391		8b				0
9a	-5	-130	393	398		9a	16	13	288	272
9b	-7	-126	350	357		9b	35	42	-284	-318
10a	6	-118	421	415		10a	45	-57	630	584
10b	24	-96	388	364		10b	71	-31	457	386
11a	-63	-102	210	272		11a	50	-5	1 930	1 880
11b	-180	-90	-1 018	-838		11b	-27	35	-1 235	-1 208
12a	-40	-91	1 066	1 107		12a	73	42	2 727	2 654
12b	-183	-85	-2 471	-2 288		12b	35	49	-1 788	-1 823

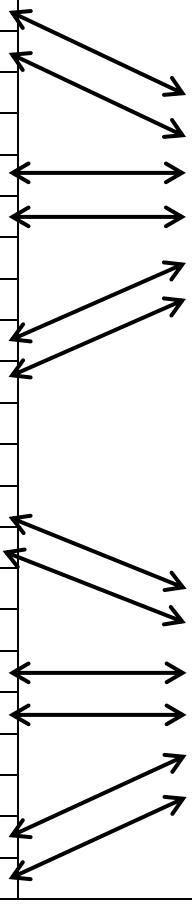

9.5 COMPARISONS BETWEEN PRESSURE AND STRAIN

As a comparison of the pressure and strain time histories after impact, measurements of both have been included on the same graphs. Figure 52 shows the measurements for GRW tanker J2580, and Figure 53 shows the measurements for GRW tanker J3910.

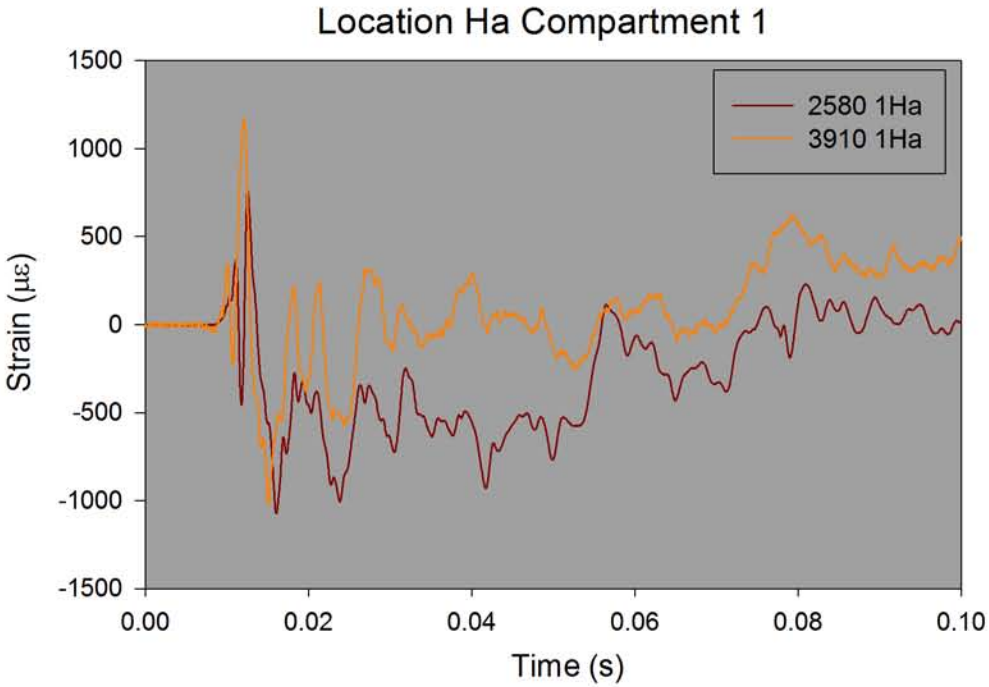

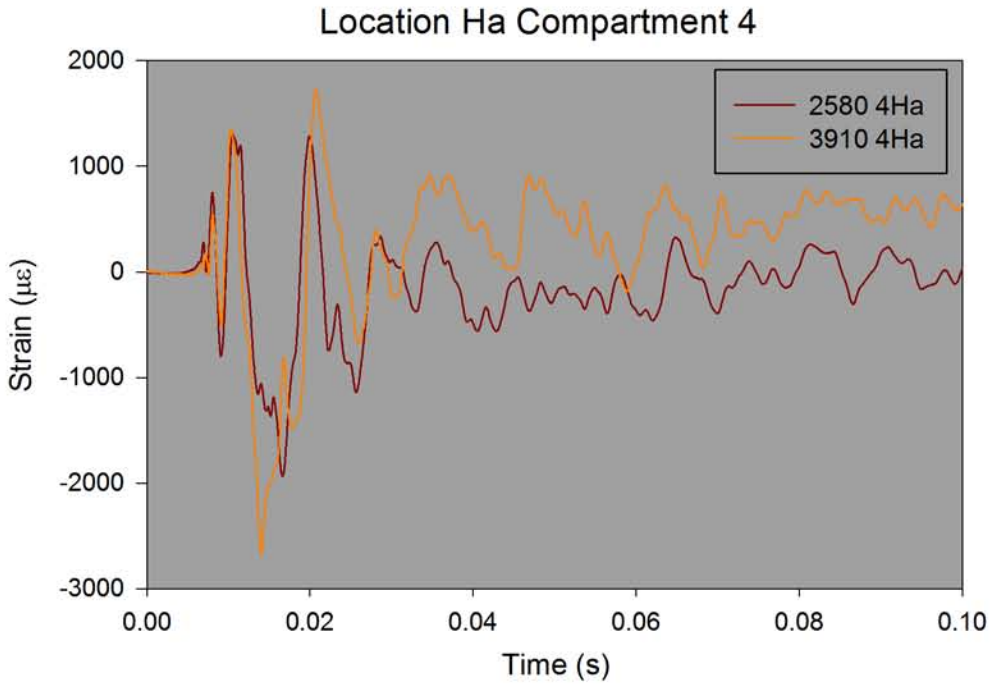

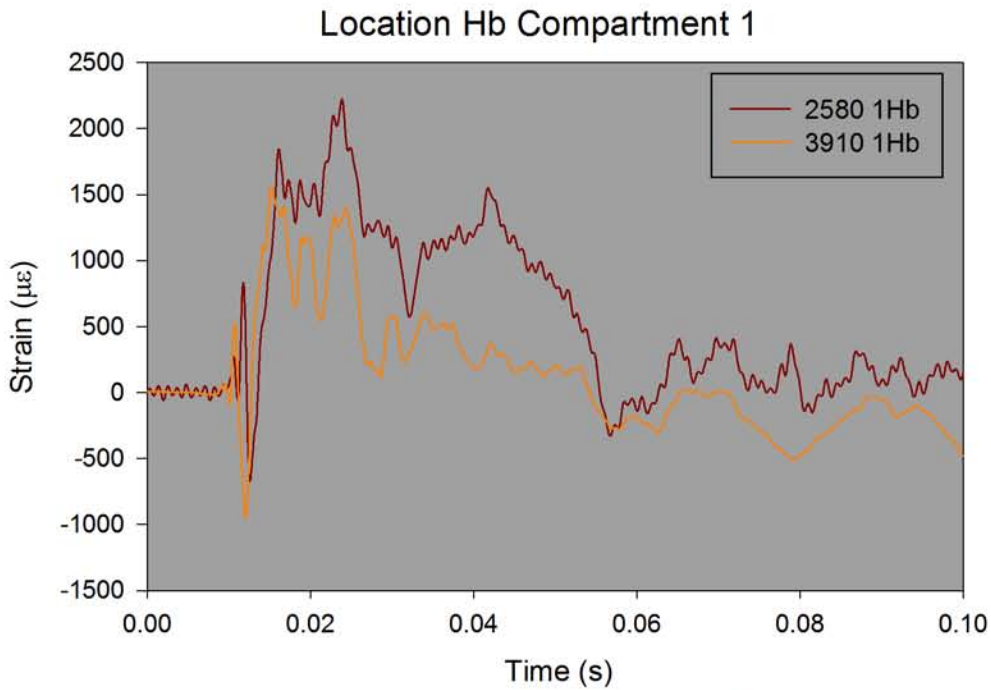

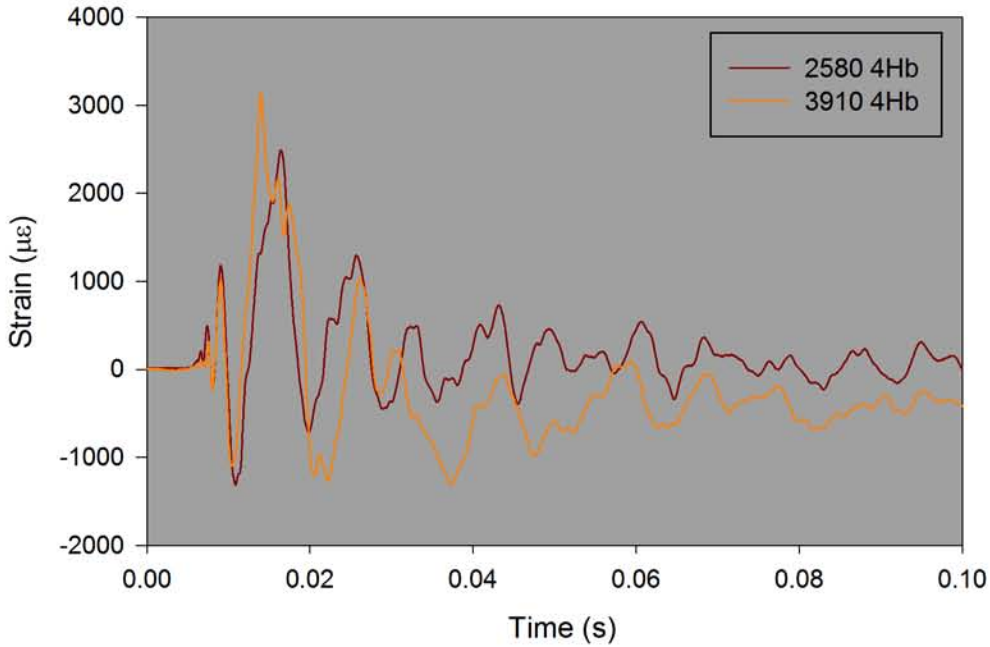

Figure 47 Strain measurement comparison - central hoop strain

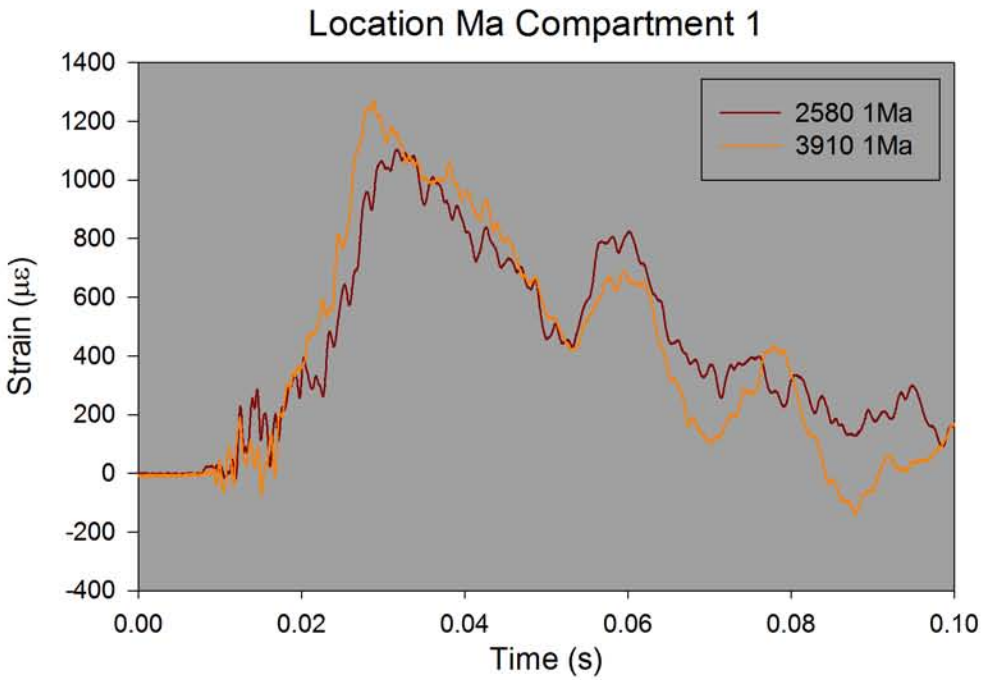

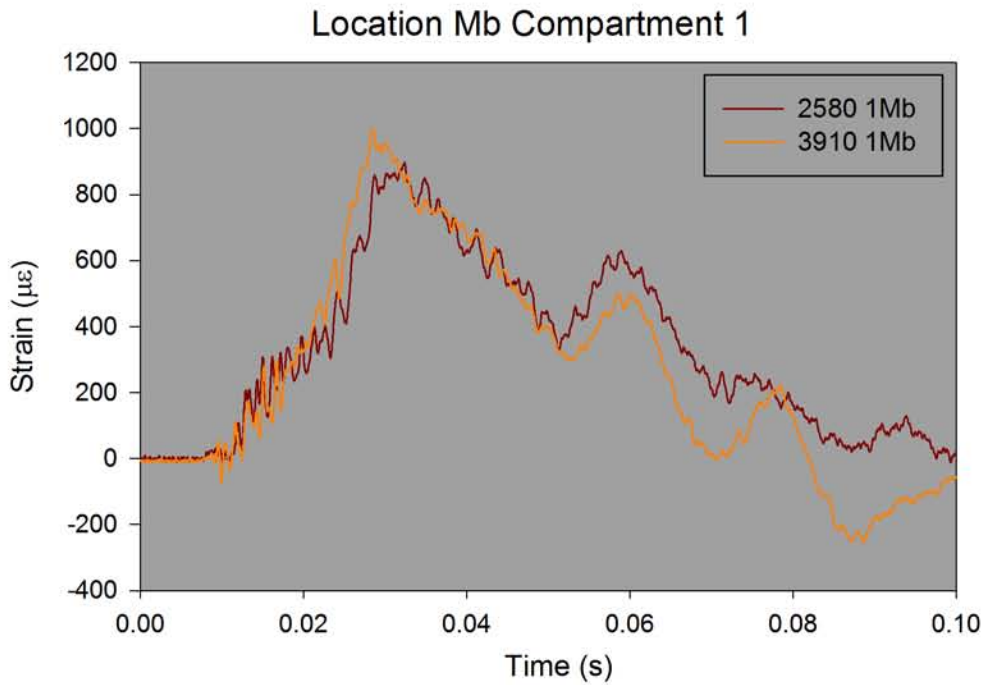

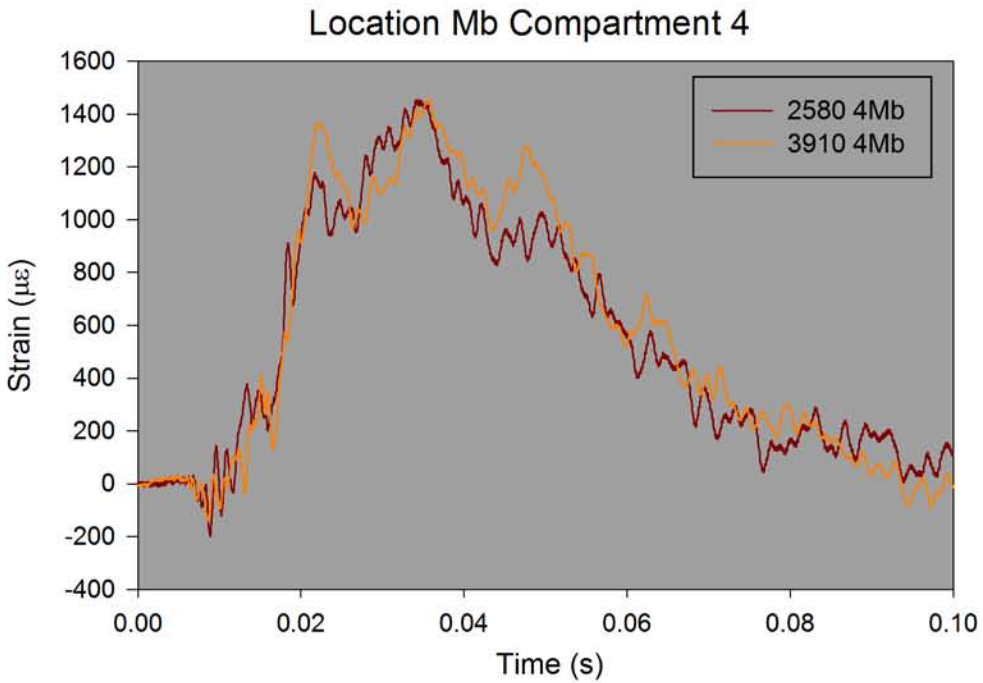

Figure 48 Strain measurement comparison - central longitudinal strain

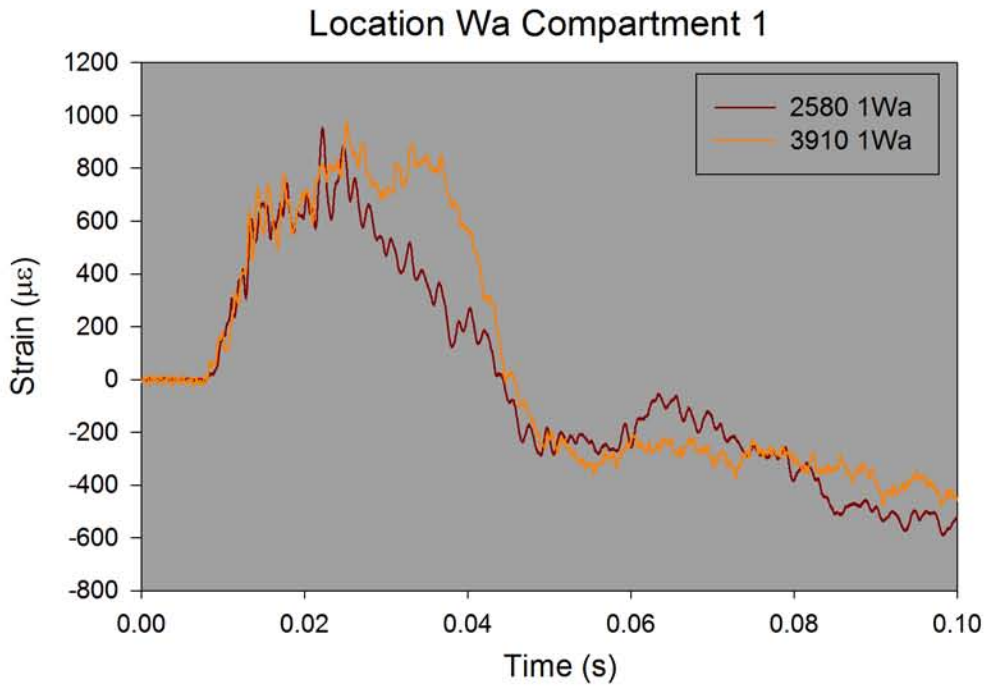

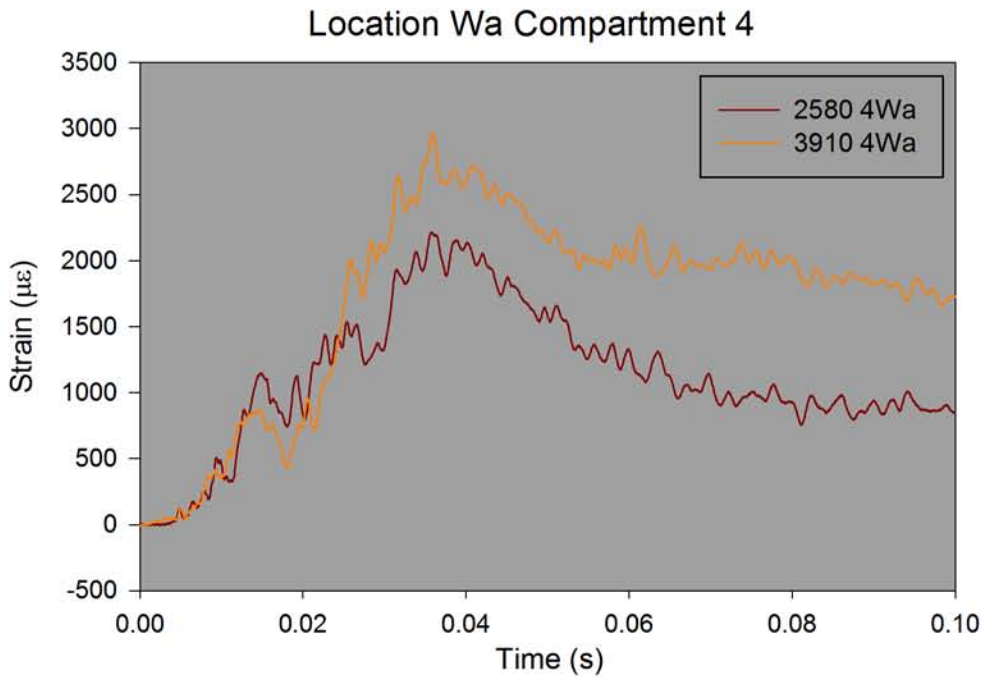

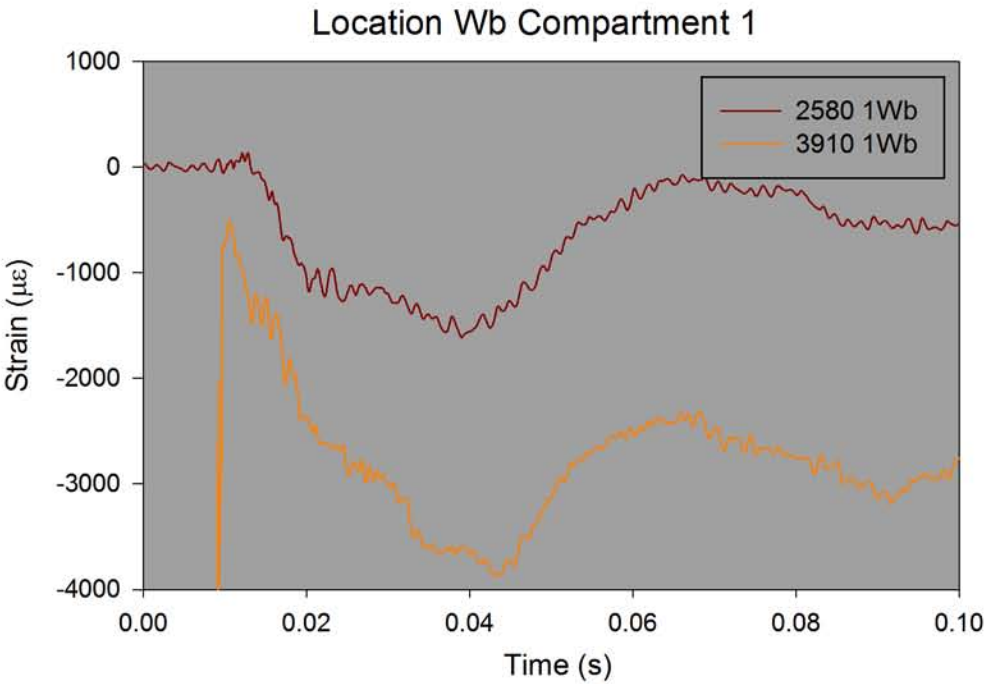

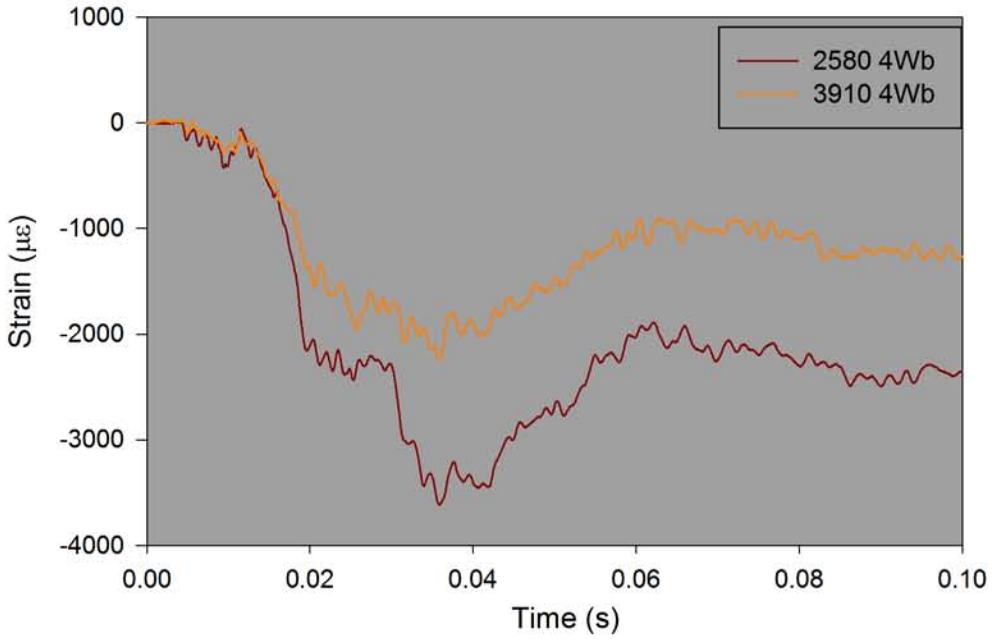

Figure 49 Strain measurement comparison - longitudinal strain near the weld at the rear bulkhead

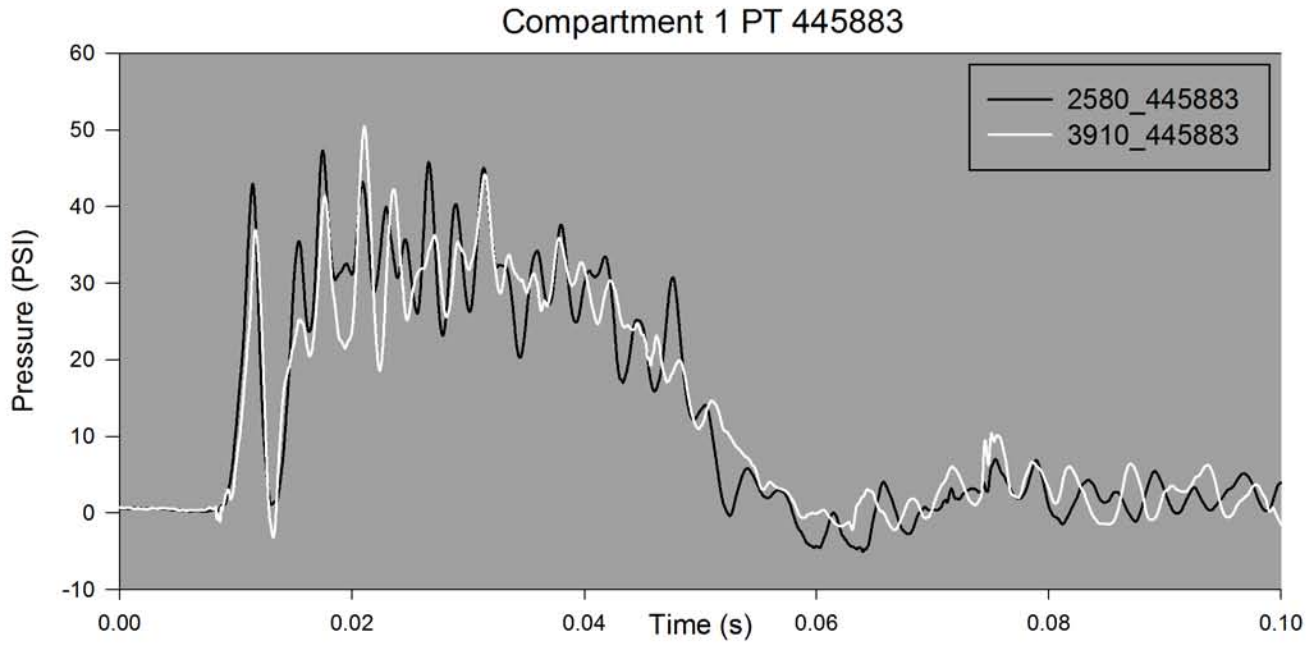

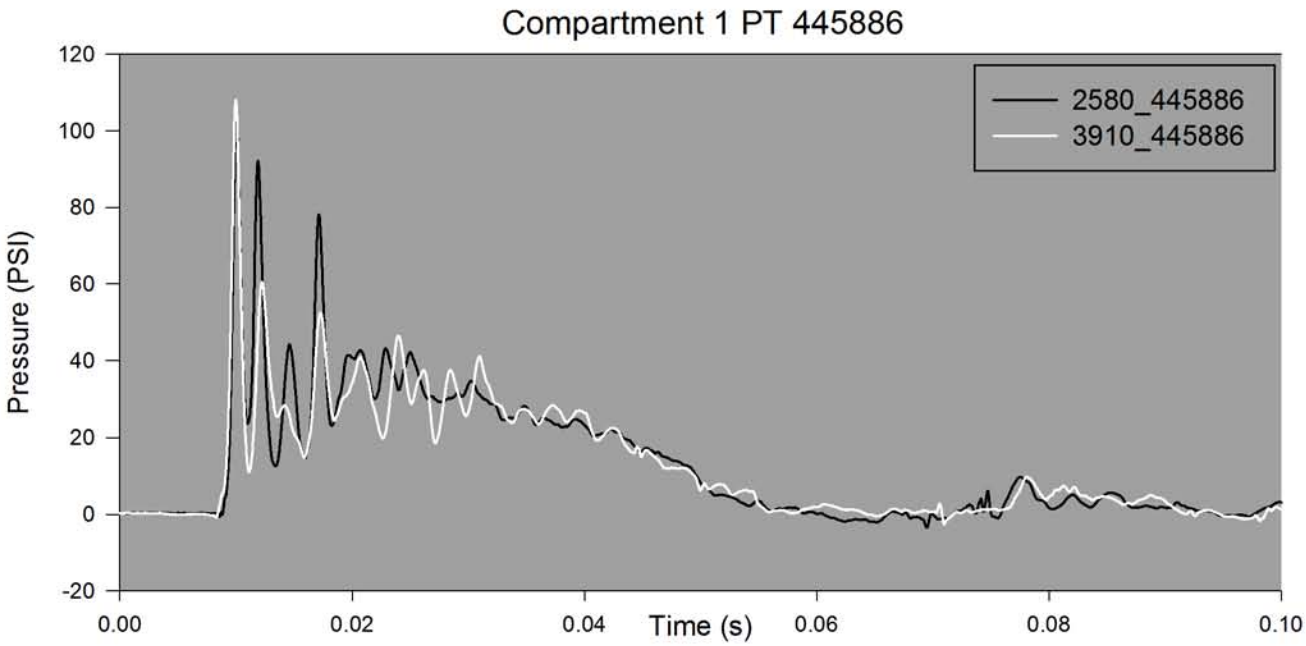

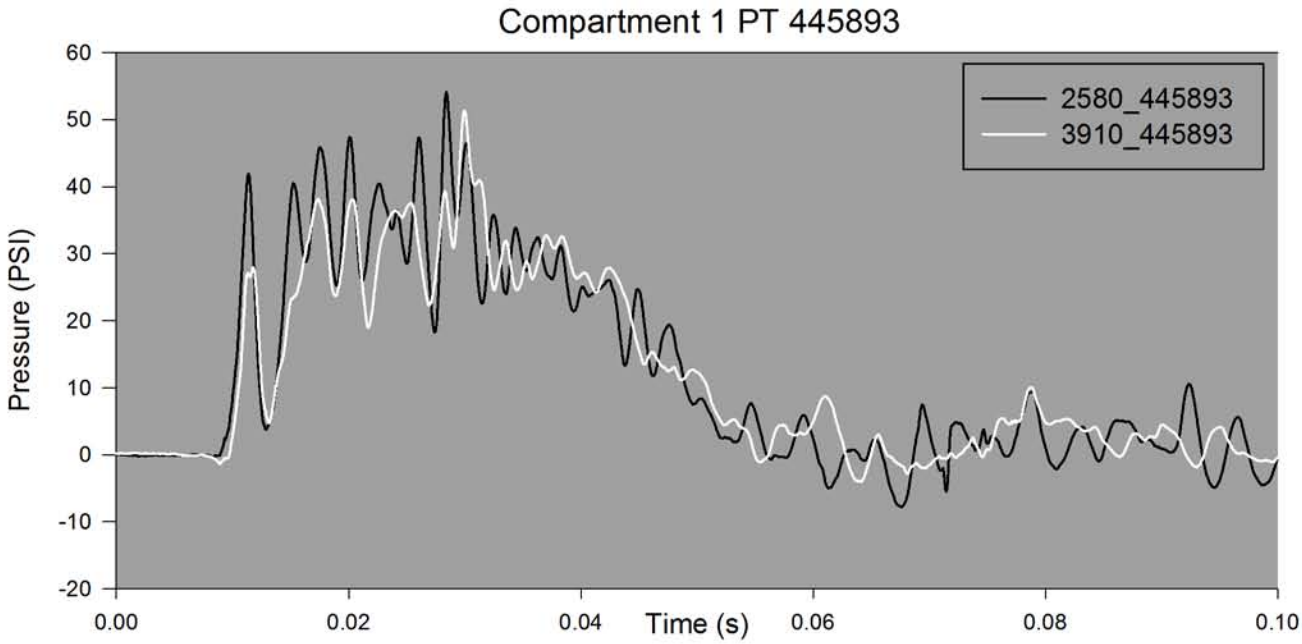

Figure 50 Pressure measurement comparison - compartment 1

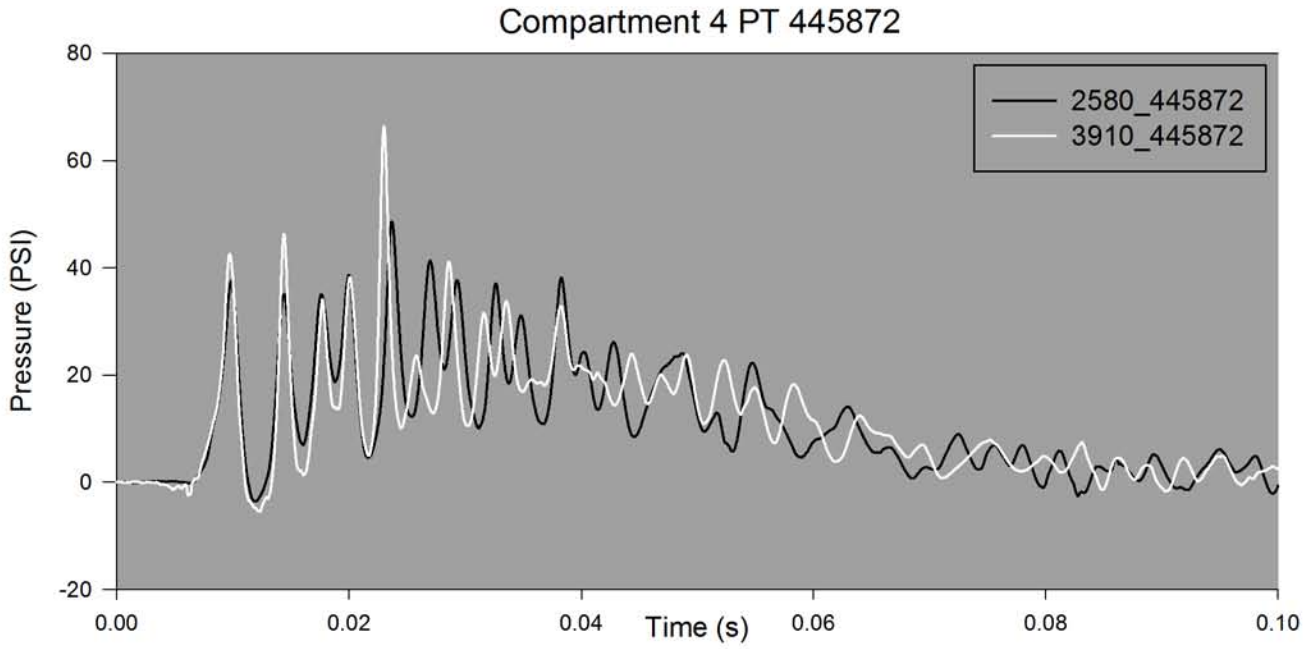

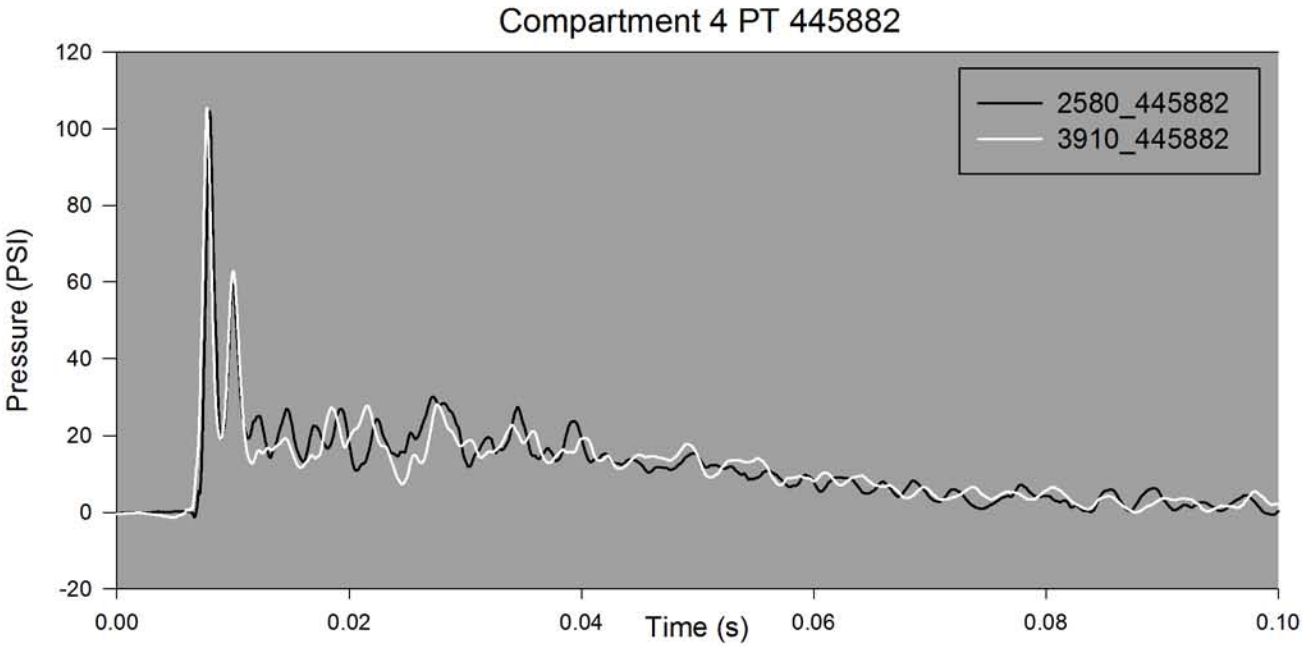

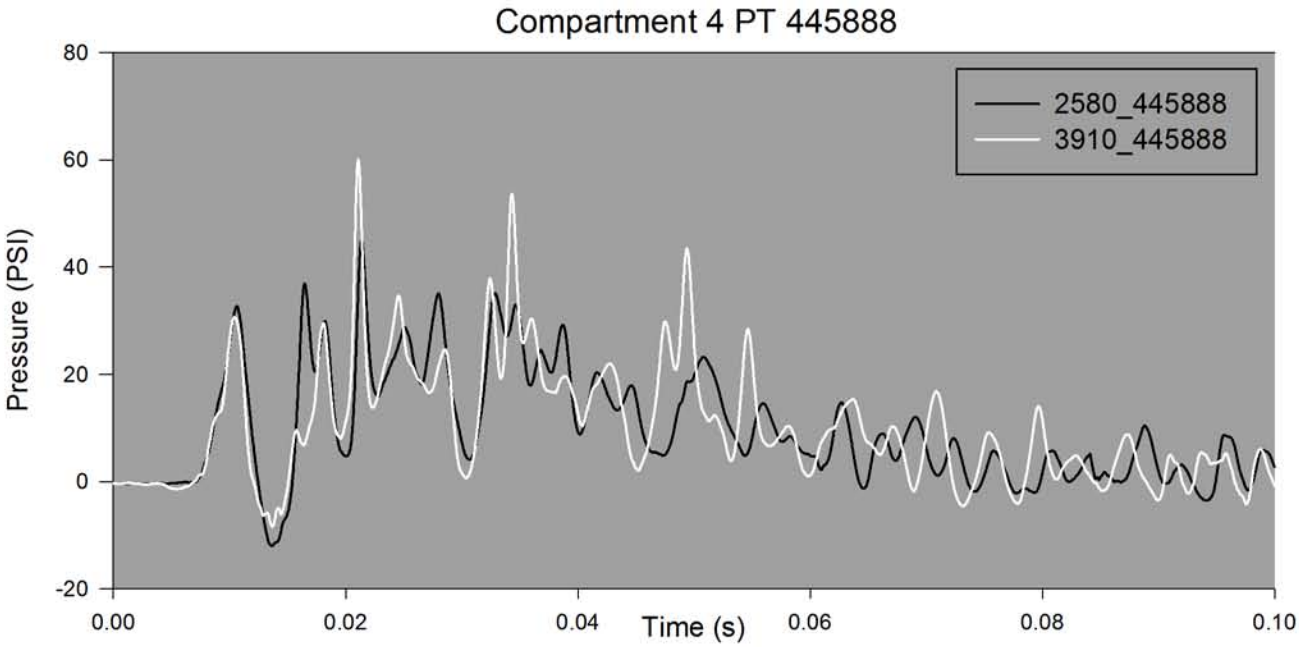

Figure 51 Pressure measurement comparison - compartment 4

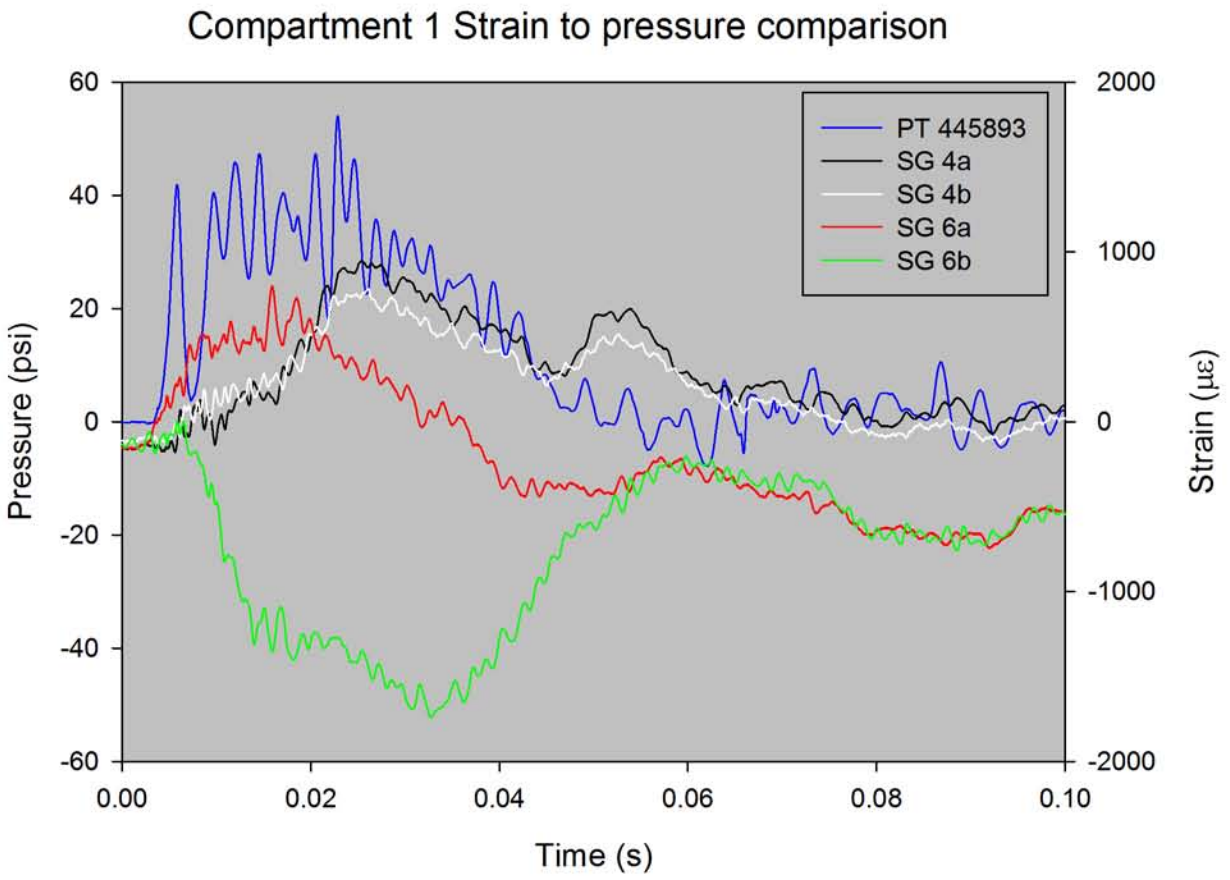

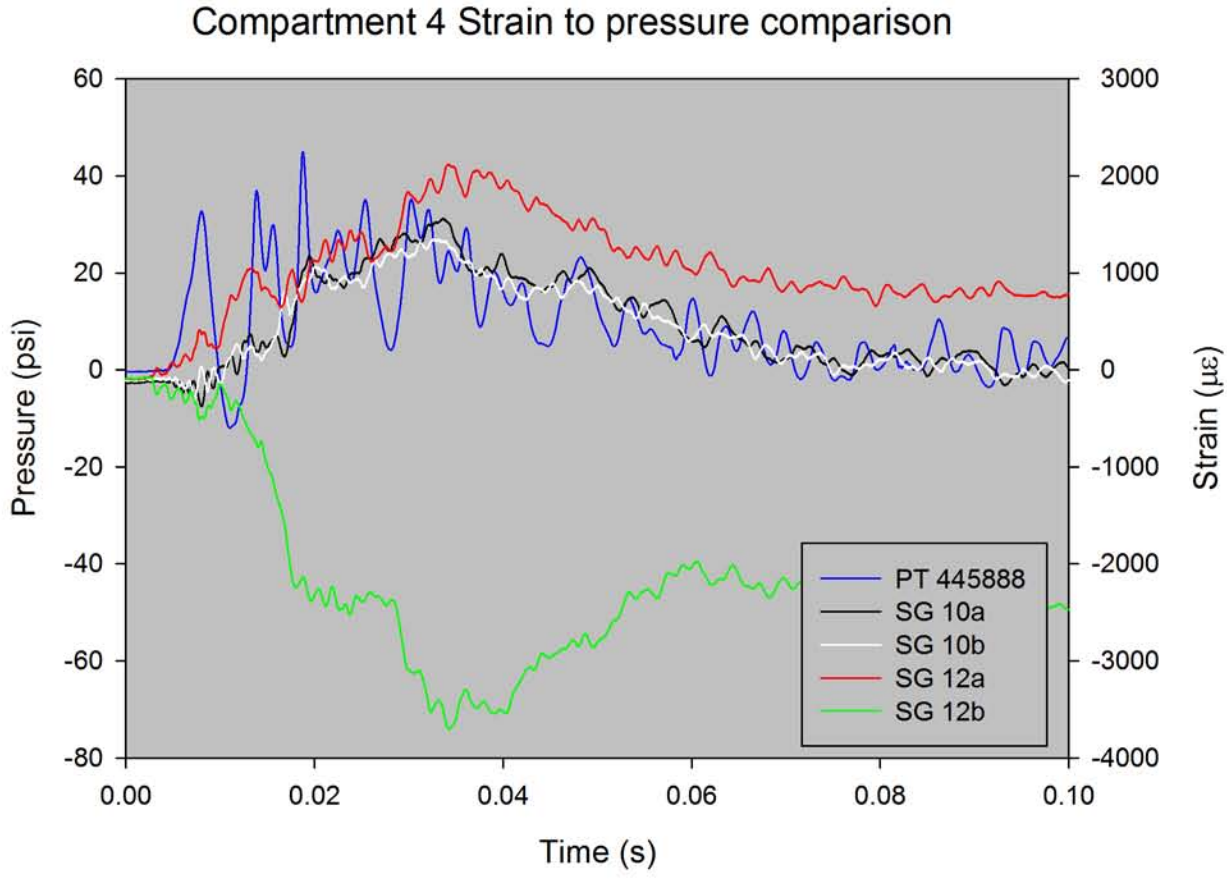

Figure 52 GRW J2580 strain and pressure measurements

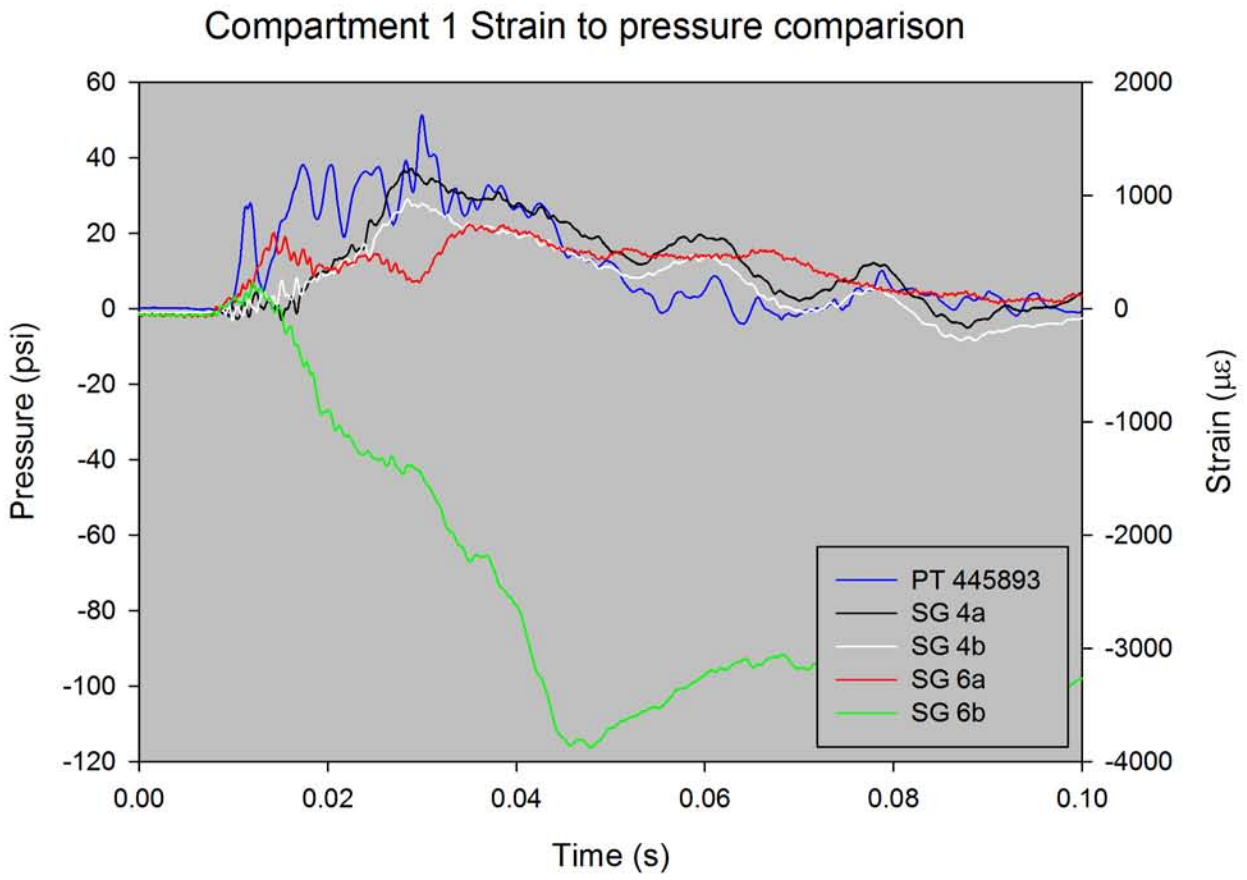

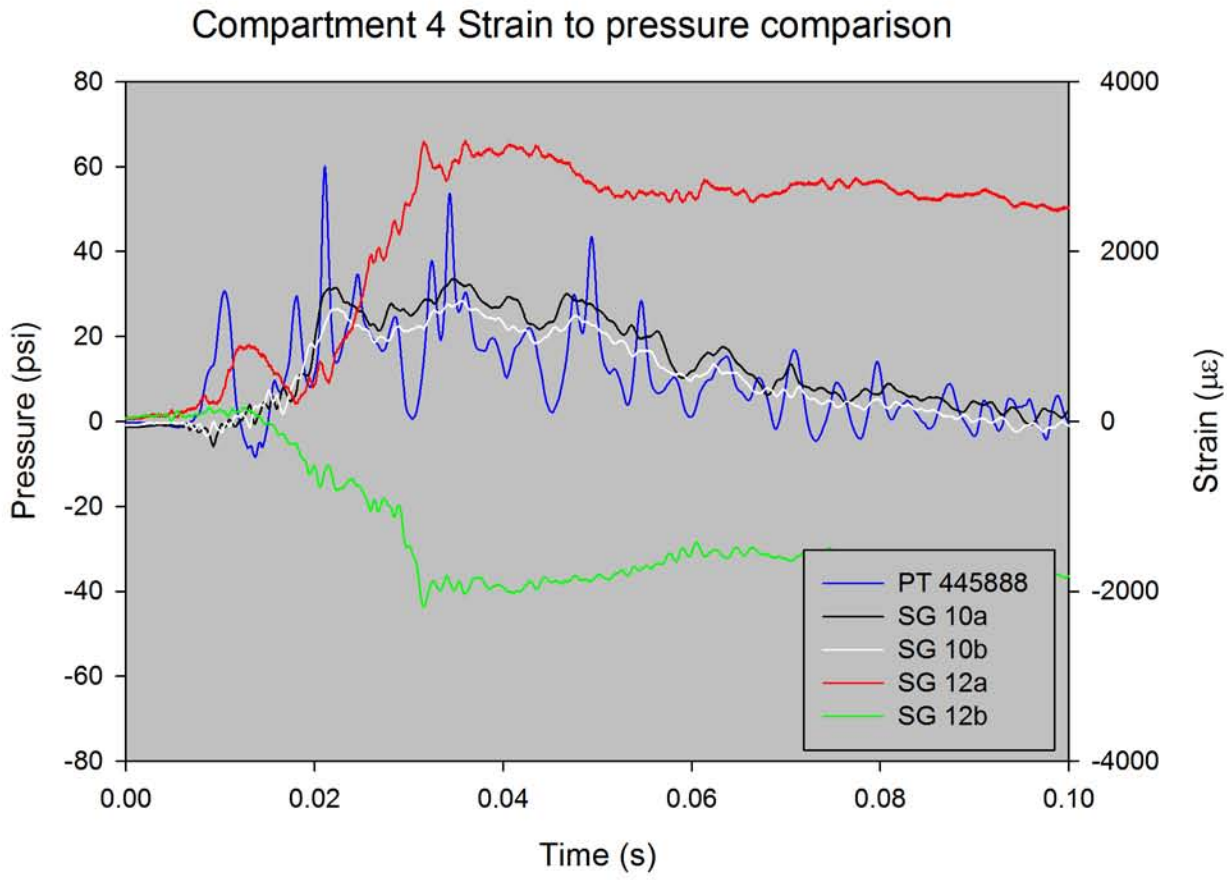

Figure 53 GRW J3910 strain and pressure measurements

9.6 SUMMARY DAMAGE ASSESSMENT

This section contains a brief discussion on the key damage observed after the topple test for each of the three tankers tested.

9.6.1 Proof of concept tanker

On the initial impact, a significant amount of water was expelled from the tanker through the manway pressure relief valves, as shown in Figure 54. Some of the pressure relief valves continued to leak after the test; most notably the valve on compartment 3 where the seal had 'unseated' (Figure 55). This is not particularly surprising as the manway seals and pressure relief valves had not been tested or adjusted before the test.

VPS1404007_016

Figure 54 Initial impact of the tanker with significant water loss from pressure relief valves – *proof of concept* tanker

VPS 1404007_053

Figure 55 Leakage from pressure relief value due to unseated seal – *proof of concept* tanker

Immediately after impact, there was a small leak from an area in the impact zone at the front of the tanker as shown in Figure 56. This was located in a buckled section where the front bulkhead met the side of the tanker.

VPS 1404007_030

Figure 56 Leak from the front of the *proof of concept* tanker

Before emptying the tanker it was found that little water remained due to leakage from all the compartments through this leak in the front bulkhead. The welds connecting all the internal bulkheads to the shell of the tanker had failed. Figure 57 shows one example of bulkhead weld failure.

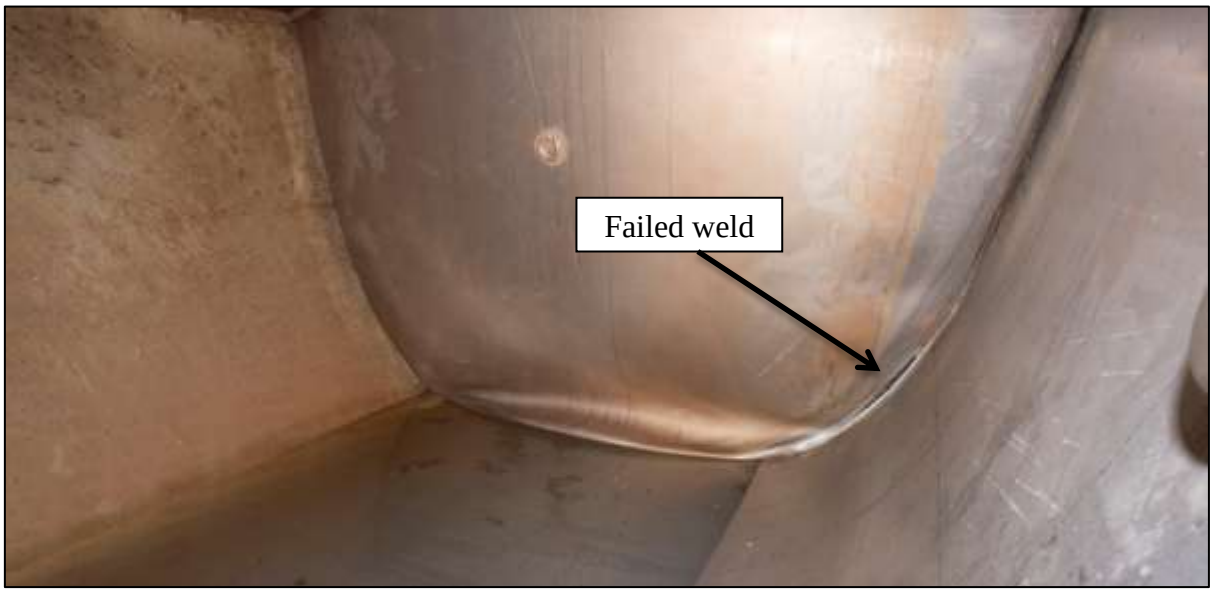

VPS 1404016_030

Figure 57 Inside the *proof of concept* tanker showing failure of bulkhead weld

Figures 58 and 59 show images from the laser scan of the tanker after the test, while still on its side. From the laser scan data before and after the test, the level of deformation at the rear was approximately 100 mm.

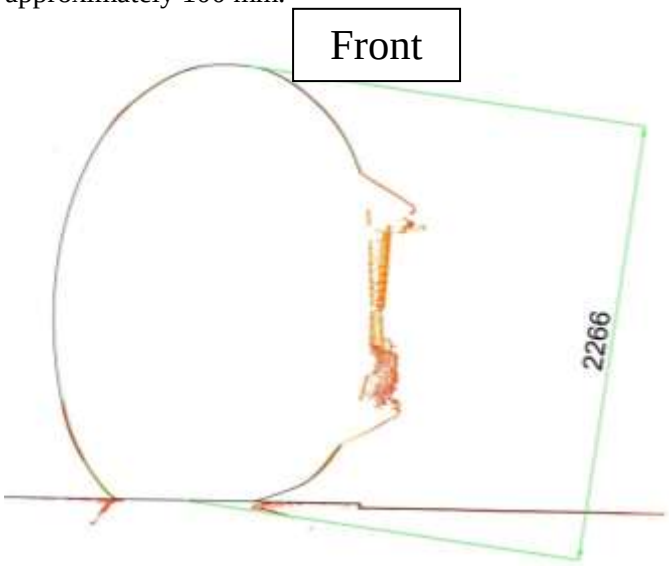

Figure 58 Deformation of *proof of concept* tanker from laser scans after test (front)
all dimensions mm

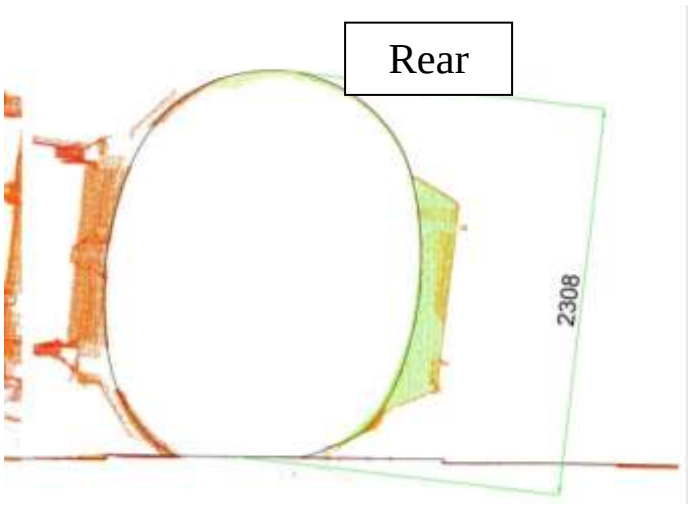

Figure 59 Deformation of *proof of concept* tanker from laser scans after test (rear)
all dimensions mm

9.6.2 GRW tanker J2580

Figure 60 shows six images form the high speed video for each end of the tanker in 20 ms steps from the moment of impact to 100 ms later.

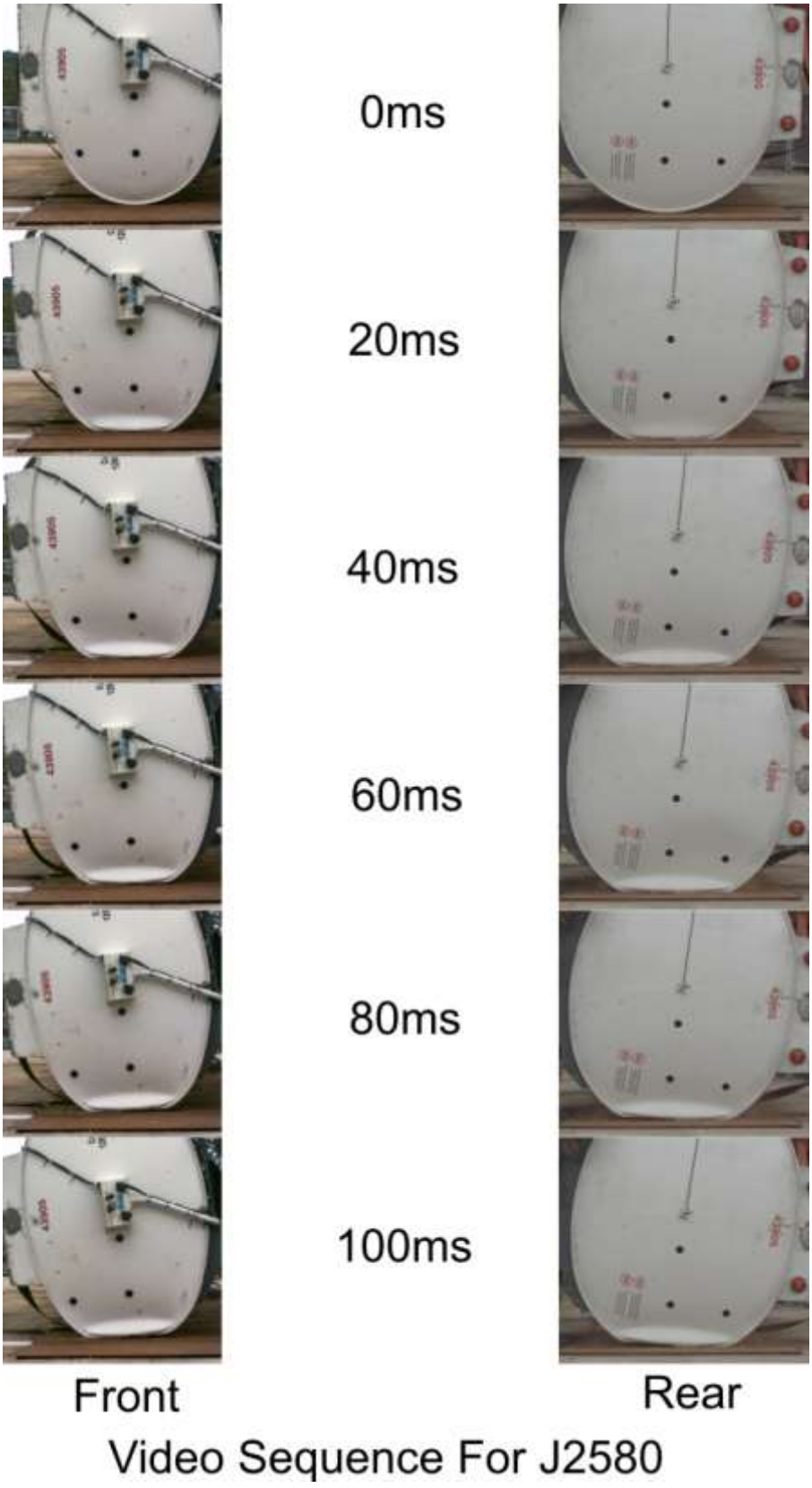

Figure 60 High speed video images during impact – GRW tanker J2580

9.6.2.1 External leaks and internal integrity of compartments

During the impact, some water was lost through the pressure relief valves (Figure 61). Examination of the videos and stills photography found that the amount of water lost in this way was minimal. Due to the lower level of water than would have been the case for road fuel, the pressure relief valves may not have been in full contact with the water at the moment of impact.

VPS1405007_026 enhanced

Figure 61 Initial impact of GRW tanker J2580 showing water loss from pressure relief valves

Immediately after the test, water could be seen leaking from the rear of the tanker (Figure 62).

VPS1405007_118

Figure 62 Leak from the rear of GRW tanker J2580

The water leaked from a rupture between the rear bulkhead and extruded band. On subsequent inspection, there was a rupture in the weld between the rear bulkhead and extruded band at the top of the impact zone. Figure 63 shows the tanker in the upright position. Figures 64 and 65 show the failure on the upper side of the impact zone more clearly.

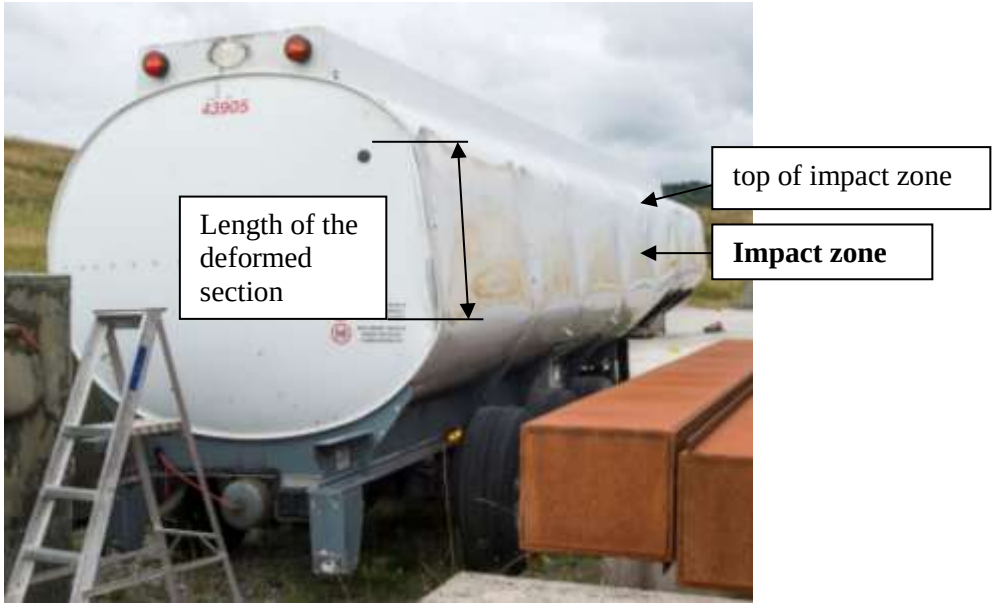

VPS 1408025_013

Figure 63 GRW tanker J2580 in the upright position – after test

VPS 1408025_017

Figure 64 GRW tanker J2580 – rupture in the weld at the top of the impact zone (1)

VPS 1408025_022

Figure 65 GRW tanker J2580 – rupture in the weld at the top of the impact zone (2)

HSL supplied TWI with a sample of the impact zone from the off-side rear (band H/8) and a sample of the equivalent portion on the near-side from GRW tanker J2580 for post-mortem assessment under WP2. During post-mortem examination, TWI observed an apparent through-wall crack along the circumferential weld at the top of the impact zone. This crack can be seen in Figure 66, which is taken from close examination of an HSL photograph of the tanker after being lifted back onto its wheels.

Internal inspection of GRW tanker J2580 prior to the test found that the profile of the extruded band on this tanker was different to GRW tankers with a later manufacture date that HSL had inspected. This inspection also found that, for GRW tanker J2580, the bulkheads were welded to the extruded bands on one side, the convex side of the bulkhead curvature, and not to both sides. The convex side of the rear bulkhead was the outside.

When the water was pumped out of each compartment, no obvious lowering of the water level in the adjacent compartments was observed; so it was not confirmed at this stage if there had been any breaches between compartments. Once the tanker had been lifted back onto its wheels, pneumatic pressure tests confirmed that all compartments had lost their internal integrity.

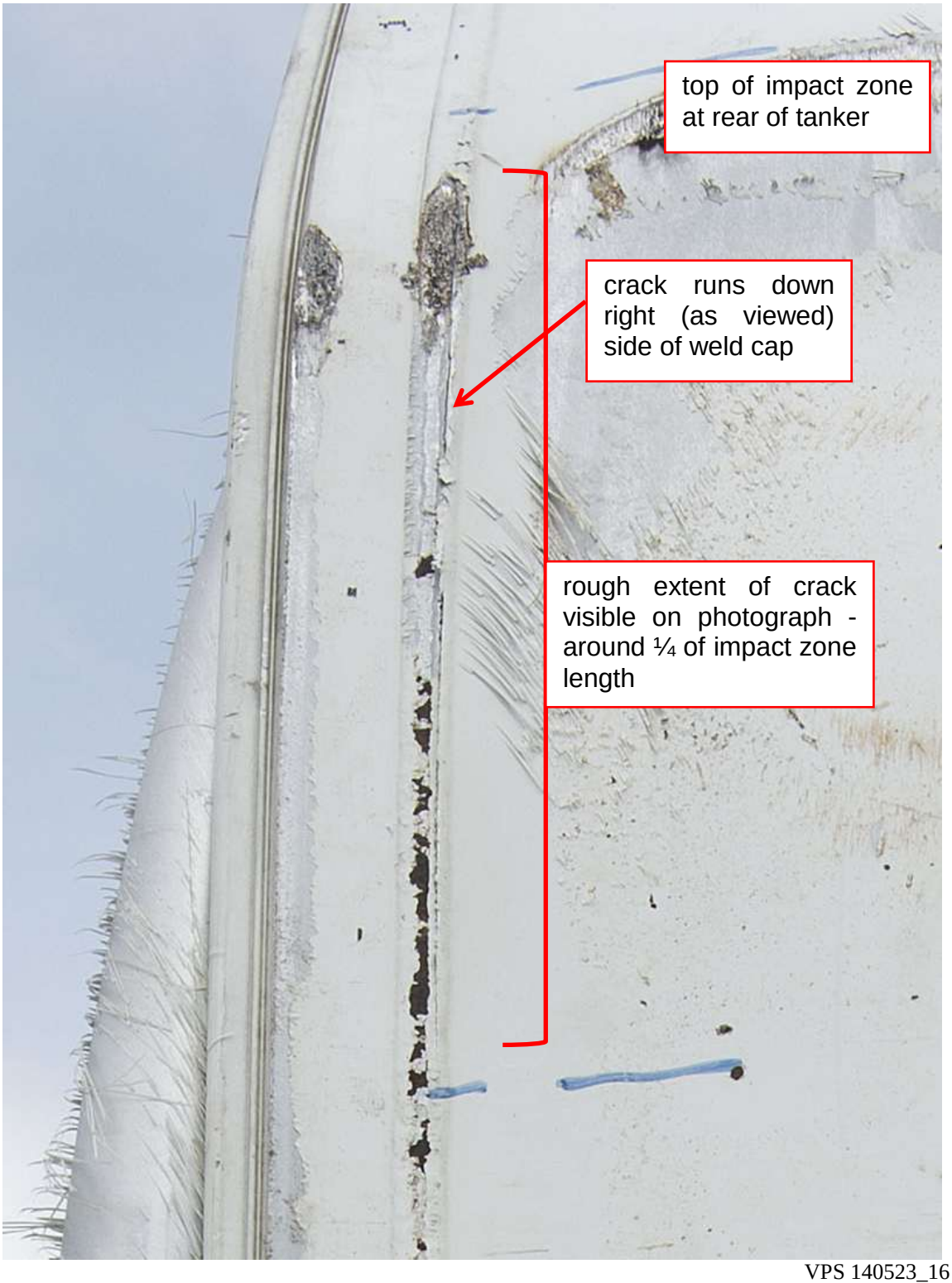

VPS 140523_16

Figure 66 GRW tanker J2580 – apparent through-wall crack along the circumferential weld at the top of the impact zone at the rear (band H/8)
taken from photograph after tanker lifted back onto its wheels

9.6.2.2 Deformation of the tanker

The front and rear profiles of the tanker, obtained from laser scans after the test while the tanker was still on its side, are shown in Figures 67 and 68. The approximate width of the tanker at both front and rear before the test was 2 530 mm, while after the test the width at the front was 2 448 mm and the width at the back was 2 429.5 mm. Therefore, the impact caused permanent deformation of approximately 82 mm at the front and 100 mm at the rear.

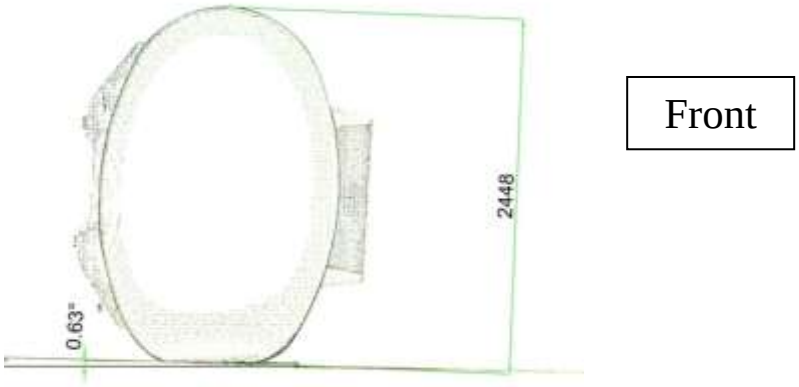

Figure 67 Deformation of GRW tanker J2580 from laser scans after test - front
dimensions in mm

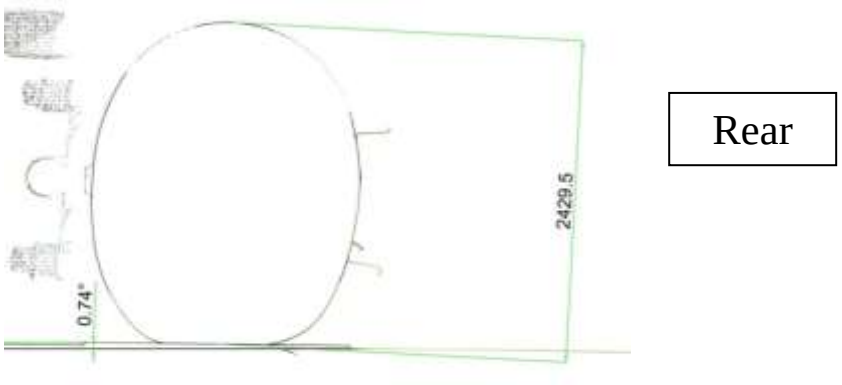

Figure 68 Deformation of GRW tanker J2580 from laser scans after test - rear
dimensions in mm

9.6.2.3 Real-world rollover damage

GRW have indicated that the damage around the joints between the extrusion band and the bulkhead/baffles is consistent with that seen in real-world rollovers.

9.6.3 GRW tanker J3910

Figure 69 shows six images from the high speed video for each end of the tanker in 20 ms steps from the moment of impact to 100 ms later.

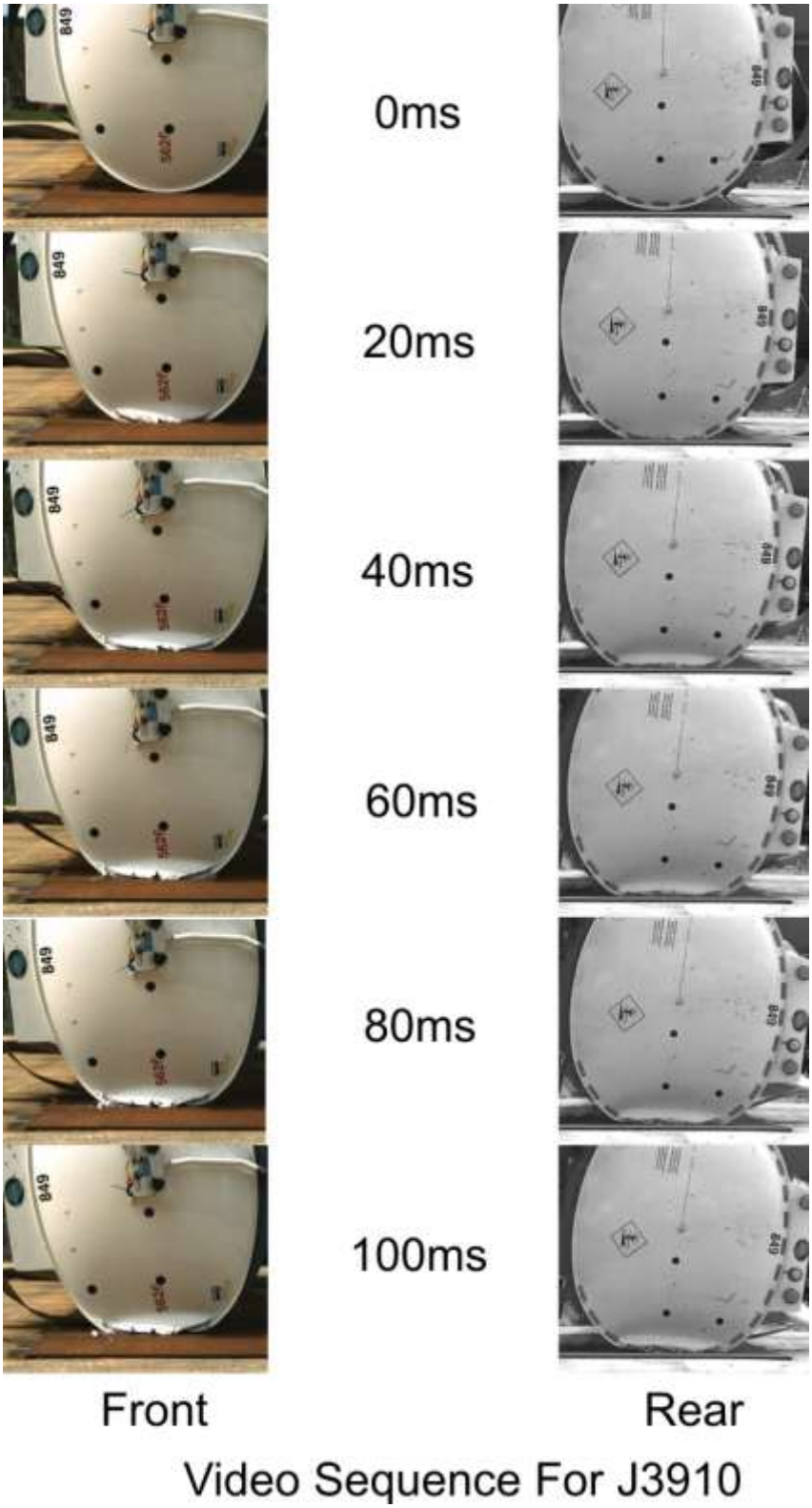

Figure 69 High speed video images during impact – GRW tanker J3910

9.6.3.1 External leaks and internal integrity of compartments

During the impact some water was lost through the pressure relief valves, as shown in Figure 70. Examination of the videos and stills photography found that the amount of water lost in this way was minimal. Again, due to the lower level of water than would have been the case for road fuel, the pressure relief valves may not have been in full contact with the water at impact.

VPS1406045_044

Figure 70 Initial impact of GRW tanker J3910 showing water loss from pressure relief valves

After the test, water could be seen leaking from the front of the tanker as shown in Figure 71.

VPS1406045_110

Figure 71 Leak from the front of GRW tanker J3910

Subsequent visual examination found a rupture at the toe of the weld between the front bulkhead and extruded band at the top of the impact zone, and a crack at the toe of the weld between the front bulkhead and extruded band at the bottom of the impact zone. Figure 72 shows the tanker in the upright position. Figures 73 and 74 show the failure at the top of the impact zone. Figures 75 and 76 show the crack at the bottom of the impact zone.

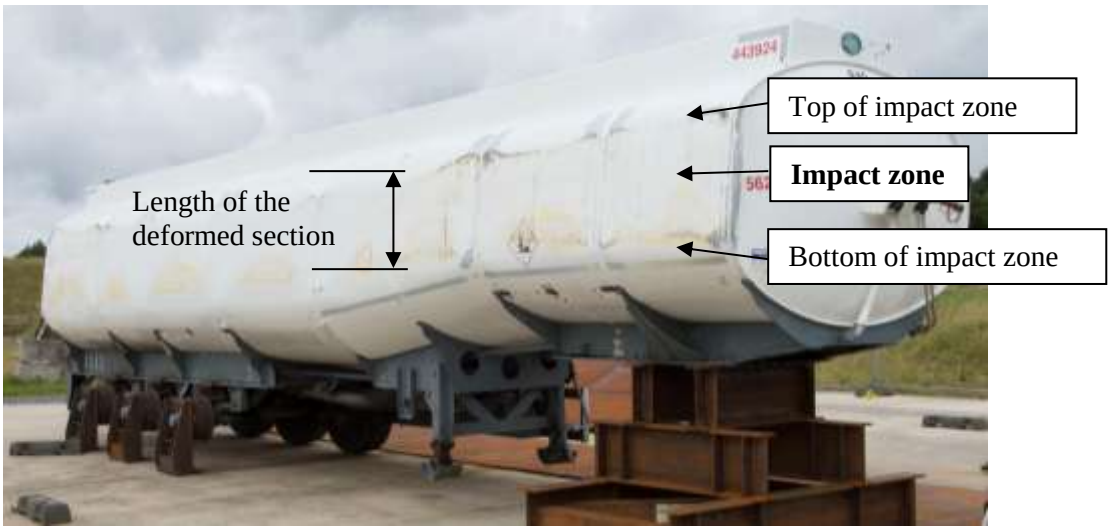

VPS 1408025_007

Figure 72 GRW tanker J3910 in the upright position – after test

VPS 1408025_025

Figure 73 GRW tanker J3910 – rupture at the toe of the weld at top of impact zone (1)

VPS 1408025_002

Figure 74 GRW tanker J3910 – rupture at the toe of the weld at top of impact zone (2)

VPS 1408025_024

Figure 75 GRW tanker J3910 – crack at the toe of the weld at bottom of impact zone (1)

VPS 1408025_006

Figure 76 GRW tanker J3910 – crack at the toe of the weld at bottom of impact zone (2)

HSL supplied TWI with a sample of the impact zone from the off-side front (band A/8) from GRW tanker J3910 for post-mortem assessment under WP2.

Internal inspection of GRW tanker J3910 before the test found that the profile of the extruded bands on this tanker were different to earlier GRW tankers HSL have inspected. This inspection also found that, for GRW tanker J3910, the bulkheads were welded to the extruded bands on both sides of the bulkhead curvature.

When the water was pumped out of each compartment, the following observations were made (see Figure 10 in Section 6.1 for compartment numbering):

- No external leaks were observed apart from the leak at the front bulkhead.
- Compartment 1 had emptied through the leak at the front bulkhead; compartment 2 had started to empty. Conclusion: the bulkhead between compartments 1 and 2 was leaking internally.
- When compartment 2 was emptied, the level did not reduce in compartment 3. Conclusion: there was no significant leak at the bulkhead between compartments 2 and 3.
- When compartment 3 was emptied, the level did not reduce in compartment 4. Conclusion: there was no significant leak at the bulkhead between compartments 3 and 4.
- When compartment 4 was emptied, the water level reduced in compartment 5. Conclusion: the bulkhead between compartments 4 and 5 was leaking internally.
- When compartment 5 was emptied, the water level did not reduce in compartment 6. Conclusion: there was no significant leak at the bulkhead between compartments 5 and 6.

Once the tanker had been lifted back onto its wheels, a pneumatic pressure test confirmed internal leaks at bulkheads between compartments 1 and 2 (band C/8), and between compartments 4 and 5 (band F/8). There was no internal leak found at the bulkhead between compartments 2 and 3, nor at the bulkhead between compartments 5 and 6. The bulkhead between compartments 3 and 4 passed the pressure test, however there was a flexing noise in the bulkhead at around 140 mb pressure.

9.6.3.2 Deformation of the tanker

The front and rear profiles of the tanker, obtained from laser scans after the test while the tanker was still on its side, are given in Figures 77 and 78. The approximate width of the tanker at both front and rear before the test was 2 522 mm, while after the test the width at the front was 2 440 mm and the width at the back was 2 415 mm. Therefore, the impact caused permanent deformation of approximately 82 mm at the front and 107 mm at the rear.

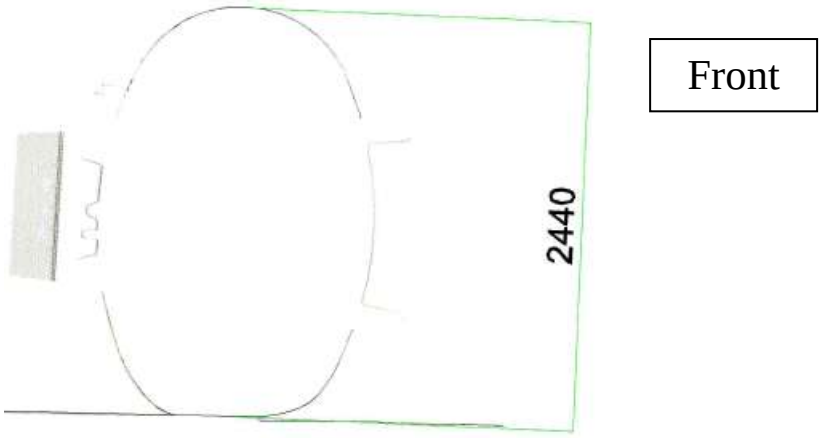

Figure 77 Deformation of GRW tanker J3910 from laser scans after test - front
dimensions in mm

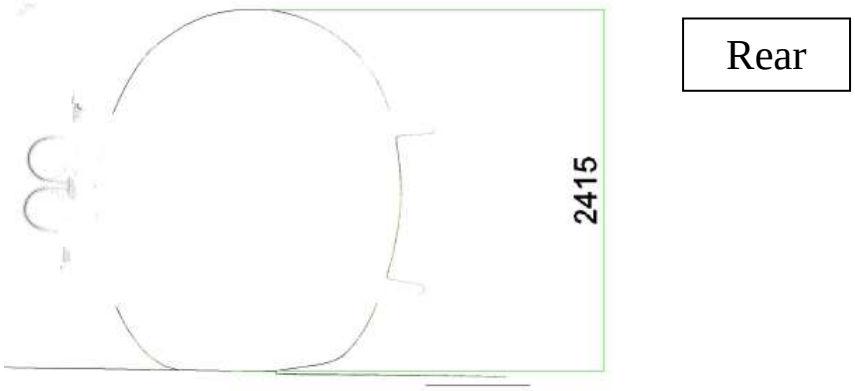

Figure 78 Deformation of GRW tanker J3910 from laser scans after test - rear
dimensions in mm

9.6.3.3 Real-world rollover damage

GRW have indicated that the damage around the joints between the extrusion band and the bulkhead/baffles is consistent with that seen in real-world rollovers.

9.6.4 GRW tankers J3910 and J2580 - length of the damaged section of the shell

Figure 79 shows lengths of the damaged sections of the shells (lengths of the 'flats' in the flattened area) and the % difference in these lengths between the two GRW tankers.

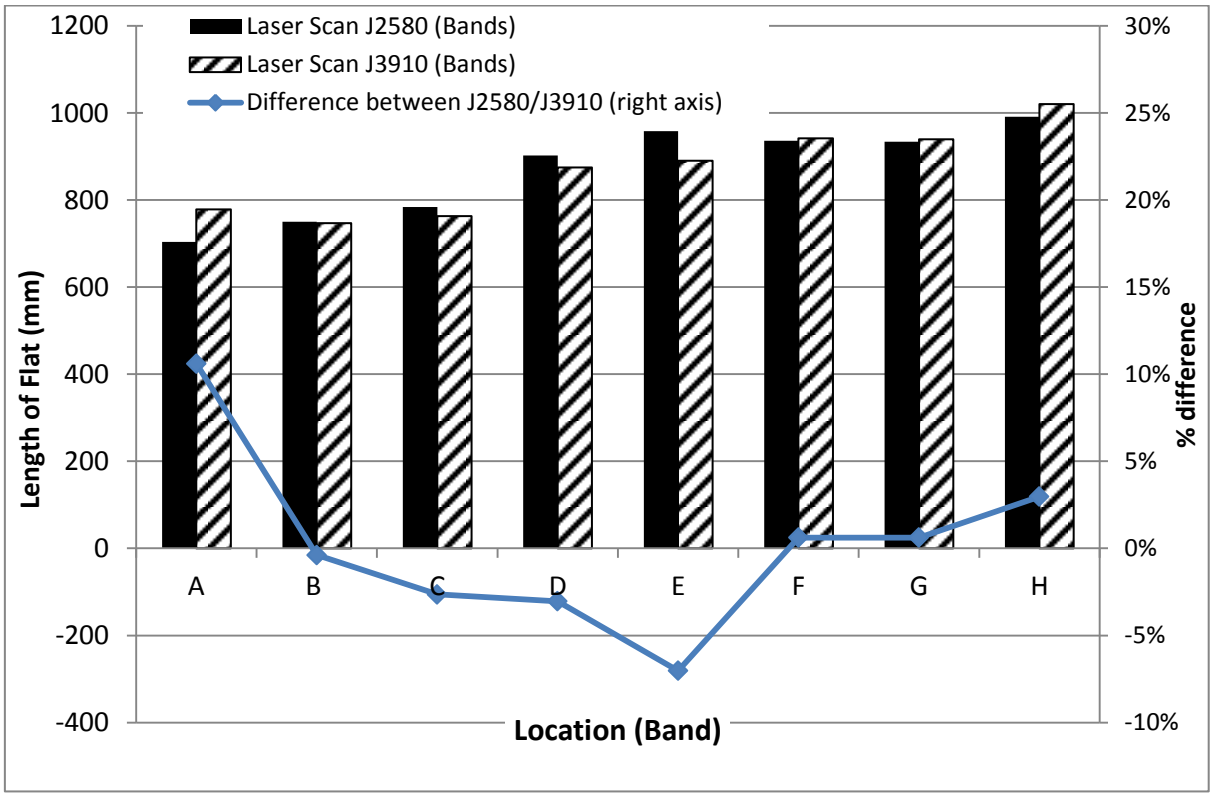

Figure 79 GRW tankers J2580 and J3910 - lengths of the damaged sections at the bands

The % difference (on the right hand axis) is based on the equation:

(length(J3910) – length(J2580))/length(J2580) x 100%

So where the % is positive, the length of the damaged section is greater for J2580, and where the % is negative the length of the damaged section is greater for J3910.

The differences are all within 12% of each other, which indicates that the structural response of the two GRW tankers was similar and test method was reproducible.

10 CONCLUSIONS

Overall, the outcomes of a *proof of concept* test and tests on two GRW tankers, J2580 and J3910, demonstrated that the topple test was a reliable test method. The test data was reproducible and was used to validate HSL's Finite Element (FE) model, and improve the understanding of tanker impact behaviour during rollover.

Test Methods, including tanker preparation
Three tankers were topple tested. First, a *proof of concept* test was conducted on a 'guinea pig' aluminium petroleum road fuel tanker. The aim of this test was to establish, with minimal test instrumentation on the tanker, that the basic test method and data logging system were sound, and so all the key features of tanker preparation, test and recovery were included in this test. The second and third tests were on GRW tanker J2580 (8-banded 6-compartment, 2008), and GRW tanker J3910 (8-banded 6-compartment, 2011): full test instrumentation was used in both tests.

After considering various approaches, HSL developed a topple test; a prepared tanker was tilted under controlled conditions until it became unstable and fell onto its offside under the influence of gravity. The tanker was filled with water because fuels were not practical for environmental and safety reasons. Impact on the offside of the tanker avoided damaging filling ports on the tanker's nearside. Information on GRW tankers was used to calculate the approximate angle at which GRW tankers would become unstable and ramps were designed to provide an initial tilt angle less than this calculated angle. The ramps were secured to a concrete test pad, with a plate steel landing pad providing a robust and repeatable impact area. After preparation, an empty tanker was placed on the ramps with its offside at, and parallel to, the bottom of the ramps.

Once ready for test, the tanker was filled with the required volume of water (equivalent to the mass of fuel for the GRW tankers) distributed across all compartments. It was then toppled sideways, pivoting around the outer edge of its offside wheels to fall onto the landing pad. The tanker was rotated into the topple position using two parallel winching systems with wide slings to spread the load and prevent high stress levels on the tanker body when winch forces were applied to the slings. Each winching system included a chain hoist and load cell and was anchored to the concrete pad. Rotating the tanker into the topple position was controlled by ensuring the load on each winch line was similar. When the point of instability was reached, the winching lines slackened and the tanker toppled onto its side due to the force of gravity.

Rectangular steel supports ('steel wheels') replaced the tanker's offside wheels to remove the risk of the tyres coming off the wheel rims during the test, and to avoid variability from uncontrolled shear movement in these tyres during the topple. The tanker was not tested with a tractor unit to avoid uncontrolled variations between tests caused by tractor unit rotation and to avoid possible failure of the kingpin due to unconventional loading. Instead, a steel frame (the '5^{th} wheel' assembly) was fitted at the tanker's kingpin plate to give the support normally provided by the tractor and to keep the tanker at the desired coupling height for the test. The tanker's suspension was blocked rigid to remove sources of uncontrolled variation, such as changes in the ride height, and to keep the tank position fixed relative to the suspension during the topple. Any tanker items not integral to the tank and suspension, or which might adversely affect the impact, or which might contain fuel, hydraulic oil or other environmentally harmful materials, were sealed or removed.

The full data gathering instrumentation for GRW tankers J2580 and J3910 comprised strain gauges, pressure transducers and accelerometers to provide data for use in validating the finite element model and characterising general impact behaviour. In total, 40 such instruments were used in these two tests. Accelerometer blocks were located at the centre point on the outside of

both the front and rear bulkheads. Arrays of strain gauges and pressure transducers were mounted in compartments C1b (rear half of front compartment) and C4 (third compartment from the rear) as follows:

- seven pressure transducers in each compartment, located at the midpoint of the compartment close to the inner tanker wall, radiating circumferentially top to bottom on the offside (impact side), the centre being at the estimated point of impact;
- twelve strain gauges in each compartment, mounted as strain gauge pairs in matching positions on the inside and the outside of the offside tanker shell. For GRW tankers J2580 and J3910 one location was near the rear bulkhead weld measuring longitudinal strain and one location was at the midpoint of the compartment measuring both longitudinal and hoop strain. For GRW tanker J3910 only, a further location was near the front bulkhead weld measuring longitudinal strain.

Two independent data loggers were used, one for each of compartments C1b and C4. During the test these loggers were synchronised with the high speed video and acquired data at 50 000 samples per second, or one recording every 0.02 millisecond. The *proof of concept* test was recorded using a range of video cameras, and the tests on GRW tankers J2580 and J3910 were recorded using thirteen video cameras ranging from standard speed (25 frames per second) to high speed (1 000 frames per second). Frames from the high speed video were analysed to obtain accurate measurements of acceleration and impact velocity at the front and rear of the tanker.

Before test, the internal welds at the extrusion bands in GRW tankers J2580 and J3910 were visually inspected; the locations of fillet welds between the extrusion band and the shell were mapped for both tankers and the locations of weld misalignments mapped for GRW tanker J3910. GRW tanker J2580 bulkheads were welded to the extrusion bands on the convex side of the bulkhead only, while GRW tanker J3910 bulkheads were welded to the extrusion bands on both sides of the bulkhead. In addition, the extrusion profiles were different between the two tankers, with a lug on the concave side of the bulkhead for GRW tanker J2580. Before the test of GRW tanker J3910, the external circumferential weld caps were surveyed to provide data for WP2. Grids of circles, intended to indicate the deformation close to the welds for WP2, were marked on the outside of this tanker above the likely impact zone at compartments C1b and C4. Tankers were laser scanned before and after test to confirm if tanker preparation caused any changes, and to record changes to tanker shape after impact.

Once surveyed and prepared, including fitting all instrumentation, the manway lids were refitted and pneumatic pressure tests conducted to confirm that GRW tankers J2580 and J3910 were fully sealed and loadworthy. Immediately before the test, the tankers were filled with water (using a calibrated water meter) to give a mass that was equivalent to the maximum rated load mass of the tankers. GRW tankers J2580 and J3910 were, thus, both filled with 31 376 litres of water, with each compartment filled to about 70% of its maximum capacity. These volumes were below the rated volumes for fuel because of the higher density of water.

Immediately after impact, leaks and other impact features found by visual examination were recorded. The tanker was then emptied and lifted back upright onto its wheels. After recovery there was further visual examination and, for GRW tankers J2580 and J3910, pressure tests were conducted to establish the internal integrity of the compartments and bulkheads.

Topple test results

The overall impact duration was a few seconds for all the tests, with most deformation occurring in the first 100 ms. The impact was close to uniform along the length of the tanker, and the impact velocities lay within the range of 1.75 to 2.62 rad/s which has been reported for rollovers in real accidents, as follows:

- The front and rear of the *proof of concept* tanker hit the ground within a few milliseconds of each other. The impact speed at the rear of the tanker was 4.25 m/s (around 2 rad/s) - due to the nature of the test, impact speed was not measured at the front of the tanker.
- GRW tanker J2580 impacted with speeds of 4.50 m/s (1.82 rad/s) at the front and 4.10 m/s (1.86 rad/s) at the rear of the tanker, with the rear hitting the ground less than 1 ms before the front of the tanker.
- GRW tanker J3910 impacted with speeds of 4.55 m/s (1.84 rad/s) at the front and 4.25 m/s (1.93 rad/s) at the rear of the tanker, with the rear hitting the ground less than 7 ms before front of the tanker.

The pressure data in both compartments were similar for GRW tankers J2580 and J3910. Short duration pressure peaks between 2 and 7.7 bar were observed during the first 20 to 30 ms of the impact; these were above the 2 bar peak used in previous rollover modelling. However, between around 20 and 40 ms after impact the pressures were around 2 bar, and after this the pressures reduced further.

The strain data in both compartments were similar for GRW tankers J2580 and J3910. Strains near the welds were higher than those at the compartment centre, with some yielding and plastic deformation observed in the strain behaviour near the welds. During impact, for both GRW tankers, high speed video captured free travelling flexural waves propagating away from the impact line around the circumference of the tanker. Such waves should result in more pronounced ripples in the circumferential strain than the longitudinal strain at the centre of the compartment and, for both GRW tankers, this was found to be the case. Signals from three of the internal strain gauges on GRW tanker J3910 were lost during filling. Although these signals re-appeared during the impact, data from these gauges was only used as an indicator of trends. This loss of data did not significantly compromise the successful outcome of the tests.

After the test, all the tankers exhibited a similar offside deformation shape with the impact area flattened. The deformation profile was similar along the length of the GRW tankers, with the level of deformation increasing from front to rear of the GRW tankers. The deformation data, both as a reduction in tanker diameter and as the length of the flattened impact chord, were similar for GRW tankers J2580 and J3910. Impact had caused a permanent reduction in tanker diameter of approximately 100 mm at the rear and 82 mm at the front of GRW tanker J2580; and of approximately 107 mm at the rear and 82 mm at the front of GRW tanker J3910.

GRW J2580 impact damage. Immediately after the test, the only visible leak from the tanker was between the rear bulkhead and extrusion band at the top of the impact area. Subsequent visual inspection found a rupture within the fillet weld between the rear bulkhead and extrusion band at the top of the impact area, with no visible damage at the bottom of the impact area. During emptying there was no evidence of any breaches between compartments. However, pneumatic pressure tests showed that all compartments had lost their internal integrity. HSL supplied TWI with samples from GRW tanker J2580, including the impact zone from the off-side rear, for post-mortem assessment under WP2. During post-mortem examination, TWI observed an apparent through-wall crack along the circumferential weld at the top of the impact zone. This crack can be seen on close examination of HSL photographs of the tanker after being lifted back onto its wheels. The detailed fractographic analysis of the J2580 and J3910 samples is addressed in the WP2 report.

GRW J3910 impact damage. Immediately after the test, the only visible leak from the tanker was between the front bulkhead and extrusion band at the top of the impact area. Subsequent visual inspection found a rupture in the toe of the fillet weld between the front bulkhead and extrusion band at the top of the impact area, and also a crack in the toe of the same weld at the

bottom of the impact area. During emptying there was evidence of leaks at the bulkhead between compartments 1 and 2, and between compartments 4 and 5. Pneumatic pressure tests confirmed that internal integrity had been lost between compartments 1 and 2, and between compartments 4 and 5, while the other bulkheads and compartments had maintained their internal integrity. HSL supplied TWI with a sample from GRW tanker J3910, including the impact zone from the off-side front, for post-mortem assessment under WP2.

GRW have indicated that the damage around the joints between the extrusion band and the bulkhead/baffles is consistent with that seen in real-world rollovers.

11 REFERENCES

[1] European Agreement on the Carriage of Dangerous Goods by Road (ADR) (2013) http://www.unece.org/trans/danger/publi/adr/adr2013/13contentse.html (summary information can be found on the HSE website at http://www.hse.gov.uk/cdg/manual/adrcarriage.htm)

[2] *Roark's Formulas for Stress and Strain* 6th Edition, Warren C Young McGraw Hill International 1989 ISBN 0-07-100373

12 APPENDIX 1 INTERNAL FILLET WELD SURVEY OF J2580 & J3910 – FILLET WELD MAPS

Detailed fillet weld location maps are provided for GRW tankers J2580 and J3910. J2580 was mapped in general by HSL, and in detail by a contractor under HSL instruction, while J3910 was mapped in detail by HSL.

12.1 APPENDIX 1.1 GRW J2580

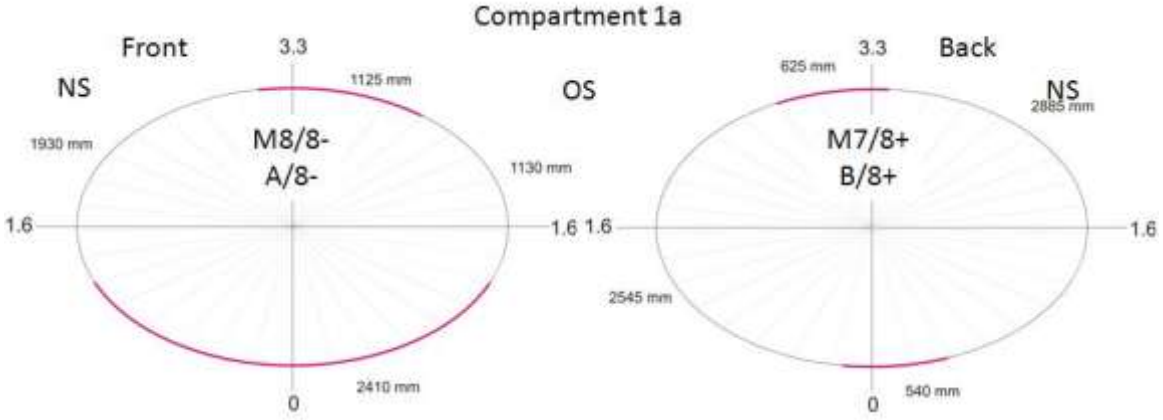

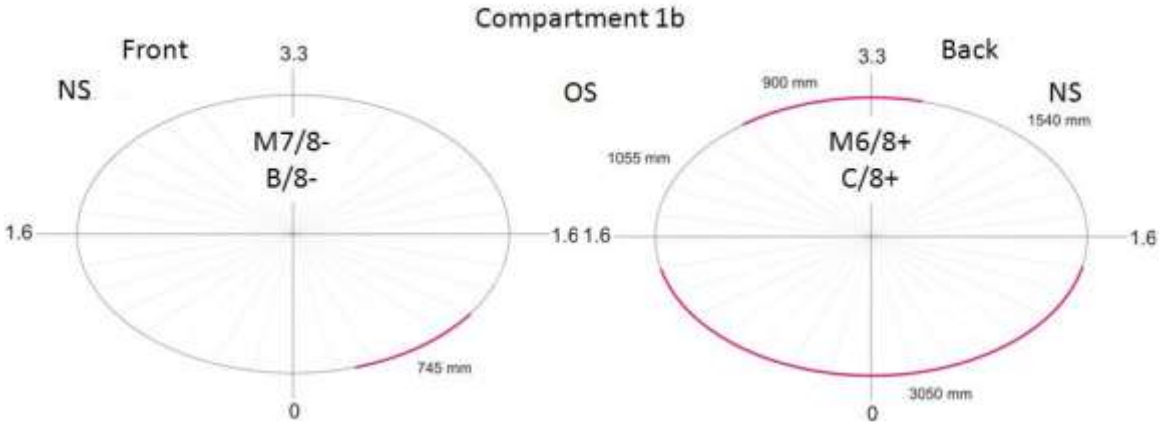

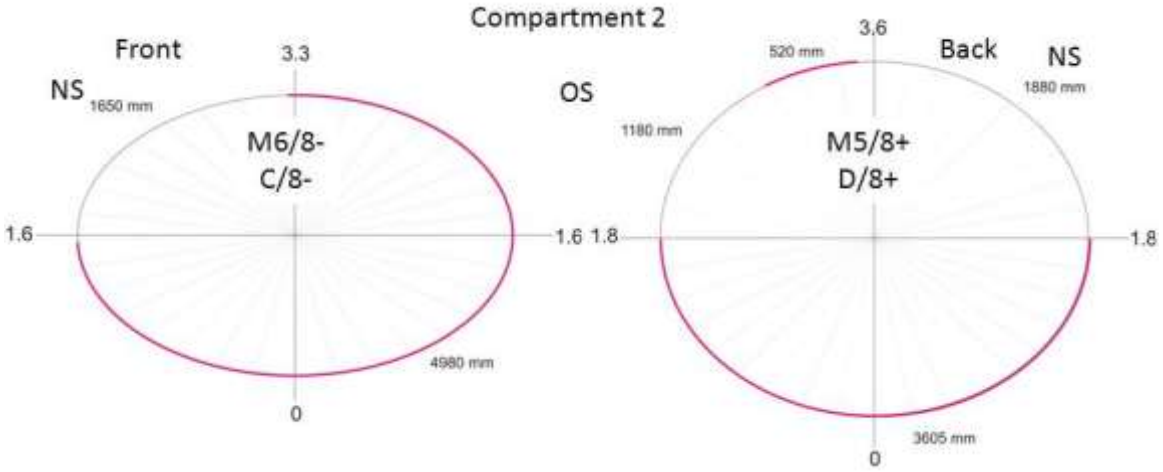

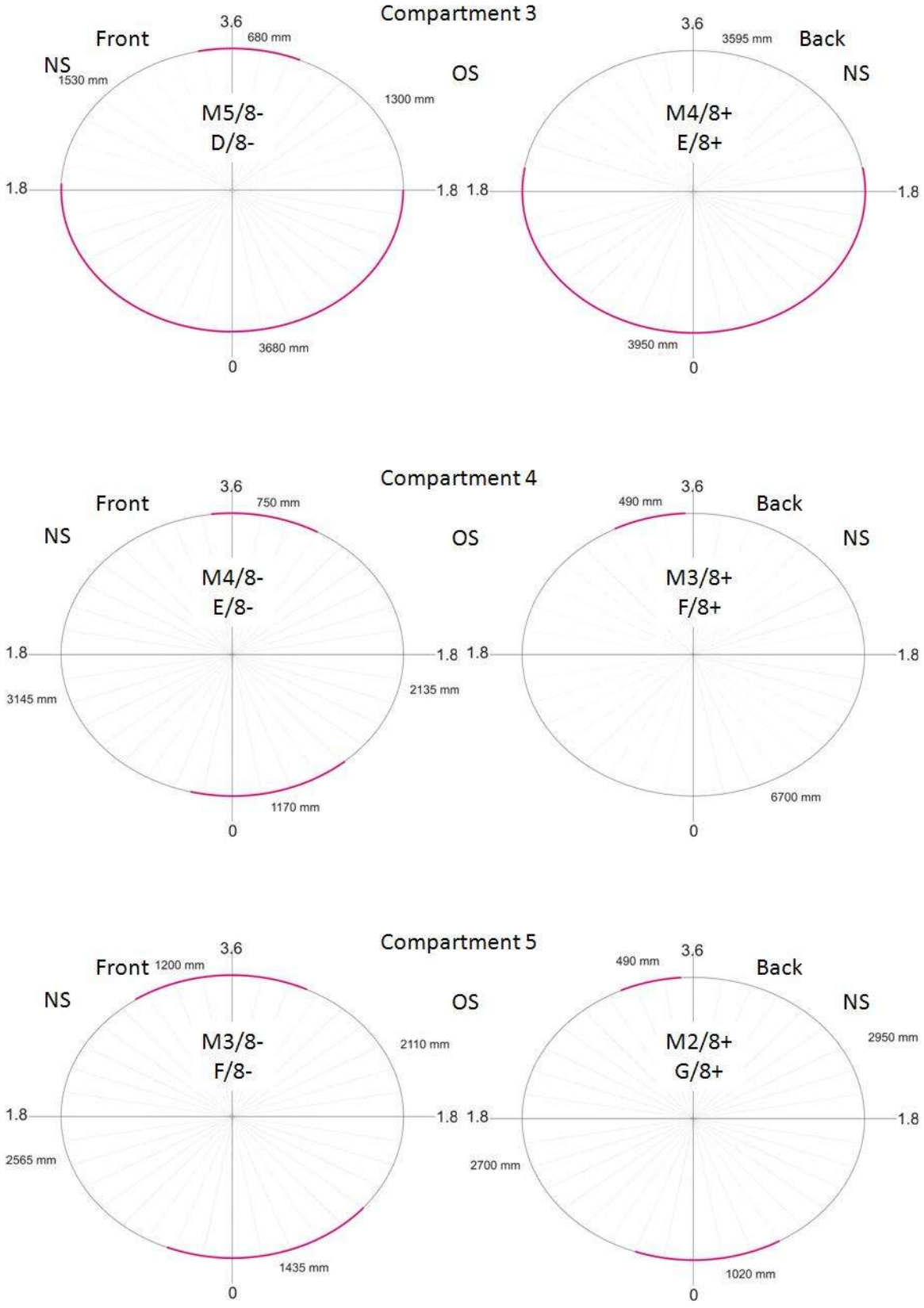
Compartment 3
Front
NS
OS
3.6
680 mm
1530 mm
1300 mm
M5/8-
D/8-
1.8
1.8
3680 mm
0
Back
NS
3.6
3595 mm
M4/8+
E/8+
1.8
1.8
3950 mm
0
Compartment 4
Front
NS
OS
3.6
750 mm
M4/8-
E/8-
1.8
1.8
3145 mm
2135 mm
1170 mm
0
Back
NS
3.6
490 mm
M3/8+
F/8+
1.8
1.8
6700 mm
0
Compartment 5
Front
1200 mm
NS
OS
3.6
M3/8-
F/8-
2110 mm
1.8
1.8
2565 mm
1435 mm
0
Back
NS
3.6
490 mm
M2/8+
G/8+
2950 mm
1.8
1.8
2700 mm
1020 mm
0

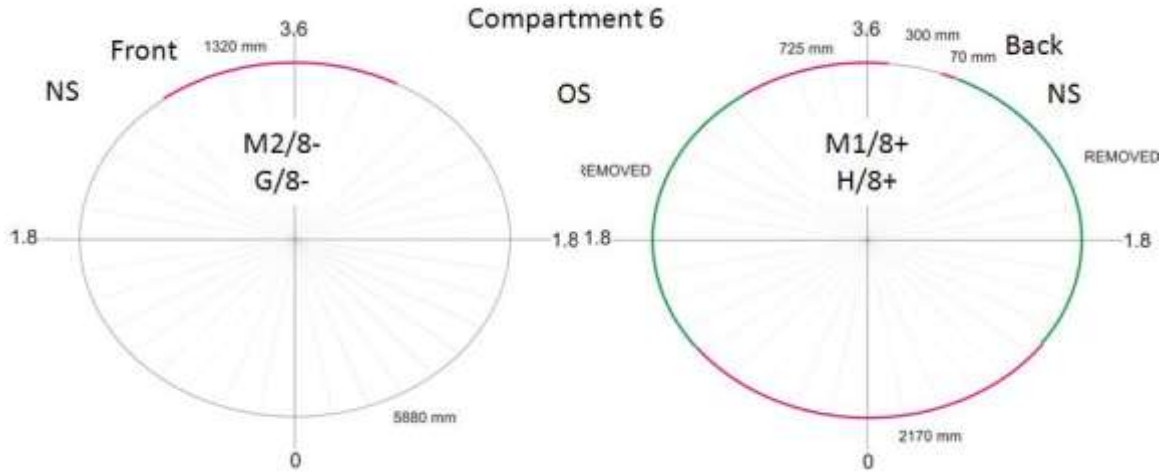

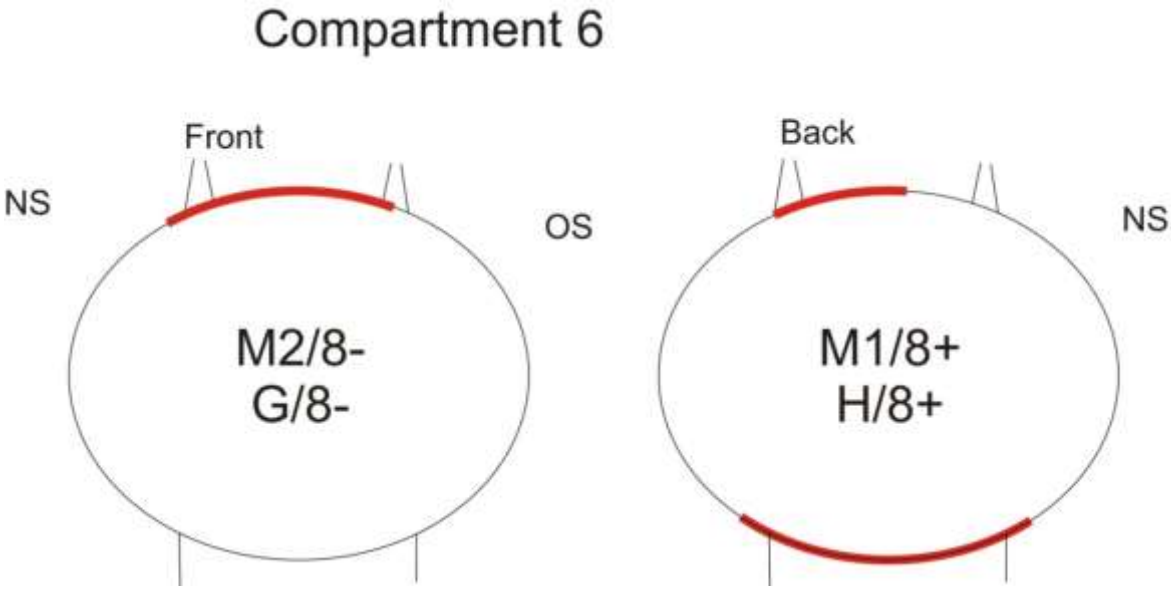

The detailed mapping of compartment 6 was conducted after samples had been taken from the rear of the compartment (band H/8+), so the less detailed map of compartment 6 is included for completeness.

12.2 APPENDIX 1.2 GRW J3910

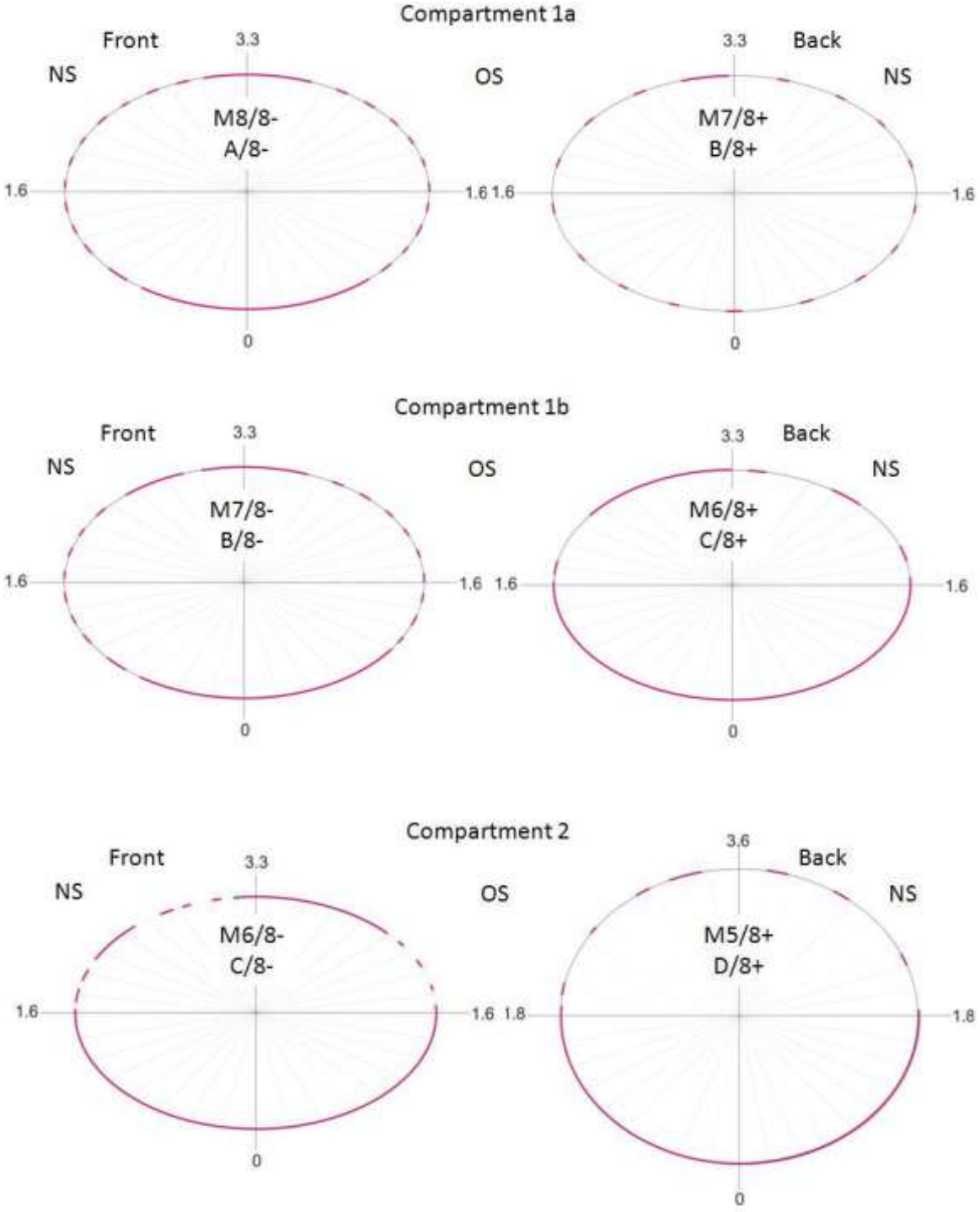

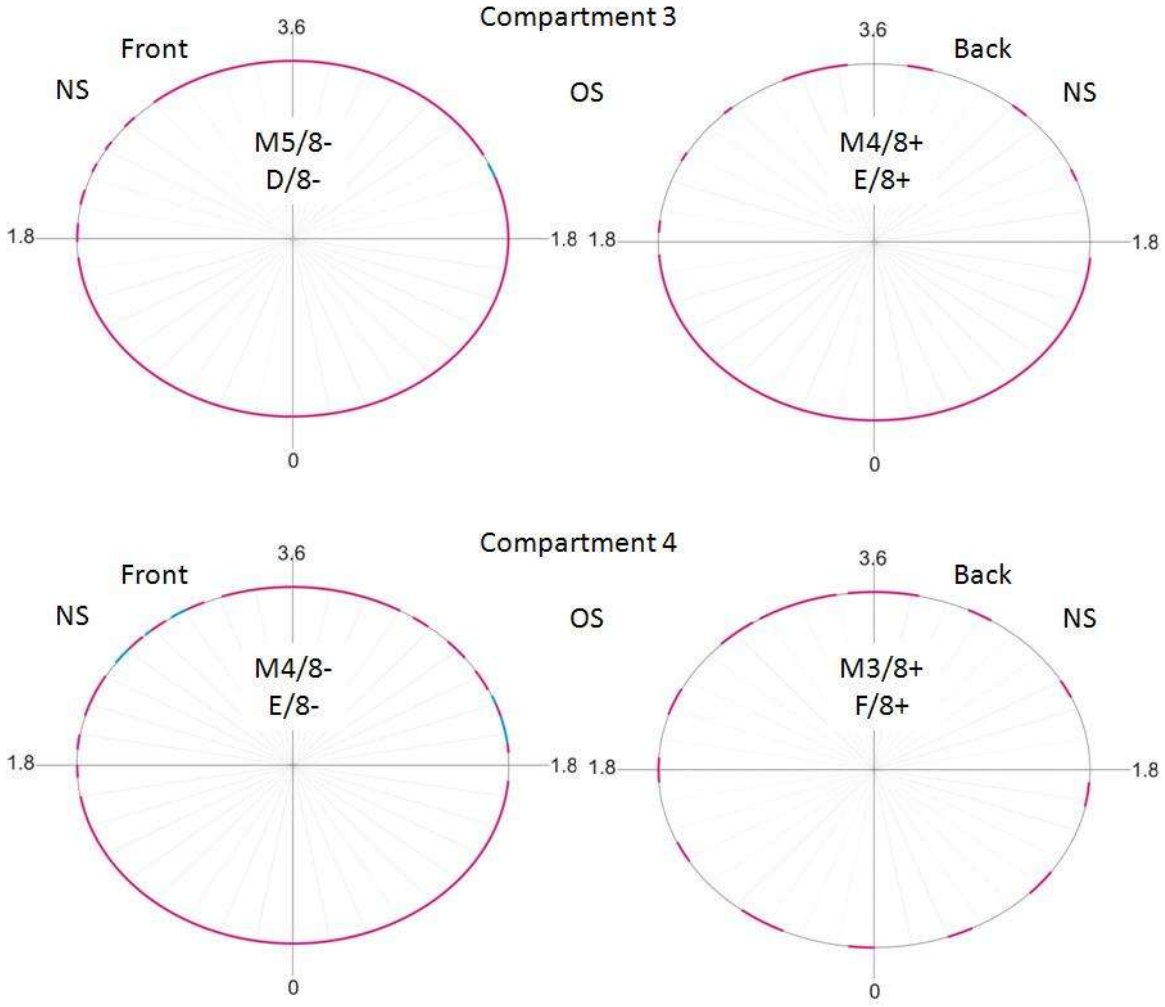
Compartment 3
Front
NS
OS
3.6
M5/8-
D/8-
1.8
1.8
0
Back
NS
3.6
M4/8+
E/8+
1.8
1.8
0
Compartment 4
Front
NS
OS
3.6
M4/8-
E/8-
1.8
1.8
0
Back
NS
3.6
M3/8+
F/8+
1.8
1.8
0

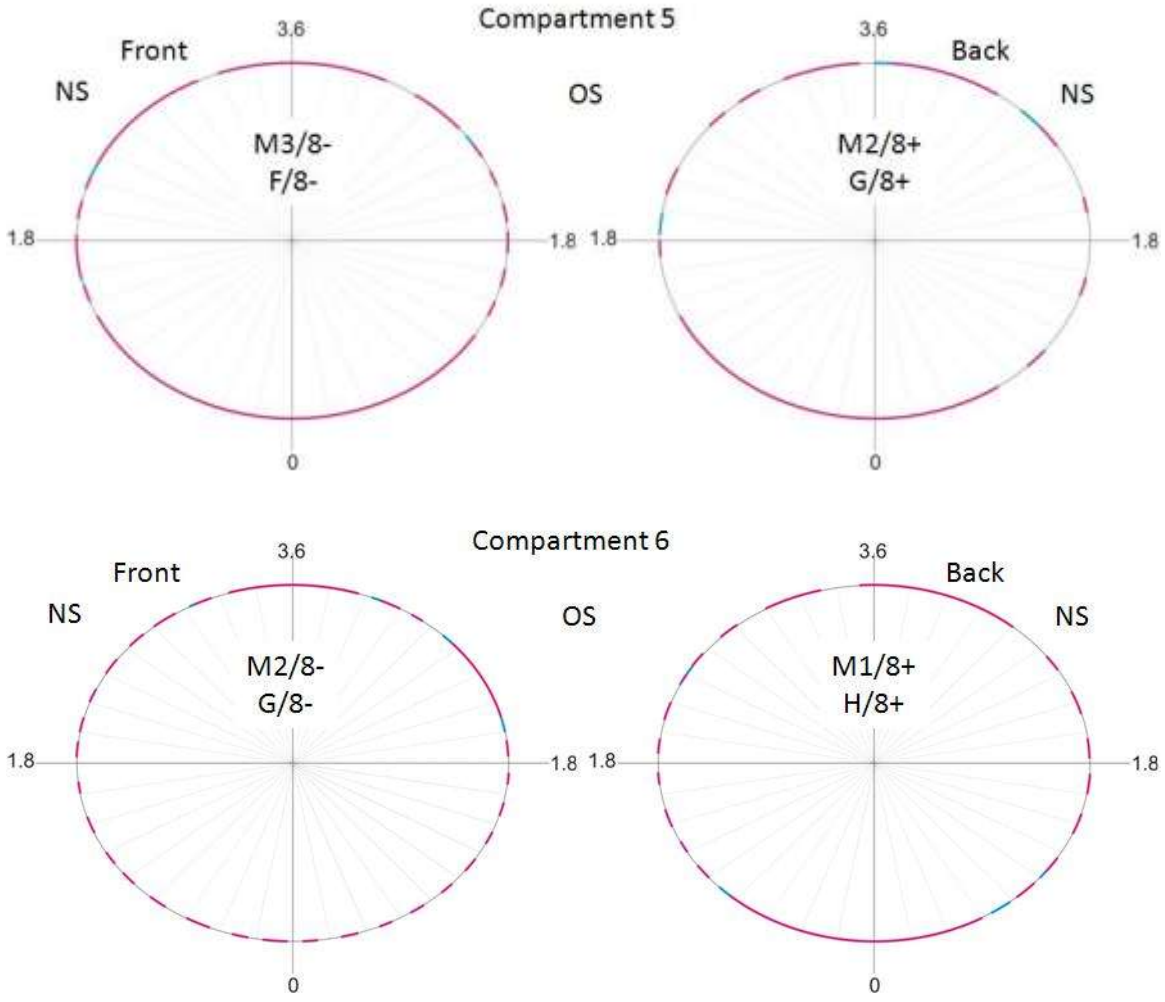
Compartment 5
Front
NS
OS
Back
NS
M3/8-
F/8-
M2/8+
G/8+
3.6
1.8
0
Compartment 6
Front
NS
OS
Back
NS
M2/8-
G/8-
M1/8+
H/8+

13 APPENDIX 2 WELD CAP SURVEY

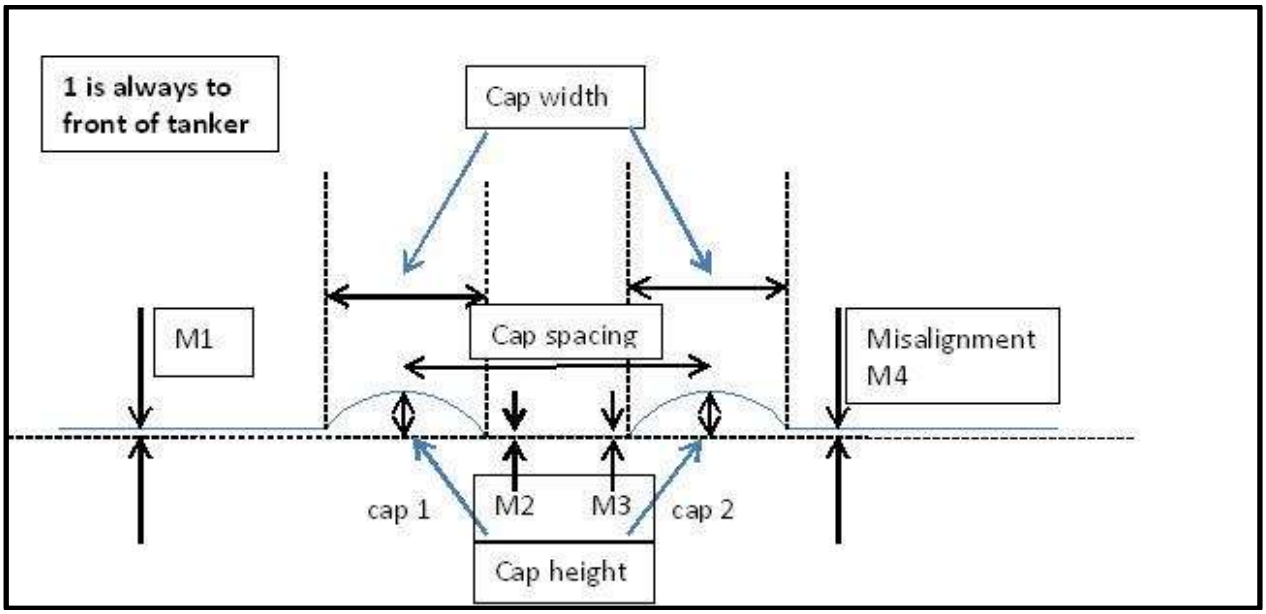

Figure A2.1 Schematic showing the weld cap survey variables

Measurements were carried out on both the offside and nearside of the tanker.
For the front and rear bands (A and H), there was only one weld cap.
For all cap and misalignment measurements - 1 is the nearest to the front of the tanker

Misalignment measurements were obtained as follows (shown in Figure A2.2):

1. Draw a line from the outer two positions of the scan data in each position (i.e. two points nominally on the main tanker surface)
2. Offset this line so it touches only the inner-most point on the scan profile
3. Take the misalignment measurements from the weld profile to this line

M1 is always to the front of the tanker

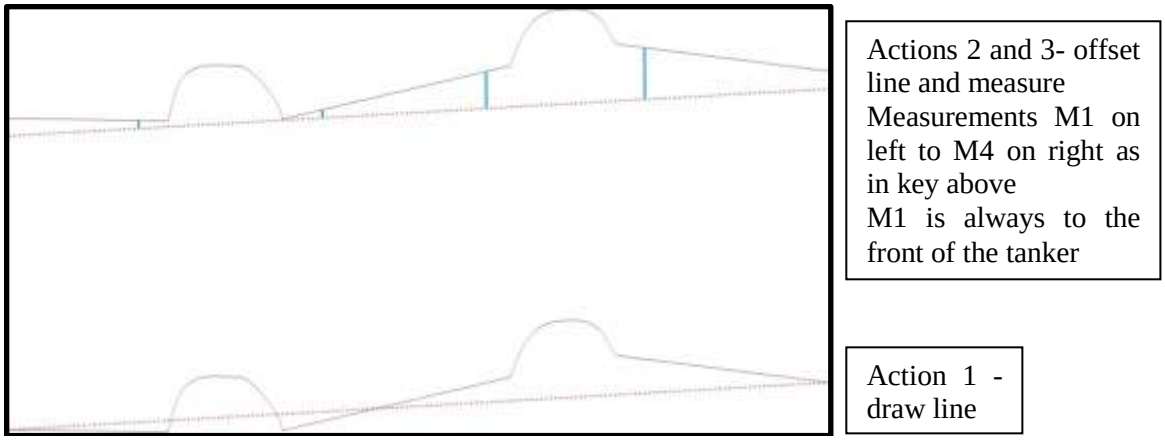

Figure A2.2 Measuring misalignment

Measurement samples (slices) were taken in three positions on the tanker surface at:

- 30° above the mid-height horizontal plane at;
- the mid-height horizontal plane; and
- 30° below the mid-height horizontal plane.

Figure A2.3 shows these positions.

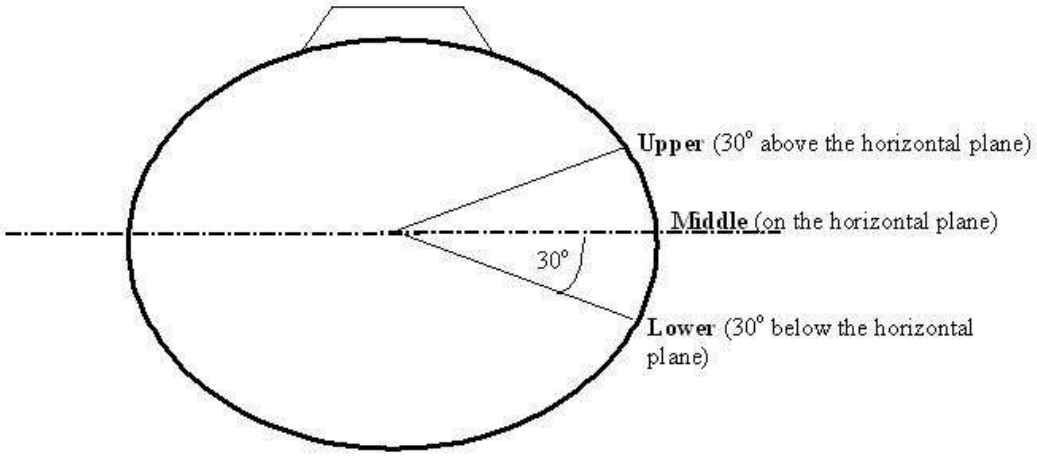

Figure A2.3 Measurement slices for the weld cap survey

Table A2.1 provides the weld cap survey dimensions.

Table A2.1 Weld cap survey data

J3910 WELD CAP DATA FROM LASER SCAN - all dimensions mm

Bands A and H - only one weld cap

Caps and misalignment - 1 is nearest front of tanker

Vehicle Offside slice	**band**		**Cap Height**		**Cap Width**		**Cap Spacing**	**Misalignment**			
	HSL	***DfT***	1	2	1	2		1	2	3	4
Upper	1	A/8	1.62	N/A	18.79	N/A	N/A	0.34	0.26	N/A	N/A
30 degrees	2	B/8	1.83	2.04	19.42	18.74	52.11	0.72	0.41	0.02	0.5
above horizontal	3	C/8	2.11	2.16	19.19	17.37	50.91	1.03	0.03	0.01	1.05
	4	D/8	2.52	1.8	19.83	19.6	52.9	1.75	0.86	0.13	1.09
	5	E/8	2.59	2.02	21.35	20.48	51.15	1.05	0.81	0.09	0.36
	6	F/8	2.21	1.93	19.1	18.97	51.23	1.9	1.15	0.07	0.21
	7	G/8	2.37	1.56	19.36	21.38	20.73	0.45	0.01	0.26	2.06
	8	H/8	1.71	N/A	19.38	N/A	N/A	0.38	0.2	N/A	N/A
Middle	1	A/8	2.18	N/A	19.28	N/A	N/A	0.2	0.27	N/A	N/A
horizontal	2	B/8	2.11	2.22	19.11	18.41	51.64	0.79	0.45	0.03	0.5
(3 o'clock)	3	C/8	1.97	2.25	19.09	18.59	50.53	0.31	0.08	0.47	1.26
	4	D/8	2.32	1.67	19.18	19.8	50.43	3.14	1.66	0.33	2.01
	5	E/8	2.26	1.83	20.61	19.34	53.52	1.15	0.84	0.07	0.68
	6	F/8	2.18	2.1	20.56	19.6	52.19	1.63	1.21	0.24	0.23
	7	G/8	1.9	2.1	22.1	20.5	51.4	1.01	0.11	0.82	1.95
	8	H/8	1.84	N/A	20.23	N/A	N/A	0.15	0.61	N/A	N/A
Lower	1	A/8	1.74	N/A	17.67	N/A	N/A	0.09	0.8		
30 degrees	2	B/8	2.18	2.04	20.27	20.83	52.22	0.87	0.4	0.06	0.59
below horizontal	3	C/8	2.03	1.86	18.96	17.53	50.48	1.21	0.5	0.15	1.11
	4	D/8	2.12	1.95	19.1	17.85	50.84	3.07	1.76	0.72	0.63
	5	E/8	1.85	1.81	18.8	19.36	50.85	0.8	0.64	0.09	0.25
	6	F/8	1.97	1.95	19.85	19.43	51.66	1.13	0.98	0.26	0.08
	7	G/8	1.62	2	18.74	19.03	50.95	0	0.05	0.79	1.47
	8	H/8	1.46	N/A	19.52	N/A	N/A	0.19	0.3	N/A	N/A

J3910 WELD CAP DATA FROM LASER SCAN - all dimensions mm

Vehicle Nearside slice		**Cap Height**		**Cap Width**		**Cap Spacing**	**Misalignment**			
	DfT	1	2	1	2		1	2	3	4
Upper	A/8	2.33	N/A	21.36	N/A	N/A	0.43	0.45	N/A	N/A
30 degrees	B/8	1.19	2.02	20.47	19.14	51.96	2.57	0.1	0	1.04
above horizontal	C/8	0.55	1.58	19.24	20.3	55.71	1.36	0.05	0.04	1.98
	D/8	N/A	1.83	N/A	19.91	N/A	N/A	N/A	0.27	0.16
	E/8	2.15	2.04	21.19	17.66	51.12	0.79	0.55	0.13	0.13
	F/8	1.85	2.12	20.8	17.11	51.41	1.18	0.98	0.31	0.27
	G/8	1.6	1.66	19.61	19.03	50.62	0.22	0.13	0.98	2.29
	H/8	1.79	N/A	19.5	N/A	N/A	0.24	0.22	N/A	N/A
Middle	A/8	1.52	N/A	18.59	N/A	N/A	0.24	0.57	N/A	N/A
horizontal	B/8	1.81	2.13	18.71	17.9	51.32	1.11	0.4	0.1	0.88
(3 o'clock)	C/8	1.52	1.95	19.51	19.21	52.2	0.12	0.52	1.28	2
	D/8	2.84	2.12	20.39	17.88	51.06	0.73	0.44	0.06	0.21
	E/8	2.32	1.96	19.6	17.37	51.57	0.48	0.44	0.01	0.36
	F/8	2.31	1.76	19.91	17.39	51.14	0.64	0.58	0.12	0.17
	G/8	2.1	2.28	18.49	18.57	49.67	0.25	0.06	0.43	0.94
	H/8	1.43	N/A	19.49	N/A	N/A	0.28	0.21	N/A	N/A
Lower	A/8	1.91	N/A	19.22	N/A	N/A	0.08	0.34	N/A	N/A
30 degrees	B/8	2.47	1.98	19.52	18.24	51.85	1.33	1.02	0.13	0.36
below horizontal	C/8	2.06	2.39	18.72	19.96	52.26	1.27	0.08	0.49	1.06
	D/8	1.07	2.04	17.68	19.06	50.93	1.96	0.55	0.06	0.67
	E/8	2.21	2.22	20.67	19.04	51.89	0.85	0.55	0.02	0.4
	F/8	2.4	2.23	20.23	18.02	51.35	1.31	0.98	0.13	0.08
	G/8	2.11	2.08	20.3	20.65	51.4	0.26	0.03	0.65	0.81
	H/8	1.71	N/A	19.94	N/A	N/A	0.1	0.16	N/A	N/A

Upper slice on band 4 scan only covered one weld

14 APPENDIX 3 GRID MEASUREMENTS

The key to the grid is shown in Figure A3.1 below.

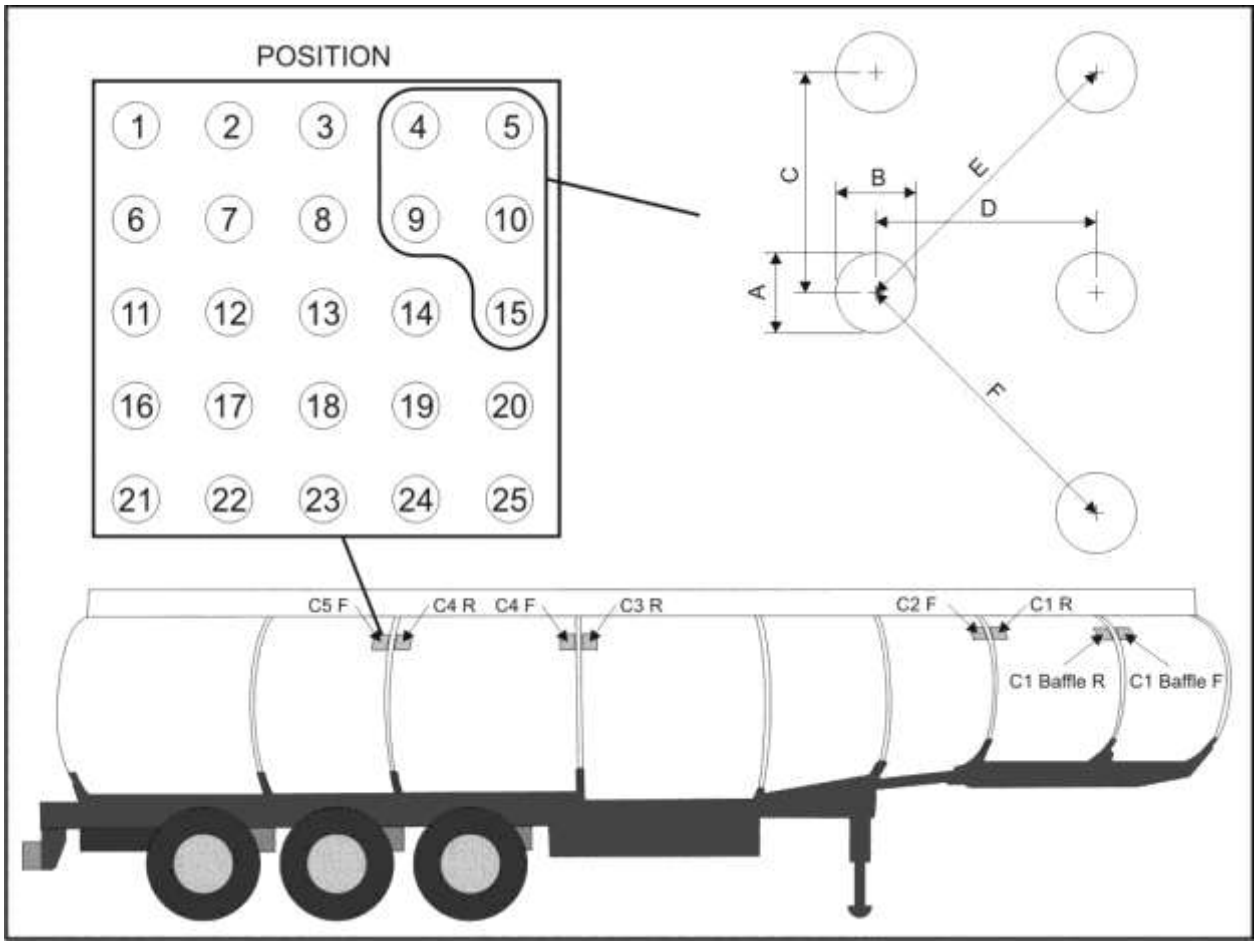

Figure A3.1 Grid Measurements on Tanker GRW J3910 – After the Test

- The circles had a nominal wall/line thickness of 3mm.
- Measurements of A&B used the inside of this line - the inner diameter
- After-test measurements are to +/-0.2mm

Table A3.1 lists the positions of the grids in relation to the bands.

As a baffle forms a partial division between compartment 1a and 1b, *C1 Baffle F* refers to the grid located to the front side of the baffle, *C1 Baffle R* refers to the grid located to the rear side of the baffle. All other locations reference their position relative to the compartment, hence *C1 R* is located to the rear of compartment 1 and *C2 F* is located to the front of compartment 2 etc.

Table A3.1 Grid position using tanker band terminology agreed by research consortium.

C1 Baffle F	band B/8 (+)	B/8 = baffle
C1 Baffle R	band B/8 (-)	
C1 R	band C/8 (+)	C/8 = bulkhead
C2 F	band C/8 (-)	
C3 R	band E/8 (+)	E/8 = bulkhead
C4 F	band E/8 (-)	
C4 R	band F/8 (+)	F/8 = bulkhead
C5 F	band F/8 (-)	

F = the grid located within the front half of the compartment

R = the grid located within the rear half of the compartment

Table A3.2 shows the reference measurements before testing.

Table A3.2 Pre-test measurements (reference values)

	Diameter A	Diameter B	Space C	Space D	Diagonal E	Diagonal F
Dimensions (mm)	19.25	19.25	28.1	28.1	39.5	39.5
Variation (mm)	±0.05	±0.05	±0.2	±0.2	±0.2	±0.2

The distances from outer edge of the weld cap to the inner edge of the circles of the closest column are shown in Table A4.3. (i.e. the column consisting of positions 1, 6, 11, 16, 21, or 5, 10, 15, 20, 25 depending on whether the grid was to the front or the rear of the band). Although these measurements were made after the test, as this distance had not noticeably changed, these measurements can be considered as a good indication of the distances before the test was carried out.

Table A3.3 Distance from the outer edge of the weld cap to the closest column of circles

Distance (mm)	Grid
10	C1 baffle F
8	C1 baffle R
10	C1 R
10	C2 F
10	C3 R
10	C4 F
8	C4 R
8	C5 F

On the grid alignment, the nominal height differences between the grids at the front and rear of each compartment are as follows:

- C5 F is 21.3 mm higher than C4 R
- C4 F is 31.8 mm higher than C3 R
- C2 F is 21.3 mm higher than C1 R

Height differences were measured between rows 21 to 25 of each grid.

Tables A3.4 to A3.11 show the grid measurements as specified in Figure A3.1.

Measurements were made with a Vernier calliper gauge (indication only); the maximum tolerance is approximately +/- 0.2 mm.

Where N/A is written, this refers to the fact that this measurement could not be made due to impact damage. Any cells that are in grey are measurements that were not possible to make.

Table A3.4 C1 Baffle (F)

Position	Dia A	Dia B	Space C	Space D	Diag E	Diag F
1	19.1	19.2		28.4		39.6
2	19.3	19.1		28.6		39.5
3	19.2	19.1		28.0		39.5
4	19.3	19.2		28.2		39.3
5	19.1	19.2				
6	18.9	19.1	27.5	28.2	39.7	39.3
7	19.0	19.0	27.9	27.9	40.1	39.5
8	19.1	19.1	28.1	28.2	39.7	39.5
9	19.1	19.1	28.0	28.2	39.7	39.5
10	19.0	19.1	27.9			
11	18.9	19.0	27.8	28.1	40.1	39.2
12	19.0	19.2	28.2	28.1	40.0	39.4
13	19.0	19.3	27.9	28.4	39.8	39.6
14	19.1	19.4	27.7	28.0	39.5	39.8
15	19.2	19.2	27.8			
16	19.1	18.9	27.9	28.2	39.6	39.2
17	19.0	19.3	27.8	28.1	40.2	
18	19.2	19.4	28.2	28.2	40.5	39.6
19	19.3	19.0	28.4	27.8	40.2	39.7
20	19.3	19.3	28.6			
21	19.0	18.8	27.9	28.6	40.6	
22	N/A	19.5	28.2	N/A	40.4	
23	N/A	19.0	N/A	N/A	N/A	
24	N/A	N/A	28.6	27.9	39.9	
25	19.4	19.2	28.4			

All dimensions in mm - measured using a vernier caliper for indication purposes only

N/A - Some lower markings on compartment one were damaged during impact

Table A3.5 C1 Baffle (R)

Position	Dia A	Dia B	Space C	Space D	Diag E	Diag F
1	18.9	19.0		28.2		39.8
2	19.0	19.2		28.0		39.7
3	18.9	18.9		28.0		40.1
4	19.0	19.1		28.3		40.0
5	19.0	19.2				
6	19.2	19.3	27.9	27.9	39.3	39.8
7	19.1	19.1	28.1	28.2	39.2	39.9
8	19.3	19.1	27.7	28.0	39.1	40.0
9	19.2	19.2	28.0	28.1	39.3	40.1
10	19.1	19.4	28.2			
11	19.3	19.3	28.0	28.0	39.6	40.0
12	19.1	19.4	28.0	28.1	39.8	40.2
13	19.2	19.1	28.1	28.2	39.5	40.3
14	19.1	19.2	28.0	28.3	39.4	40.7
15	19.3	19.4	27.7			
16	19.4	19.1	28.8	28.3	40.0	40.4
17	19.3	19.5	28.6	28.1	40.0	39.9
18	19.3	19.1	28.4	28.5	39.4	40.3
19	19.3	19.5	28.0	28.3	38.8	40.9
20	19.2	19.6	28.4			
21	19.2	19.1	28.3	28.1	40.0	
22	19.4	19.0	28.1	27.8	39.4	
23	N/A	18.8	28.3	28.0	39.6	
24	19.1	19.3	28.8	28.8	38.8	
25	19.5	19.4	28.1			

All dimensions in mm - measured using a vernier caliper for indication purposes only

N/A - Some lower markings on compartment one were damaged during impact

Table A3.6 C1 R

Position	Dia A	Dia B	Space C	Space D	Diag E	Diag F
1	18.9	19.0		28.3		39.4
2	18.5	18.7		28.3		39.1
3	18.6	19.0		27.7		39.1
4	18.9	19.0		27.9		39.4
5	18.6	19.2				
6	18.6	19.0	27.6	27.9	39.8	39.2
7	18.6	19.0	27.8	28.0	40.3	39.5
8	18.8	18.9	28.2	28.0	39.7	39.1
9	18.6	19.0	28.0	27.9	39.7	39.5
10	18.6	19.0	28.0			
11	18.5	19.2	27.5	28.3	39.8	39.3
12	18.6	18.9	28.0	27.8	39.9	39.8
13	18.6	19.4	27.8	27.9	40.0	39.2
14	18.4	18.9	28.2	28.1	40.0	39.4
15	18.6	19.1	27.9			
16	18.6	19.0	27.6	28.2	40.0	39.3
17	18.6	19.2	27.6	27.8	39.6	39.5
18	18.9	19.2	27.8	28.0	39.6	39.4
19	19.0	19.2	27.6	27.9	39.9	40.0
20	18.7	19.1	27.9			
21	19.0	19.3	27.9	28.0	40.2	
22	19.1	19.3	28.0	28.1	40.1	
23	19.0	19.1	27.8	28.2	39.9	
24	19.0	19.0	27.9	28.0	39.8	
25	19.1	N/A	28.1			

All dimensions in mm - measured using a vernier caliper for indication purposes only

N/A - Some lower markings on compartment one were damaged during impact

Table A3.7 C2 F

Position	Dia A	Dia B	Space C	Space D	Diag E	Diag F
1	19.0	18.9		28.2		39.9
2	18.9	18.9		28.3		39.5
3	19.7	19.0		28.3		39.4
4	18.7	19.2		28.3		39.2
5	18.6	19.0				
6	18.8	19.0	28.3	28.0	39.6	39.5
7	18.7	18.9	28.0	28.1	39.7	39.7
8	18.8	19.1	27.7	28.4	39.6	39.6
9	18.5	19.1	27.8	28.1	39.2	39.5
10	18.7	18.7	27.6			
11	18.7	19.0	27.7	28.2	39.7	39.8
12	18.7	19.0	27.8	28.1	39.6	39.8
13	18.8	18.9	27.7	28.2	39.6	39.7
14	18.7	19.1	27.5	28.4	39.1	39.3
15	18.6	18.8	27.4			
16	18.9	19.0	27.8	28.1	39.8	39.8
17	18.7	19.0	28.0	27.9	39.7	40.0
18	18.6	19.0	27.6	28.4	39.7	39.9
19	18.5	19.2	27.8	28.1	39.6	39.6
20	18.6	18.8	27.6			
21	18.8	19.0	27.9	28.2	39.7	
22	18.7	19.2	27.8	28.5	39.5	
23	18.8	19.3	27.8	28.3	39.5	
24	18.9	19.1	27.9	28.0	39.5	
25	18.7	19.0	27.7			

All dimensions in mm - measured using a vernier caliper for indication purposes only

Table A3.8 C3 R

Position	Dia A	Dia B	Space C	Space D	Diag E	Diag F
1	19.0	19.3		28.2		39.4
2	19.1	19.1		28.0		39.5
3	19.1	19.2		27.5		39.1
4	19.3	19.3		27.6		39.3
5	18.9	19.3				
6	19.0	19.1	27.8	28.0	39.7	39.5
7	19.0	19.0	27.8	28.1	39.9	39.4
8	19.1	19.2	28.1	27.9	39.5	39.6
9	19.0	19.2	27.8	27.9	39.3	39.6
10	19.1	19.3	28.0			
11	19.0	19.0	28.1	28.1	39.5	39.5
12	19.1	19.2	28.1	27.7	39.6	39.2
13	19.2	19.0	28.0	27.8	39.8	38.9
14	19.0	19.1	28.1	28.2	39.9	39.2
15	19.2	19.2	28.0			
16	18.9	19.1	27.7	27.8	39.5	39.3
17	19.0	19.2	27.5	28.0	39.7	39.3
18	19.0	19.3	27.8	28.1	39.4	39.3
19	19.1	19.2	27.5	28.1	39.8	39.4
20	19.0	19.3	27.8			
21	19.1	19.2	28.0	28.1	39.6	
22	19.2	19.2	27.9	28.5	39.8	
23	19.1	19.3	27.9	28.1	39.6	
24	19.0	19.1	28.1	27.9	39.4	
25	19.3	19.3	28.0			

All dimensions in mm - measured using a vernier caliper for indication purposes only

Table A3.9 C4 F

Position	Dia A	Dia B	Space C	Space D	Diag E	Diag F
1	18.9	18.9		27.9		39.7
2	19.0	19.1		27.7		39.6
3	19.0	18.9		27.9		39.6
4	19.0	18.9		28.0		39.5
5	19.1	19.3				
6	18.8	19.0	28.1	28.0	39.6	39.6
7	18.8	19.0	28.0	28.0	39.7	39.5
8	19.0	19.0	28.0	27.9	39.7	39.5
9	19.0	18.9	28.0	28.0	39.9	39.5
10	18.9	19.1	28.1			
11	19.0	19.1	28.0	28.1	39.7	39.6
12	18.9	19.1	27.7	27.8	39.2	39.7
13	19.0	18.8	28.2	28.0	39.6	39.9
14	19.1	19.2	27.7	28.3	39.6	39.9
15	19.0	19.1	27.9			
16	18.7	19.0	27.9	27.9	39.6	39.7
17	18.9	19.0	28.4	27.9	39.5	39.7
18	18.9	19.0	27.8	27.9	39.5	39.6
19	19.0	19.1	28.1	28.3	39.6	39.9
20	19.0	19.2	28.0			
21	19.1	19.0	28.1	28.0	39.5	
22	19.0	19.1	28.0	28.3	39.5	
23	18.9	19.0	27.9	28.0	39.1	
24	19.1	19.0	27.9	28.2	39.7	
25	19.2	19.2	28.0			

All dimensions in mm - measured using a vernier caliper for indication purposes only

Table A3.10 C4 R

Position	Dia A	Dia B	Space C	Space D	Diag E	Diag F
1	18.7	19.3		27.9		39.5
2	18.9	19.1		27.8		39.4
3	19.0	19.4		28.0		39.5
4	19.1	19.4		28.1		39.3
5	18.9	19.1				
6	18.8	19.2	27.7	28.0	39.5	39.3
7	18.9	19.3	27.8	28.2	39.4	39.2
8	18.9	19.1	27.7	28.0	39.6	39.1
9	18.9	19.4	27.8	28.0	39.6	39.6
10	19.4	19.5	28.4			
11	19.0	19.1	27.9	28.0	39.8	39.2
12	19.0	19.1	27.8	28.0	39.9	39.4
13	18.9	19.4	28.1	28.3	39.7	39.5
14	19.0	19.4	28.1	28.2	39.7	39.3
15	19.1	19.1	28.0			
16	18.8	19.1	27.9	28.0	40.0	38.8
17	19.0	19.0	27.7	28.3	39.9	39.5
18	18.8	19.4	27.8	28.0	39.7	39.2
19	18.9	19.0	27.9	28.0	39.8	39.5
20	19.1	19.2	27.2			
21	18.9	19.4	27.7	28.3	40.0	
22	19.3	19.4	27.8	28.5	40.1	
23	19.6	19.5	28.0	28.0	40.0	
24	19.2	19.4	28.0	28.1	40.1	
25	19.1	19.4	28.3			

All dimensions in mm - measured using a vernier caliper for indication purposes only

Table A3.11 C5 F

Position	Dia A	Dia B	Space C	Space D	Diag E	Diag F
1	19.0	19.2		28.5		39.8
2	19.0	19.1		27.9		39.4
3	19.1	19.0		28.2		39.6
4	19.1	19.2		28.1		39.9
5	18.9	19.0				
6	18.9	19.2	27.7	28.0	39.2	39.5
7	19.1	19.0	28.0	28.0	39.2	39.7
8	18.9	19.0	28.0	28.1	39.4	40.0
9	18.9	19.1	28.1	28.2	39.4	39.7
10	18.9	19.0	28.2			
11	18.9	19.1	27.7	28.1	39.4	39.7
12	18.7	18.9	27.7	28.2	39.5	39.9
13	19.1	19.1	28.0	28.2	39.4	39.7
14	19.0	19.1	27.6	28.4	39.3	39.9
15	18.9	19.2	27.7			
16	19.0	19.3	28.1	28.0	39.6	39.7
17	19.0	19.0	27.9	28.2	39.6	39.8
18	19.0	19.0	28.1	28.0	39.4	40.0
19	19.1	19.0	27.9	28.2	39.6	40.1
20	19.2	19.1	28.2			
21	19.3	19.1	28.4	28.1	39.5	
22	19.3	19.1	28.3	28.2	39.5	
23	19.2	19.1	27.8	28.1	39.6	
24	19.3	19.1	27.9	28.4	39.4	
25	19.2	19.2	28.0			

All dimensions in mm - measured using a vernier caliper for indication purposes only